



Norwegian University of
Science and Technology

Analysis of Ventilation Strategies for ZEB

Magnus Owren Sangnes

Master of Energy and Environmental Engineering

Submission date: June 2016

Supervisor: Hans Martin Mathisen, EPT

Norwegian University of Science and Technology
Department of Energy and Process Engineering

EPT-M-2016-112

MASTER THESIS

for

Student
Magnus Owren Sangnes

Spring 2016

Analysis of ventilation strategies for ZEB

*Analyse av strategier for ventilasjon av ZEB***Background and objective**

The research programme Zero Emission Buildings (ZEB) includes so-called pilot buildings as a part of the research. Powerhouse Kjørbo is an older office building that has been renovated to become a zero emission building. See <http://www.powerhouse.no/prosjekter/kjorbo/> for more information.

Powerhouse Kjørbo has a displacement ventilation system. Measurements indicate that the ventilation effectiveness is lower than expected. There might be several causes, like stagnant zones or short-circuiting between supply and extract.

To ensure the quality of future building and system design it is of interest to do closer studies of the ventilation strategy used at Kjørbo, and how it possibly can be improved.

The final goal of the thesis is to contribute to improved background knowledge about how to design efficient ventilation solutions for ZEB office buildings.

The work is a continuation of the candidate's specialization project.

The task is connected to the NTNU-SINTEF Zero Emission Building (ZEB) research activity on pilot buildings.

The following tasks are to be considered:

1. Conduct a literature study related to displacement ventilation and scaled model experiments
2. Design and build a scaled laboratory model of Kjørbo
3. Perform field measurements of the ventilation system at Kjørbo
4. Validate the model against the prototype (Kjørbo)

5. Perform tests to improve the design of the ventilation system

-- " --

Within 14 days of receiving the written text on the master thesis, the candidate shall submit a research plan for his project to the department.

When the thesis is evaluated, emphasis is put on processing of the results, and that they are presented in tabular and/or graphic form in a clear manner, and that they are analyzed carefully.

The thesis should be formulated as a research report with summary both in (in both) English and Norwegian, conclusion, literature references, table of contents etc. During the preparation of the text, the candidate should make an effort to produce a well-structured and easily readable report. In order to ease the evaluation of the thesis, it is important that the cross-references are correct. In the making of the report, strong emphasis should be placed on both a thorough discussion of the results and an orderly presentation.

The candidate is requested to initiate and keep close contact with his/her academic supervisor(s) throughout the working period. The candidate must follow the rules and regulations of NTNU as well as passive directions given by the Department of Energy and Process Engineering.

Risk assessment of the candidate's work shall be carried out according to the department's procedures. The risk assessment must be documented and included as part of the final report. Events related to the candidate's work adversely affecting the health, safety or security, must be documented and included as part of the final report. If the documentation on risk assessment represents a large number of pages, the full version is to be submitted electronically to the supervisor and an excerpt is included in the report.

Pursuant to "Regulations concerning the supplementary provisions to the technology study program/Master of Science" at NTNU §20, the Department reserves the permission to utilize all the results and data for teaching and research purposes as well as in future publications.

The final report is to be submitted digitally in DAIM. An executive summary of the thesis including title, student's name, supervisor's name, year, department name, and NTNU's logo and name, shall be submitted to the department as a separate pdf file. Based on an agreement with the supervisor, the final report and other material and documents may be given to the supervisor in digital format.

- Work to be done in lab (Water power lab, Fluids engineering lab, Thermal engineering lab)
- Field work

Department of Energy and Process Engineering, 13. January 2016



Olav Bolland
Department Head



Hans Martin Mathisen
Academic Supervisor

Research Advisor:

Preface

This thesis is part of the Master of Science degree for the Department of Energy and Process Engineering at the Norwegian University of Science and Technology (NTNU) in Energy and Environmental Engineering, with specialization in Energy and Indoor Environment. The thesis is connected to the NTNU-SINTEF Zero Emission Building (ZEB) research activity on pilot buildings.

The thesis is a study into the indoor climate of the renovated zero emission and energy positive office building Powerhouse Kjørbo. The purpose of the thesis is to analyze the applied strategy for ventilation at Kjørbo from measurements during field work and in a reduced-scale building model.

Trondheim, June 17, 2016, 2015

Magnus Owren Sangnes

Acknowledgements

I would like to thank my supervisor Hans Martin Mathisen for guidance throughout this thesis, for help on designing the reduced-scale model, and for providing helpful insights and arguments regarding the planning and execution of the field work and laboratory experiments. Great thanks goes to Odin Budal Søgne, for excellent cooperation during the field work and later analysis of the results. Søgne has been very helpful and provided knowledge and numerous tips from experience with his previous work. To Lars Konrad Sørensen, who helped me build the reduced-scale model and provided clever solutions during the build period, thank you very much. I would also like to thank Olav Rådstoga, who aided me in the preparations of the field work.

Abstract

Powerhouse Kjørbo is an office building renovated to become a zero emission and energy positive building. It has a displacement ventilation system, which aims at providing a good indoor climate with low energy consumption. Previous measurements indicate that the ventilation effectiveness is lower than expected. There might be several causes, like stagnant zones, obstructions to the air flow or short-circuiting between air supply and extract. This thesis aims to investigate these issues.

A reduced-scale building model was built in a laboratory to resemble the office landscape in the prototype (Powerhouse Kjørbo). Tracer gas measurements, velocity mapping, and temperature measurements were conducted to examine the ventilation efficiency, gain understanding of the air flows and validate the model against the prototype in order to achieve similarity.

Fieldwork was conducted in the prototype building. Tracer gas measurements, velocity mapping, duct traversing, smoke visualization and registration of presence were performed to examine the ventilation efficiency, gain understanding of the air flows and determine flow rates and average occupancy.

The tracer gas measurements in the prototype show that the air change efficiency is lower than expected for displacement ventilation. This indicate existence of short-circuiting or stagnant zones. The local air change indexes indicate displacement characteristics in the zones, but mixing of the stratified air layers seem to occur and the bookshelves are assumed to work as obstructions to the air flow. Comparison of local indexes suggest that short-circuiting and stagnant zones also occur in areas of the building apart from the office landscape. A minor air leakage within the heat exchanger is still present.

The tracer gas measurements in the model show that the air change efficiency is similar to

the prototype, but the local air change indexes differ significantly. Excessive air leakage and suboptimal temperature differences are the most likely causes. Improvements made to the air-tightness were confirmed by the tracer gas measurements. Similar to the prototype, the bookshelves in the model seem to pose as obstructions to the air flows.

The temperature measurements in the model reveal a temperature difference which is relatively stable, but insufficient to match the Archimedes number to the prototype. The cooling capacity of the air handling unit, air leakage, and uninsulated ducts are identified as the main causes.

The velocity mapping and smoke visualization in the prototype indicate that the diffuser discharge is unstable, most likely caused by the large diffuser area. The issue affect the air distribution and may cause short circuiting. The adjacent zone were determined to be one meter, and no occupants or objects are found within this zone.

The velocity mapping in the model reveal that the diffuser discharge flow towards different parts of the office landscape than in the prototype. This is assumed to affect the similarity.

Comparison of the results conclude that the model and the prototype do not share satisfying similarity yet. The local air change indexes differs too much, the air flow patterns are not similar enough and the air leakage in the model is unacceptably high. However, there are indications that the air flows in certain zones are behaving similarly. It is believed that the model and prototype can share similarity after improvements have been made to the air leakage, temperature difference and control of the simulated air coming from the part of the prototype excluded from the modeling.

Sammendrag

Powerhouse Kjørbo er et kontorbygg rehabilitert til å bli et nullutslipps pluss hus. Det har et fortregningsventilasjonsystem som har som mål å forsyne bygget med et godt inneklima til et lavt energiforbruk. Tidligere målinger antyder at ventilasjonseffektiviteten er lavere enn forventet. Det kan være flere årsaker til dette, som stagnante soner, hindringer for luftstrømmen eller kortslutninger mellom tilluft og avtrekk. Denne oppgaven forsøker å undersøke disse årsakene.

En redusert skala modell ble bygget i et laboratorium for å simulere kontorlandskapet i prototypen (Powerhouse Kjørbo). Sporgassmålinger, kartlegging av hastigheter og temperaturmålinger ble gjennomført for å undersøke ventilasjonseffektiviteten, forstå luftstrømmene og validere modellen mot prototypen for å oppnå likhet.

Feltarbeid ble utført i prototypen. Sporgassmålinger, kartlegging av hastigheter, kanaltraversering, røykvisualisering og registrering av tilstedeværelse ble gjennomført for å undersøke ventilasjonseffektiviteten, forstå luftstrømmene og bestemme luftmengder og gjennomsnittlig tilstedeværelse.

Sporgassmålingene i prototypen viser at luftvekslingseffektiviteten er lavere enn forventet for fortregningsventilasjon. Dette antyder eksistens av kortslutning og stagnante soner. De lokale luftvekslingsindikatorerne antyder fortregningskarakteristikk i sonene, men omrøring av de stratifiserte luftlagene ser ut til å forekomme, og bokhyllene er antatt å virke som hindre for luftstrømmen. Sammenligning av de lokale indikatorerne antyder at kortslutning og stagnante soner også forekommer i deler av bygningen utenom kontorlandskapet. En mindre luftlekkasje er fortsatt tilstede i varmeveksleren.

Sporgassmålingene i modellen viser at luftvekslingseffektiviteten er relativt lik som i prototypen, men at de lokale luftvekslingsindikatorerne avviker betydelig. Utbredt luftlekkasje

og suboptimal temperaturdifferanse er de mest sannsynlige årsakene. Forbedringer i lufttettheten utført mellom forsøkene ble bekreftet av sporgassmålingene. I likhet med prototypen, virker bokhyllene i modellen å utgjøre hindre for luftstrømmene.

Temperaturmålingene i modellen avslører en temperaturdifferanse som er relativt stabil, men utilstrekkelig til å oppnå samme Arkimedesnummer som i prototypen. Kjøleevnen til ventilasjonsaggregatet, luftlekkasje og uisolerte kanaler ble identifisert som hovedårsakene.

Kartleggingen av hastighetene og røykvisualiseringen i prototypen antyder at luftstrømmen fra tilluftsventilene er ustabil, mest sannsynlig forårsaket av det store ventilarealet. Dette problemet innvirker på luftdistribusjonen og kan føre til kortslutning. Nærsonen ble bestemt til å være en meter, og ingen personer eller gjenstander befinner seg innenfor denne avstanden.

Kartleggingen av hastighetene i modellen avslører at luftstrømmen fra ventilen beveger seg mot andre deler av kontorlandskapet enn den gjør i prototypen. Dette er antatt å ha innvirkning på likheten.

Sammenligning av resultatene konkluderer med at modellen og prototypen ikke deler tilstrekkelig likhet enda. De lokale luftvekslingsindikatorerne avviker for mye, strømningsbildet er ikke likt nok, og luftlekkasjen i modellen er uakseptabelt høy. Likevel er det antydning at luftstrømmene i visse soner oppfører seg med en viss likhet. Det antas at modellen og prototypen kan dele likhet etter forbedringer har blitt oppnådd i luftlekkasjen, temperaturdifferansen og kontroll over den simulerte luften som kommer ifra den delen av prototypen som ble utelatt fra modelleringen.

Contents

Preface	i
Acknowledgements	iii
Abstract	v
Sammendrag	vii
Abbreviations	xix
Nomenclature	xxi
1 Introduction	1
1.1 Powerhouse	1
1.2 Background	2
1.2.1 Concerns on the Indoor Air Quality	3
1.3 Objectives	5
1.4 Scope and Limitations	5
1.5 Approach	8
1.6 Literature Study	9
2 Background Theory	11
2.1 Displacement Ventilation	11
2.1.1 Convection Flows	12
2.1.2 The Adjacent Zone	14
2.1.3 Displacement Ventilation in Open Office Areas	15
2.1.4 Distribution of Air	15

2.1.5	Instability in the Diffuser Discharge	16
2.1.6	Constant Air Volume (CAV) and Variable Air Volume (VAV) Method of Ventilation	17
2.1.7	Demand Controlled Ventilation	17
2.1.8	Heating and Cooling with Displacement Ventilation	18
2.2	Ventilation Effectiveness	18
2.2.1	Air Change Rate	19
2.2.2	Age of Air	20
2.2.3	Air Change Efficiency	21
2.2.4	Contaminant Removal Effectiveness (CRE)	22
2.2.5	Conditions for Using the Measures	22
2.2.6	Tracer Gas Measurements	23
2.2.7	Step Change Response Methods	24
2.2.8	Calculating Ventilation Effectiveness from Measured Concentrations	25
2.3	Similarity	28
2.3.1	The concept of similarity	28
2.3.2	Similarity Requirements	29
2.4	Traversing an Air Duct to Determine Average Air Velocity and Air Flow Rate	34
2.4.1	Traversing a Round Duct	34
3	Fieldwork Methodology	37
3.1	Tracer Gas Measurements	37
3.1.1	Principle	38
3.1.2	Method	39
3.2	Air Velocity Mapping in the Adjacent Zone of a Wall Diffuser	41
3.2.1	Method	42
3.3	Air Flow Rate in Duct	44
3.3.1	Method	44
3.4	Smoke Visualization	45
3.5	Presence of People	45
3.6	Discussion	45

4	Reduced-scale Building Model	47
4.1	Prototype Building	47
4.1.1	Design and Layout of the Ventilation System in the Prototype Building	48
4.2	Reduced-scale Building Model Description	49
4.2.1	Building Materials	51
4.2.2	Internal Heat Gains	51
4.2.3	Design of the Ventilation System in the Model	53
4.3	Model Parameters	55
4.4	Tracer Gas Measurements in the Model	56
4.4.1	Method	56
4.5	Air Velocity Mapping in the Adjacent Zone of a Wall Diffuser in the Model	58
4.6	Temperature Measurements in the Model	58
4.6.1	Method	59
4.7	Discussion	60
5	Experimental Results	61
5.1	Tracer Gas Measurements	61
5.1.1	Results from Fieldwork	62
5.1.2	Results from Model	69
5.2	Temperature Measurements	77
5.2.1	Results from Model	77
5.3	Diffuser Air Velocity Mapping	85
5.3.1	Results from Fieldwork	85
5.3.2	Results from Model	86
5.4	Traversing of Duct	87
5.5	Smoke Visualization	88
5.6	Comparison of Prototype and Model Results	89
5.7	Discussion	93
6	Conclusion	95
6.1	Recommendations for Further Work	96
	Appendices	103

A	Location of Tracer Gas Sampling Points	105
B	Air Velocity Data	109
C	Charts of Diffuser Air Velocity Mapping	113
D	Excel Worksheet for Tracer Gas Calculations	119
E	Equipment	125
	E.1 Tracer Gas Measurement Mquipment and Mpparatus	125
	E.2 Air Velocity Measurements	126
	E.3 Air Flow Rate Measurements	127
	E.4 Smoke visualization	127
	E.5 Temperature Measurements	127
	E.6 Sampling Intervals of Equipment	127
F	Presence of People During a Work Day	129
G	Floor Plans and Drawings of the Model and Prototype	131
H	Calibration of Equipment	137
	H.1 Errors in Calibration Methodology	137
I	Data Sheet for Damper and Channel fan	143
J	Risk Assessment Report	147

List of Figures

- 1.1 Floor plan of second floor of building four. The diffusers in question are highlighted by blue circles. The zones suspected of having stagnant zones are highlighted in red. The red oval indicate a separating wall. Figure is based on illustration by Søgne (2015) 4
- 1.2 View of the east corner in the office landscape. Observe that the corner is almost completely closed in by bookshelves 4
- 2.1 The concept of displacement ventilation (Price Industries, 2011) 12
- 2.2 Air layers (Price Industries, 2011) 12
- 2.3 Thermal plume from point source and heated cylinder (Price Industries, 2011) 13
- 2.4 Local convection forces provide better air quality in the breathing zone (Ingebrigtsen, 2015) 13
- 2.5 Adjacent zone of diffusers (Price Industries, 2011) 15
- 2.6 Air distribution around obstructions (Price Industries, 2011) 16
- 2.7 Unstable discharge flow occurs frequently in large supply units (Skistad, 2002) 17
- 2.8 The age of the air at different points in the room (Ingebrigtsen, 2015) 20
- 2.9 Principle of step up and step down method of tracer gas injection and measurement. Figure based on illustration by Søgne (2015). 25
- 2.10 Calculations of the concentration curve for step up and step down measurements. Figure based on illustration by Søgne (2015). 26
- 2.11 Location of measuring points using the log-Tchebycheff method (TSI Air-flow Instruments, 2015) 36

3.1	Principle illustration of tracer gas measurements. Figure based on illustration by Søgne (2015)	38
3.2	Location of sampling points for tracer gas measurement on March 9, 2016 - first set	40
3.3	Tracer gas dosage equipment	41
3.4	Diffuser chosen for air velocity mapping (red circle). Figure based on illustration by Søgne (2015)	42
3.5	Air velocity measurement grid (red dots indicate anemometer location)	43
3.6	Measuring points in duct (red dots indicate anemometer location)	44
4.1	Cross section of the prototype building (Projectplace, 2015)	48
4.2	View of the office landscape in the prototype	48
4.3	Overview of 2nd floor with air supplies, exhaust and radiators highlighted (red line indicate the modeled area). Based on illustration by Søgne (2015)	49
4.4	Floor plan of model. The height of the model is 750mm.	50
4.5	Outside view of the model	50
4.6	Inside view of the model office landscape	51
4.7	Area of the model with electric Floor heating (the yellow area indicate the floor heating, and the red arrows indicate the air flow from the diffusers)	53
4.8	Location of sampling points for tracer gas measurement on June 2, 2016 and June 4, 2016	57
4.9	Air velocity measurement grid (red dots indicate anemometer locations)	58
4.10	Location of thermocouples	59
5.1	Tracer gas measurement on March 9, 2016 - first set	63
5.2	Tracer gas measurement on March 9, 2016 - second set	66
5.3	Tracer gas measurement on March 10, 2016	68
5.4	Tracer gas measurement on June 1, 2016 - first set	70
5.5	Tracer gas measurement on June 1, 2016 - second set	72
5.6	Tracer gas measurement on June 2, 2016	74
5.7	Tracer gas measurement on June 4, 2016	76
5.8	Temperature measurements at June 1, 2016	79

5.9	Temperature difference between floor and ceiling at four different locations in the model at June 1, 2016	80
5.10	Temperature measurements at June 2, 2016	82
5.11	Temperature difference between floor and ceiling at four different locations in the model at June 2, 2016	83
5.12	Temperature measurements at June 4, 2016	84
5.13	Temperature difference between floor and ceiling at four different locations in the model at June 4, 2016	85
5.14	Air velocities at a height of 100mm - prototype	86
5.15	Air velocities at a height of 25mm - model	87
5.16	Air velocities in duct with diameter of 400 mm	88
5.17	Smoke rises up through in the center stairwell	89
5.18	Comparison of air velocities at similar heights in prototype and model . . .	90
5.19	Comparison of tracer gas measurement in prototype and model	91
A.1	Location of sampling points for tracer gas measurement on March 9, 2016 - second set	105
A.2	Location of sampling points for tracer gas measurement on March 10, 2016	106
A.3	Location of sampling points for tracer gas measurement on June 1, 2016 - first set	106
A.4	Location of sampling points for tracer gas measurement on June 1, 2016- second set	107
C.1	Air velocities at height of 30mm- prototype	113
C.2	Air velocities at height of 100mm - prototype	114
C.3	Air velocities at height of 400mm- prototype	114
C.4	Air velocities at height of 700mm - prototype	115
C.5	Air velocities at height of 7.5mm - model	115
C.6	Air velocities at height of 25mm - model	116
C.7	Air velocities at height of 100mm - model	116
C.8	Air velocities at height of 175mm - model	117
E.1	Tracer gas sampler and monitor equipment	125

F.1	Presence of people on 2nd floor at different times on March 10. The numbers indicate the number of people in the specified area	130
H.1	Calibration certificate of the N_2O filter of the Brüel & Kjær Multi-gas monitor Type1302	138
H.2	Calibration certificate of the TSI VelociCalc 9555-P	139
H.3	Calibration certificate of the TSI VelociCalc 9555-P	140

List of Tables

- 2.1 Scale ratios 29
- 2.2 Anemometer probe insertion depth relative to duct diameter (TSI Airflow
Instruments, 2015) 36
- 3.1 Height of tracer gas sampling points 40
- 4.1 Summary of the internal heat gains in the prototype and the equivalent
representation in the model 53
- 4.2 Summary of the air flow sources in the prototype and the equivalent rep-
resentation in the model 54
- 4.3 Summary of values and dimensionless parameters for full scale prototype
and reduced-scale model 55
- 4.4 Sampling point heights 57
- 4.5 Thermocouple height 60
- 5.1 Summary of tracer gas measurement at March 9, 2016 - first set 64
- 5.2 Summary of tracer gas measurement at March 9, 2016 - second set 66
- 5.3 Summary of tracer gas measurement at March 10, 2016 68
- 5.4 Summary of tracer gas measurement at June 1, 2016 - first set 71
- 5.5 Summary of tracer gas measurement at June 1, 2016 - second set 72
- 5.6 Summary of tracer gas measurement at June 2, 2016 75
- 5.7 Summary of tracer gas measurement at June 4, 2016 77
- 5.8 Summary of measurement set on June 1, 2016 (°C) 80
- 5.9 Temperature differences in the model (°C) 81
- 5.10 Summary of measurement set on June 2, 2016 (°C) 82
- 5.11 Summary of measurement set on June 4, 2016 (°C) 84

5.12	Comparison of air change efficiencies prototype and model	92
5.13	Comparison of air change efficiencies prototype and model	93
B.1	Air velocity data prototype duct \varnothing 400 (m/s)	110
B.2	Air velocity data for the prototype (m/s)	111
B.3	Air velocity data for the model (m/s)	112
E.1	Tracer gas properties	126
H.1	Error from zero point (0°C)	141

Abbreviations

AHU Air Handling Unit. 39–41, 54, 60, 78, 97

CAV Constant Air Volume. 3, 17, 48

CO₂ Carbon dioxide. 23

CRE Contaminant Removal Effectiveness. 22, 23, 97

DCV Demand Controlled Ventilation. 17, 18

HVAC Heating, Ventilation and Air Conditioning. 7, 17

N₂O Nitrous Oxide. 23, 126

PK Powerhouse Kjørbo. 2, 15

SF₆ Sulphur hexafluorid. 23

VAV Variable Air Volume. 3, 17, 41, 48, 62

Nomenclature

$\langle \bar{\tau} \rangle$	Room mean age of air [s]
$\bar{\tau}_P$	Mean age of air at point P
$\bar{\tau}_r$	Actual average air change time [s]
\bar{v}_d	Average velocity in duct [m/s]
β	Thermal expansion coefficient of air [K^{-1}]
$\Delta\rho$	Density difference between colder and warmer air [kg/m^3]
Δp	Pressure difference between colder and warmer air [Pa]
ΔT	Temperature difference between colder and warmer air [K]
\dot{V}_{tg}	Tracer gas flow rate [l/min]
ϵ^a	Air change efficiency
ϵ_P^a	Local air change index at point P
λ	Slope for exponential trend of the tail area [-]
ν	Kinematic viscosity [m^2/s]
Φ	Heat flow [W, W/m]
Φ_c	Heat removal [W, W/m]
ρ	Air density [kg/m^3]

τ_n	Nominal time constant [s]
Θ_e	Exhaust air temperature [$^{\circ}\text{C}$]
Θ_s	Supply air temperature [$^{\circ}\text{C}$]
A_d	Area of duct [m]
c	Contaminant concentration in the room [mg/m^3 , <i>ppm</i> , <i>etc.</i>]
c_0	Concentration at zero time [mg/m^3 , <i>ppm</i> , <i>etc.</i>]
c_{∞}	Constant concentration at infinite time [mg/m^3 , <i>ppm</i> , <i>etc.</i>]
C_e	Contaminant concentration in the exhaust [mg/m^3 , <i>ppm</i> , <i>etc.</i>]
C_s	Contaminant concentration in the supply [mg/m^3 , <i>ppm</i> , <i>etc.</i>]
C_{mean}	Mean contaminant concentration in the room [mg/m^3 , <i>ppm</i> , <i>etc.</i>]
C_{oz}	Mean contaminant concentration in the occupied zone [mg/m^3 , <i>ppm</i> , <i>etc.</i>]
c_{tg}	Tracer gas concentration [ppm]
F_v	Viscous friction force [N]
F_{ρ}	Buoyancy force [N]
F_i	Inertia force [N]
F_p	Pressure force [N]
g	Acceleration of gravity [m/s^2]
L	Characteristic length [m]
L_M	Characteristic length in the model [m]
L_P	Characteristic length in the prototype [m]
N	Air change rate [h^{-1}]

p_i	Pressure drop over the damper [Pa]
Q	Air flow rate [m^3/h]
q	Air flow rate [l/s]
q_v	Air flow rate [l/s]
$q_{v,z}$	Vertical air flow rate [l/s]
t	Time [s]
t_A	Time elapsed from molecule A enter room until it reach point P1 [s]
t_B	Time elapsed from molecule B enter room until it reach point P1 [s]
t_C	Time elapsed from molecule C enter room until it reach point P1 [s]
u	Characteristic air velocity [m/s]
V	Volume [m^3]
v_d	Velocity in duct [m/s]
v_z	Vertical air velocity [l/s]
z	Height co-ordinate [m]

Chapter 1

Introduction

The research programme Zero Emission Buildings (ZEB) includes pilot buildings as a part of the research. Powerhouse Kjørbo is an older office building that has been renovated to become a zero emission building. See <http://www.powerhouse.no/prosjekter/kjorbo/> for more information.

Powerhouse Kjørbo has a displacement ventilation system. Measurements indicate that the ventilation effectiveness is lower than expected. There might be several causes, like stagnant zones or short-circuiting between air supply and extract.

To ensure the quality of future building and system design it is of interest to do closer studies of the ventilation strategy used at Kjørbo, and how it possibly can be improved. This is achieved through fieldwork at Kjørbo and measurements in a reduced-scale building model designed and constructed during the work of this thesis.

This chapter will present the background for the thesis, objectives to be considered, scope and limitations, approach, and method for the literature study. It will also provide a brief explanation of the Powerhouse concept, with the purpose of motivating the reader in understanding why the study of this building is being performed.

1.1 Powerhouse

The Powerhouse concept is a cooperation between property manager Entra Eiendom, contractor Skanska, architect office Snøhetta, environmental organization ZERO, aluminium

companies Hydro and Sapa, and Consulting firm Asplan Viak ([Powerhouse, 2015](#)). The aim of the project is to prove that it is possible to build energy positive buildings in the cold climate of Norway.

The definition of a Powerhouse varies from country to country. The Powerhouse Alliance in Norway has defined it in this way:

"A Powerhouse shall during its lifetime generate more energy than it uses for materials, production, operation, renovation and demolition."

This means that the building have to produce more energy than what is invested in production, construction, operation and disposal during the whole of its 60 year lifetime. The energy usage includes bound energy in materials and energy spent disposing of the whole building structure after it lifetime has ended. Powerhouse Kjørbo was the alliance's first project and is Norway's first energy positive building. Two additional Powerhouse projects are planned: a new building at Brattørkaia in Trondheim, Sør-Trøndelag and another rehabilitation project at Kjørbo, similar to the one in this study.

1.2 Background

Powerhouse Kjørbo (PK) is a project consisting of two office buildings that has been renovated to become zero emission buildings (ZEB). In addition they are energy positive, which mean they will during their lifespan of 60 years generate more more energy than they consume (bound energy in materials are also included). The energy generation comes from photovoltaic panels on the roof of the building and the nearby parking structure. The process of renovating an older house to become energy positive and achieve BREEAM Outstanding is the first of its kind in the world ([Powerhouse, 2015](#)). The buildings are located at Kjørbo in Sandvika, Bærum, Norway, and are two of the buildings in the larger Kjørbo-park business area originally constructed in the mid 80's.

The building utilizes modern energy and environmentally effective solutions such as an extremely air tight and insulated envelope, energy efficient displacement ventilation with effective heat exchangers, an high COP heat pump system with heat wells in the ground, energy saving windows with shading and smart use of thermal mass in the form of exposed

concrete in walls and ceilings (Asplan Viak, 2012).

1.2.1 Concerns on the Indoor Air Quality

In order to provide a good indoor environment the ventilation is provided from a demand controlled combined constant and variable air volume system with CO_2 and temperature sensors (Asplan Viak, 2012). The meeting rooms and the office landscape have variable air flow rates (VAV) while the the cell offices have a constant air flow rate (CAV). The only exhaust for the ventilation air is the centered staircase shaft (apart from small exhausts in the technical rooms and toilets). There have been raised concerns that the air quality may not be satisfactory in some areas of the office landscape (Danielsen, 2014; Søgner, 2015). Studies regarding heat distribution and level of CO_2 in these areas have been done, but it is necessary for more study into the detailed movement of the airflow in this part of the building to be able to determine the ventilation effectiveness and air quality.

To ensure good indoor air quality to all occupants it is important that the whole room is evenly ventilated, i.e that all parts of the room receives the desired amount of fresh air. Figure 1.1 show the ventilation air ducts and diffusers in the second floor of building four. Except for point exhaust vents in the toilets, the stairwell in the middle of the building is the only extract for the ventilation air. The principle of this ventilation strategy is that air supplied from the diffusers will distribute evenly along the whole floor area before rising and flowing along the ceiling towards the stairwell.

Observe that the two diffusers located in the east quadrant of the floor, highlighted by blue circles, are quite far away from the east area of the office landscape (highlighted in red). There are bookshelves placed in the area which may work as obstructions for the air flow. In the east corner, highlighted in red, the bookshelves are placed towards each other in a way that form a wall on the south and north facing sides of the corner (see Figure 1.2). Down by the floor, where the cold fresh supply air is supposed to flow, there is a gap only about one meter wide for the air to flow through into the corner. There are concerns that this give an inadequate cross section for the air supply into this area, and thus give a poor air change efficiency.



Figure 1.1: Floor plan of second floor of building four. The diffusers in question are highlighted by blue circles. The zones suspected of having stagnant zones are highlighted in red. The red oval indicate a separating wall. Figure is based on illustration by [Søgnen \(2015\)](#)



Figure 1.2: View of the east corner in the office landscape. Observe that the corner is almost completely closed in by bookshelves

The area in the south of the landscape, highlighted in red may trap air and heat which gives stagnant zones and cause the area to have poor air quality. Note that there is a separating wall, highlighted by a red oval, that prevent the air in flowing south/east around the middle structure and into the stairwell. Originally, there are not any CO_2 or temperature sensors in the highlighted areas, so no information can be collected from here. In general, the sensors for the building are located close to the diffusers and the radiators, which may not give the best control over the air quality or room temperature, as suggested by [Danielsen \(2014\)](#) and ([Søgnen, 2015](#)). These observations arise the question if the air quality in this area is satisfactory, and investigation into this is planned for this thesis.

1.3 Objectives

The final goal of the thesis is to contribute to improved background knowledge about how to design efficient ventilation solutions for ZEB office buildings.

The tasks to be considered are:

1. Conduct a literature study related to displacement ventilation and scaled model experiments.
2. Design and build a scaled laboratory model of Kjørbo.
3. Perform field measurements of the ventilation system at Kjørbo.
4. Validate the model against the prototype (Kjørbo).
5. Perform tests to improve the design of the ventilation system.

1.4 Scope and Limitations

This thesis present an analysis of the ventilation strategy of ZEB office buildings. A reduced-scale model was considered to be a good way of evaluating different ventilation strategies. The main focus of this thesis is divided into two parts. The first main focus was to analyze the ventilation strategy and acquire reference values in order to evaluate

the prototype and validate the model. The second main focus was constructing a solid, reliable and well functioning model. Designing, building and equipping a model of this size (6 m x 3 m x 0,75 m) and complexity takes a considerable amount of time. The remaining time for conducting experiments, validating and improving the model was therefore restricted. A decision was made to focus on the validation of the model, instead of performing experiments with changed model parameters and furniture placement before a satisfactory reliability was achieved. It was assumed that doing such experiments would provide give inaccurate result.

The chosen measure for analyzing the ventilation strategy and efficiency is the air change efficiency. Tracer gas experiments are considered to be a useful method for determining the efficiency in both the prototype and the model. The thesis give an evaluation of the ventilation efficiency, but due to the time restriction of the model experiments, the scope of the measurements and analysis are not as extensive and in-depth as originally planned.

It was observed that the tracer gas concentration in the supply air was not constant during the step up period. This is due to inaccuracy of the gas injection equipment and inaccuracy in the total air flow rate of the ventilation system. The unstable supply air gas concentration can be observed in all of the measurements in both the prototype and the model. This reduces the reliability of the step up measurements considerably, and therefore it was decided to omit the step up results completely, and place focus on the step down results, which were considered more accurate.

More detailed smoke visualization in the prototype could have been favorable, but due to the location of the prototype and the time span of the fieldwork this was not achievable. Smoke measurements in the model could not be conducted due to the time constraint and difficulties with the smoke equipment.

Temperature measurements in the model were not intended as a complete temperature mapping. The purpose was to provide an indication of the temperature gradient between the floor and the roof in selected parts of the room, and also as a measure of the temperature difference between the supply and exhaust air. The measurements are done for similarity analysis and model validation purposes.

Due to the time span of the field work, and lack of easy accessible equipment, the log-

Tchebycheff method for traversing an air duct could only be partially followed. One duct traversing were conducted instead of the recommended number of three.

The field measurements and model representation are limited to the second floor of building four. This floor is considered to have a room arrangement and person load that are representative for the rest of the building, and also compares to the the design conditions for the HVAC system. The outlay of the ventilation system in this floor is for the most part equal to the other floors, except the fourth, and it is considered suitable for doing measurements in.

The organization of this thesis is as follows:

- Chapter 2 present the background theory for this thesis. Theory on displacement ventilation, distribution of air and ventilation effectiveness are presented. Similarity theory and requirements associated with constructing a reduced-scale model are explained. Methodology for traversing an duct to determine the average air velocity and flow rate are presented.
- Chapter 3 present the methodology of the fieldwork conducted at Powerhouse Kjørbo. This includes description of the principles and methodology of tracer gas measurements, air velocity mapping of the adjacent zone of a wall diffuser, determination the air flow rate in a duct, smoke visualization and the registration of presence of people on a single floor of a building. The results of the fieldwork is presented in Chapter 5
- Chapter 4 present the prototype building and the reduced-scale building model, as well as methodology of the the experiments performed in the model. The chapter include building and system descriptions of the prototype and the model. Methodology and experimental set up is presented for tracer gas measurements, temperature measurements and air velocity mapping in the model. The results of the model experiments are presented in Chapter 5.
- Chapter 5 present the results from the fieldwork and the model experiments. Model results are compared to the prototype in order to determine if they share similarity. The results presented in this chapter are: tracer gas measurements in prototype and model; air velocity mapping in prototype and model; smoke visualization in proto-

type; duct traversing in prototype; presence of people in prototype and temperature measurements in model.

- Chapter 6 present the conclusions of the thesis, and give recommendations for further work.
- References and appendices follow Chapter 6.

1.5 Approach

This master's thesis is a continuation of the project work from the fall semester of 2015. The objective of the project work was to gain knowledge of displacement ventilation and reduced-scale models, and to determine if constructing such a model would be a good way to evaluate the ventilation system at Powerhouse Kjørbo. The project work concludes that making a model is indeed a suitable way to evaluate the system and find ways of improving the ventilation strategy.

Field measurements were performed in the prototype, Powerhouse Kjørbo, in order to establish a reference for the ventilation strategy, efficiency and effectiveness. Tracer gas measurements was conducted in the prototype to determine air change efficiency and local air change indexes. Air velocity mapping of a wall diffuser discharge was performed in order to compare with the model diffusers. An air duct was traversed in order to determine the average velocity and the air flow to the diffusers. Air flow patterns were visualized by using smoke in an attempt to gain greater understanding of how the air distributes in the office landscape. Presence of people were registered to establish a reference for personal heat gains in the building.

A reduced scale building a model was created to resemble the prototype. Validation of the model was conducted in order to make it behave like the prototype as much as possible. Tracer gas measurements was conducted in the model to determine air change efficiency, and compare it to the prototype. Air velocity mapping in the adjacent zone of a wall diffuser in the model was performed and compared with the prototype. Air flow patterns in the model were visualized by injecting smoke into the ventilation system, with the purpose of acquiring more understanding of how the air distributes in the office

landscape.

1.6 Literature Study

Several media has been taken advantage of to obtain information for the literature study. The most frequently used are hard cover and on-line books, article databases such as Scopus, Science Direct, AIVC Airbase, Springer and Pub.Med, and journals and guidebooks from organizations such a REHVA and ASHRAE. In the online literature search, approximation operators have been used to narrow the results and find the relevant information. Keywords and proximity operators for the search have been, among others: "reduced-scale building model", "displacement ventilation"; "similitude OR similarity theory"; "scale W/3 model AND 'displacement ventilation'".

Chapter 2

Background Theory

This chapter presents the background theory for this thesis. It explains the concept of displacement ventilation, and presents the basic theory. It explains different ways of measuring ventilation efficiency and effectiveness, and describes the principle and methodology of step up and step down method of tracer gas measurements to determine the air change efficiency and local air change indexes. Further, the chapter presents an overview of similarity theory and requirements, the modelling laws related to the performed experiments and the parameters used for evaluating a reduced-scale model against the full-scale prototype. The chapter also presents theory for traversing a duct to determine the average air velocity and air flow rate.

2.1 Displacement Ventilation

Displacement ventilation is the technique of letting warm contaminants rise to the ceiling and extract the contaminated air at ceiling level (Skistad, 2002; Ingebrigtsen, 2015). Fresh, cold air is supplied at floor level. The principle of air distribution at Powerhouse Kjørbo is displacement ventilation. As shown in Figure 2.1, air is supplied at a low level and distributes evenly along the floor, before rising towards the ceiling and into the exhausts. For this to happen it is crucial that the supply air from the diffuser has a lower temperature than the room air. If this is not the case the air will rise straight to the ceiling and get extracted without changing any of the air in the occupied zone. This unwanted situation is called short circuiting. Displacement ventilation is especially practical in rooms with

large ceiling heights where the contaminants are added to the room in combination with heat (Skistad, 2002). This makes it suitable for places with high person occupancy such as conference/meeting rooms, cinemas, libraries and restaurants.

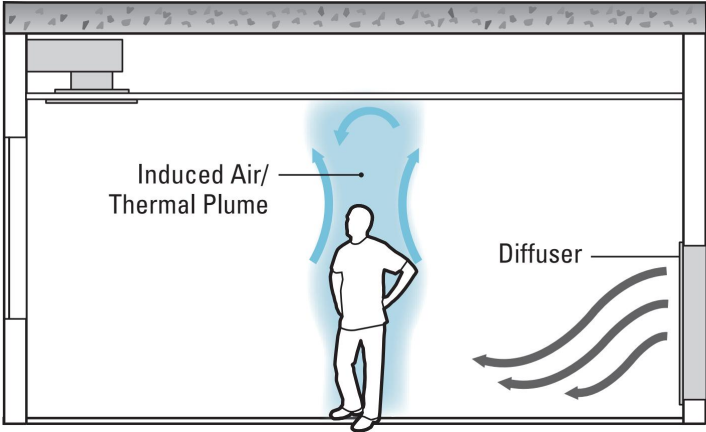


Figure 2.1: The concept of displacement ventilation (Price Industries, 2011)

2.1.1 Convection Flows

Natural convection flows are the driving force of displacement ventilation. A natural convection flow is the current of air that rises above a heat source like computers or persons, rises or descends along a warm or cold surface, due to buoyancy (Skistad, 2002). The convection flow that rises above a warm object is called a thermal plume. All plumes encountered in practical ventilation have developed fully turbulent flow (Skistad, 2002).



Figure 2.2: Air layers (Price Industries, 2011)

A vertical temperature gradient forms in a displacement ventilated zone (Price Industries, 2011). Air movement between layers of different temperatures, as shown in Figure 2.2

is caused by convection forces. The flows occur around heat sources or cold sinks and are caused by buoyancy differences. Figure 2.3 show how these plumes cause air to rise upwards, and drag with it the surrounding air, making the plume wider. A similar plume will form around a person. As illustrated in Figure 2.4, the plume effect will transport colder fresh air from the lower levels of the room along the surface the body up to the breathing zone, and is why displacement ventilation work so well in providing fresh air to occupants of a room. It is important that the room is supplied with enough air to feed the plumes, otherwise the plumes will drag contaminated air from the layers above, which disturb the stratification and cause unwanted mixing effects in the layers.

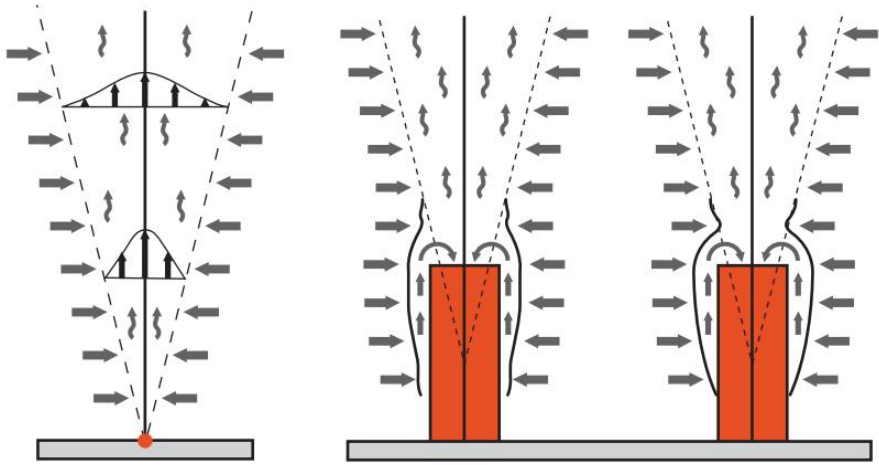


Figure 2.3: Thermal plume from point source and heated cylinder (Price Industries, 2011)



Figure 2.4: Local convection forces provide better air quality in the breathing zone (Ingebrigtsen, 2015)

The vertical air flow rate, $q_{v,z}$, of the plume at a height z above a point heat source is as follows (Skistad, 2002):

$$q_{v,z} = 5 \Phi^{1/3} z^{5/3} \quad (2.1)$$

where:

Φ = convective heat flux

z = height above heat source

The flow rate in the convection flow increases proportional to the height above the source, due to entrainment of the surrounding air. The amount of air in the plume is dependent of the temperature and the shape of the heat source, and the temperature of the surrounding air.

The centerline velocity, v_z , of the plume at a height z above a point heat source is as follows (Skistad, 2002):

$$v_z = 0,128 \Phi^{1/3} z^{-1/3} \quad (2.2)$$

2.1.2 The Adjacent Zone

The adjacent zone of a diffuser is an important factor in displacement ventilation. It is defined as the distance from the wall where the diffuser is placed to where the air flow is below a certain velocity (Ingebrigtsen, 2015). For comfort ventilation this velocity is documented as 0.2 m/s, specified with a temperature of the supply air of 3 K below the room temperature at 1.1 m above the floor (Skistad, 2002). The blue areas in Figure 2.5 illustrates the adjacent zone of different diffusers. The diffusers should be placed such that the adjacent zone is not obstructed by furniture or occupants, to avoid draught and unfavourable distribution of the supply air. The adjacent zone increase or decrease proportional to the air flow rate (Mysen and Schild, 2014).

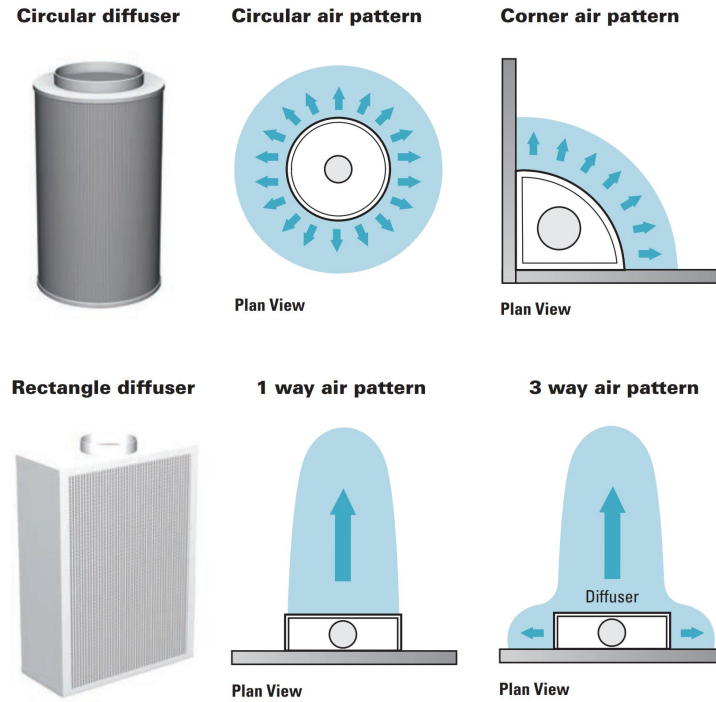


Figure 2.5: Adjacent zone of diffusers ([Price Industries, 2011](#))

2.1.3 Displacement Ventilation in Open Office Areas

Displacement ventilation is found to be suitable for larger open areas as long as certain parameters such as supply air temperature, ceiling height (preferably above 3m) and placement of diffusers and furniture are considered ([Skistad, 2002](#)). The ceiling height at PK is exactly three meters and the supply temperature are kept below the room temperature. The placement of furniture may not be optimal however.

2.1.4 Distribution of Air

Since displacement ventilation deal with very low air velocities it is crucial that the air distribute evenly over the whole floor area. In order to understand how the air will distribute in a room, it is important to consider what objects are in it, and where they are placed. As seen in Figure (2.6) the air from a diffuser flows around the obstructions, but take some time to distribute evenly behind them. Obstructions can cause the air flow to stagnate or change direction, and result in a disturbed air flow pattern. At PK, the office landscape is arranged as work stations with desks and chairs in groups of four, with bookshelves working as partitioning between the work stations. Problems can occur if

the partitioning is placed too close together or in a fashion that creates a barrier to the air flow.

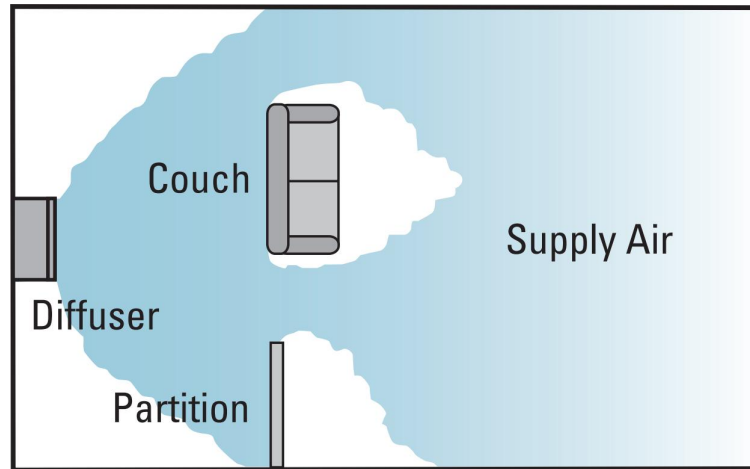


Figure 2.6: Air distribution around obstructions ([Price Industries, 2011](#))

Keeping thermal stratification is a very important factor in controlling and maintaining satisfactory air quality. Experiments conducted by [Matsumoto and Ohba \(2004\)](#) and [Bjørn and Nielsen \(2002\)](#) suggest that moving objects such as a walking person influence the air distribution in displacement ventilated rooms, and cause mixing of the stratified layers. Their results show that the moving objects mode and speed had significant effect on the temperature gradient and ventilation effectiveness. Since PK is an office building, it must be expected that people are moving around during the day.

2.1.5 Instability in the Diffuser Discharge

According to [Skistad \(2002\)](#), instability in the discharge flow can occur in a diffuser when the perforated sheet exceeds a certain size. The effect is especially prominent in low-velocity diffusers, and the cause of this issue is that the small jets from each of the holes in the sheet create suction between them. This can result in an unstable flow from the diffuser (see [Figure 2.7](#)).

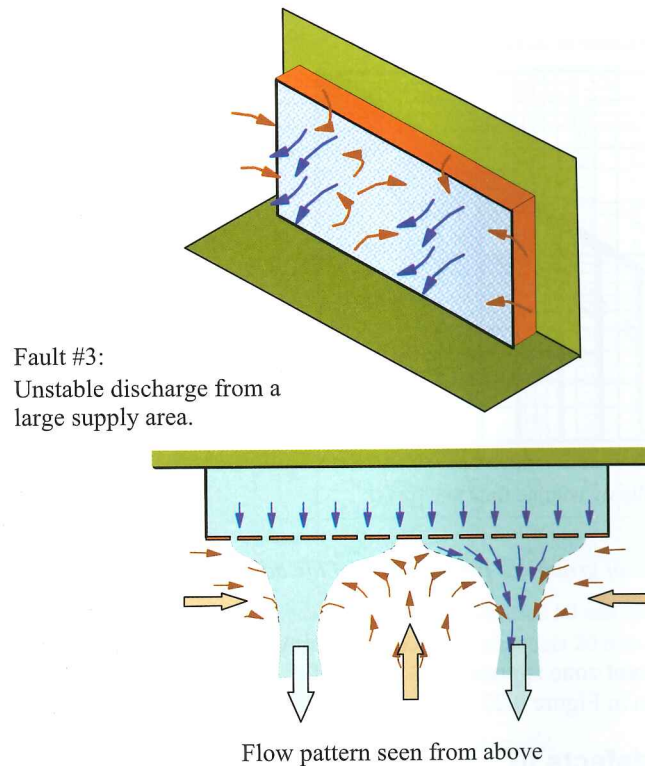


Figure 2.7: Unstable discharge flow occurs frequently in large supply units (Skistad, 2002)

2.1.6 Constant Air Volume (CAV) and Variable Air Volume (VAV) Method of Ventilation

There are mainly two ways to control the air flow to a zone or room, by use of the CAV or the VAV method. The first means, hence the name, that a constant air flow rate is supplied to the room, while the temperature of the air is varied according to the heat demand (Nilsson, 2003). The VAV method is the opposite, where the air temperature is kept constant while the air flow rate can be varied as needed. Variation of the air flow rate is achieved by controlled dampers in the air ducts and valves or by speed control of the fans (Nilsson, 2003).

2.1.7 Demand Controlled Ventilation

Another step into the control of air flow is the concept of demand controlled ventilation (DCV). With this incorporated into the HVAC system, the air flow rate or air temperature to each zone is constantly adjusted based on a number of parameters such as temperature, level of CO_2 , humidity or the presence of people (Nilsson, 2003). Sensors placed in the

zone give input to a control unit that in order adjust the air supply to correct the offset. Use of DCV can greatly reduce the energy demand for ventilation in a building (SINTEF Energiforskning, 2007).

2.1.8 Heating and Cooling with Displacement Ventilation

Since displacement ventilation relies on buoyancy forces and convection flows in order to function as intended, this technique of ventilation is not applicable for space heating. Note however that the outdoor air can be heated before it is supplied to the zone, but only to a temperature lower than the indoor air. If air with a higher temperature than the room air is supplied, this causes short-circuiting, and should be avoided at all costs as it result in a terrible ventilation efficiency (Ingebrigtsen, 2015).

Displacement ventilation is suitable for cooling by supplying air with a colder temperature than the room air. The temperature of the supply air can vary but usually lies 2 – 4 °C below the room temperature (Ingebrigtsen, 2015). The heat removed from a room can be calculated from the temperature difference between the supply and exhaust air, and the air volume flow rate (Skistad, 2002; Nilsson, 2003):

$$\Phi_c = q_v \cdot \rho \cdot c_p \cdot (\Theta_e - \Theta_s) \cdot 10^3 \quad (2.3)$$

where:

Φ_c = heat removal

q_v = air flow rate

Θ_e = exhaust air temperature

Θ_s = supply air temperature

2.2 Ventilation Effectiveness

The main purpose of ventilation is to supply fresh and clean air to the room and extract contaminants as efficiently as possible. To express the quality of the ventilation system

the terms air change efficiency and contaminant removal effectiveness are used (Skistad, 2002; Ingebrigtsen, 2015). The two terms are described as follows:

- *contaminant removal effectiveness*, ϵ^c , is the measure of how well contaminants are removed from the room (Brouns et al., 1991) and
- *air change efficiency*, ϵ^a , which is the measure of how quickly the air in the room is replaced (Sutcliffe, 1990).

In addition, we have local values:

- *local air quality index*, ϵ_P^c , is the measure the local concentration at a particular point (Mathisen et al., 2004).
- *local air change index*, ϵ_P^a , which characterises the conditions of the air exchange efficiency at a given point (Mathisen et al., 2004).

and more generally:

- *air change rate*, N , which represent the amount of air that is added to the room related to the room volume.

2.2.1 Air Change Rate

The air changes rate, N is a widely used number for expressing ventilation performance due to its simple calculation (Ingebrigtsen, 2015). It is defined by:

$$N = \frac{Q}{V} \tag{2.4}$$

where:

Q = Air flow rate

V = Room volume

The air changes rate does not contain any information on how good the ventilation in the occupied zone is. If there is a high degree of short-circuiting, the added air will not improve the room air quality. in such cases the air changes rate will give a wrong

impression of the ventilation quality. The air change rate should therefore not be used to describe the ventilation system effectiveness (Ingebrigtsen, 2015).

2.2.2 Age of Air

The ventilation effectiveness is measured using tracer gas. The concentration of tracer gas must therefore be related to the age of the air.

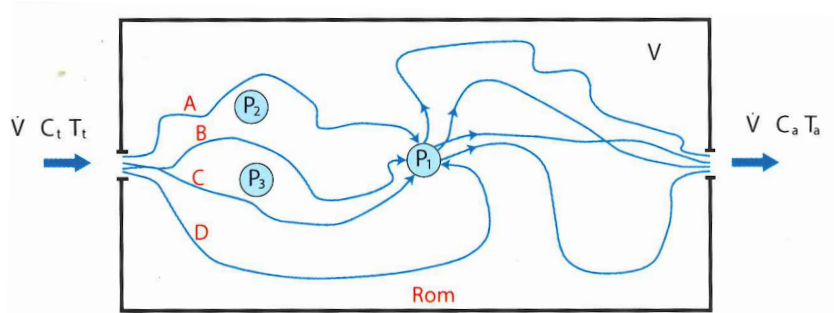


Figure 2.8: The age of the air at different points in the room (Ingebrigtsen, 2015)

The age of air at a particular location is the average time elapsed since molecules of air at that location entered the building (see Figure 2.8). The mean age of air, \bar{t}_{P1} in point $P1$ is expressed by (Ingebrigtsen, 2015):

$$\bar{t}_{P1} = \frac{t_A + t_B + t_C + \dots}{\text{number of molecules}} \quad (2.5)$$

where:

t_A = Time elapsed from molecule A enter room until it reach point $P1$

t_B = Time elapsed from molecule B enter room until it reach point $P1$

t_C = Time elapsed from molecule C enter room until it reach point $P1$

The average age of the exhaust air, also known as the nominal time constant, is given by:

$$\tau_n = \frac{V}{Q} \quad (2.6)$$

Observe that the nominal time constant is the inverse of the air change rate, seen in Equation 2.4.

2.2.3 Air Change Efficiency

Air change efficiency tells how quickly the air in the room is replaced with fresh air, in regards to what is theoretically possible (Ingebrigtsen, 2015). The factor is calculated by performing tracer gas measurements. Mathisen et al. (2004) define the air change efficiency as the the ratio between the shortest possible air change time for the air in the room (nominal time constant), and the actual average air change time. The factor is expressed by:

$$\epsilon^a = \frac{\tau_n}{\bar{\tau}_r} \cdot 100 = \frac{\tau_n}{2 \langle \bar{\tau} \rangle} \cdot 100 [\%] \quad (2.7)$$

where:

τ_n = nominal time constant

$\bar{\tau}_r$ = actual average air change time

$\langle \bar{\tau} \rangle$ = room mean age of air

The upper limit for the the efficiency is $\epsilon^a = 100$ %, which is obtained by ideal piston flow. Fully mixed flow has an efficiency of $\epsilon^a = 50$ %. Displacement flow lies in the region $\epsilon^a = 50 - 100$ %

The local air change index, ϵ_P^a , describe the condition at a particular point in the room. It is defined as the ratio between the nominal time constant and the local mean age of air, $\bar{\tau}_P$, at point P.

$$\epsilon_P^a = \frac{\tau_n}{\bar{\tau}_P} \cdot 100 \% \quad (2.8)$$

There is no upper limit for the local air change index. Fully mixed flow has an efficiency of $\epsilon_P^a = 100$ %. Displacement flow lies in the region $\epsilon^a = 100 - \infty$ %.

2.2.4 Contaminant Removal Effectiveness (CRE)

The contaminant removal effectiveness (CRE) is another way to determine the ventilation effectiveness. It gives an idea of how well the room is ventilated by the added air. The factor is calculated by performing tracer gas measurements. It is also normal to estimate an effectiveness based on renowned research on the field (Ingebrigtsen, 2015). For displacement this can be $\epsilon_c = 1,0 - 1,3$ for comfort systems and $\epsilon_c = 1,5 - 2,0$ for industrial systems. The contaminant removal effectiveness is as follows (Ingebrigtsen, 2015; Skistad, 2002):

$$\epsilon^c = \frac{C_e - C_s}{C_{mean} - C_s} \quad (2.9)$$

where:

C_e = contaminant concentration in the exhaust

C_s = contaminant concentration in the supply

C_{mean} = mean contaminant concentration in the room

or for the occupied zone:

$$\epsilon^c = \frac{C_e - C_s}{C_{oz} - C_s} \quad (2.10)$$

where:

C_{oz} = Mean contaminant concentration in the occupied zone

2.2.5 Conditions for Using the Measures

The air change efficiency and contaminant removal effectiveness can only be used to evaluate the ventilation effectiveness of a room which only exchange air with the outside, and has no inflow of air from other parts of the building (Mathisen et al., 2004).

When deciding on whether to use the air change efficiency or the CRE, the positions of the contaminants must be considered. If the locations are known and constant the

ventilation system should focus on removing the contaminants locally to avoid further spread (Mathisen et al., 2004). The measure to use should be CRE. If the case is anything else, the focus should be on exchanging the air as quickly as possible, and the air change efficiency should be the choice of measure.

2.2.6 Tracer Gas Measurements

Tracer gas experiments are used to find the nominal time constant and to simulate contaminant concentrations in order to calculate air change efficiency and contaminant removal effectiveness. The method is quite time consuming and requires expensive equipment such as gas analysers.

The gas used in the experiments must be a non-toxic gas and should normally not be found in indoor air. The density should be similar to the density of air in order to facilitate easy mixing (Mathisen et al., 2004). The gas should be possible to detect even in very small concentrations. Common gases to use in tracer gas measurements are sulphur hexafluorid (SF_6) and nitrous oxide (N_2O). Carbon dioxide (CO_2) can also be used if the background concentration is constant.

There are several principles of tracer gas experiments (Ingebrigtsen, 2015; Mathisen et al., 2004):

- **Constant concentration** - A constant, known amount of tracer gas are introduced to the room until a constant concentration of gas is achieved in the exhaust air. Can require large amounts of tracer gas.
- **Step-up** - Starting with no zero concentration at C_1 , a constant dosage of tracer gas are added, and we measure the time it takes for the gas to reach a certain concentration C_2 .
- **Step-down** - A constant dosage of tracer gas has been added to the room prior to the experiment. At time t_0 and concentration C_1 we stop the dosage, and measure the time it takes for gas to descend to zero or a certain concentration C_2 . The technique is not suitable for small air changes.
- **Pulse** - Pulses of tracer gas with known concentration and amount is added to the

room. The amount of gas at a point or in an exhaust are measured, with respect to time. This method is suitable for large room as it consumes less tracer gas. It requires precise equipment.

2.2.7 Step Change Response Methods

Step Down Response Method

Step-change response can be divided into the step-up and the step-down response. In step down tests, tracer gas is injected in the room and mixed with the room air until the concentration is uniform. The gas is usually injected through the ventilation system to ensure good mixing in the entire room. Mixing fans placed around the room is also a good way of creating an even concentration. Monitoring of the concentration start at the time the gas injection is turned off, and last until the concentrations in the room has decreased to zero or a certain concentration. Figure 2.9 illustrate the concentration development in the injection and the monitoring of tracer gas. The right half of Figure 2.10 illustrate a typical development of the concentration decay in a step down experiment. The curves for both step up and step down manifests themselves logarithmic. Therefore, when analyzing tracer gas measurements, it is important to study the curve plots in logarithmic scale as well as linear. The rise or decay of the gas concentration present themselves as straight lines in a logarithmic plot, which mean the development is stable. If this is not the case, irregularities in the the equipment or unwanted air flows may be the case (Mathisen et al., 2004).

Step Up Response Method

In step up tests, the monitoring of concentration start at the same time as the initial injection of gas. Gas is injected until the room reach a uniform concentration. Figure 2.9 illustrate the concentration development in the injection and the monitoring of tracer gas. The left half of Figure 2.10 illustrate the rise in concentration for a typical step up experiment.

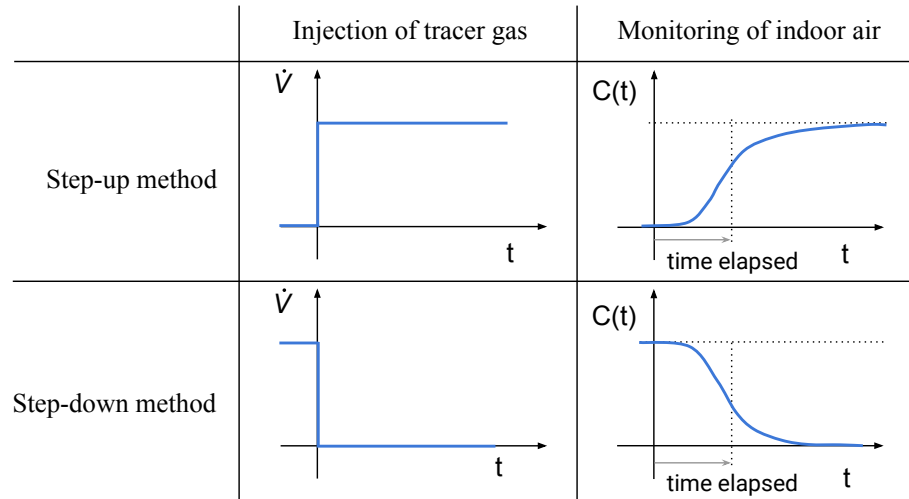


Figure 2.9: Principle of step up and step down method of tracer gas injection and measurement. Figure based on illustration by Søgne (2015).

2.2.8 Calculating Ventilation Effectiveness from Measured Concentrations

Mathisen et al. (2004) gives a procedure for calculation the air change efficiency and local air change index:

1. Make a logarithmic plot of the concentration as a function of time. This should be a straight line for the most part, but the curve usually becomes irregular at the lowest concentrations. This is due to signal noise from the gas monitor, and the this part should be deleted from the analysis. Denote the last usable concentration c_n
2. Calculate the slope of line from the straight part of the curve. This is used to extrapolate the measurements from n to infinity. This part of the curve is called the tail.
3. Calculate the efficiency according to the formulas given in the following section.

Air Change Efficiency and Local Air Change Index

Figure 2.10 show the characteristics of a concentration/time plot resulting from a consecutive step up and step down experiment. Note that for the step up, the area over the curve must be calculated, while for the step down the area under the curve is the part to

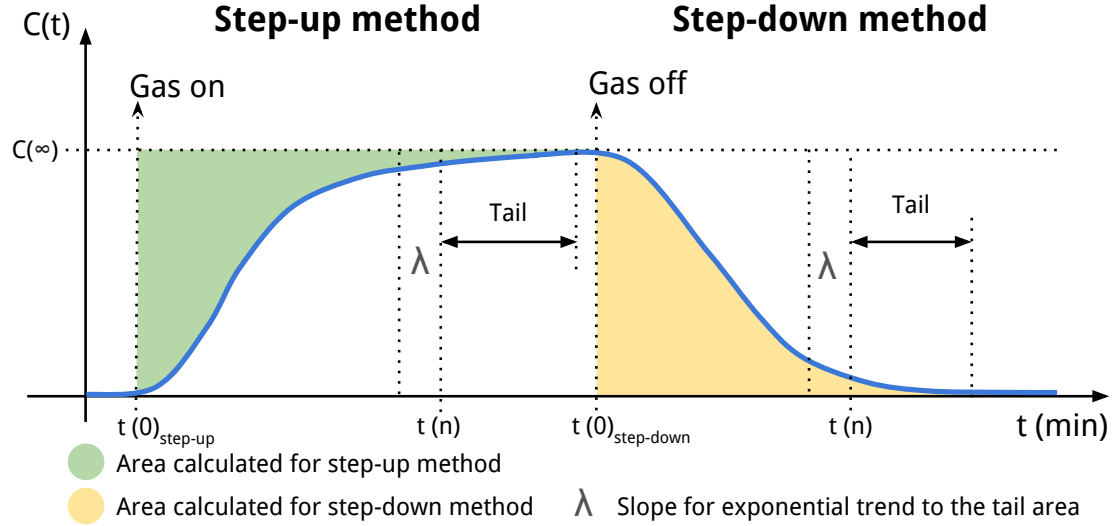


Figure 2.10: Calculations of the concentration curve for step up and step down measurements. Figure based on illustration by Søgne (2015).

focus on. Mathisen et al. (2004) present equations for calculating the air change efficiency and local air change index from a concentration curve plot. The mean age of the air in the room is calculated from the weighted area under the curve:

$$\langle \bar{\tau} \rangle = \frac{\sum_{i=1}^n \left[\frac{c_i + c_{i-1}}{2} \cdot (t_i - t_{i-1}) \cdot \frac{t_i + t_{i-1}}{2} \right] + \frac{c_n}{\lambda} \cdot \left[\frac{1}{\lambda} + t_n \right]}{\sum_{i=1}^n \left[\frac{c_i + c_{i-1}}{2} \cdot (t_i - t_{i-1}) \right] + \frac{c_n}{\lambda}} \quad (2.11)$$

where:

c = tracer gas concentration in the room

t = time

λ = slope for exponential trend of the tail area

The nominal time constant is calculated by:

$$\tau_n = \frac{\sum_{i=1}^n \left[\frac{c_i + c_{i-1}}{2} \cdot (t_i - t_{i-1}) \right] + \frac{c_n}{\lambda}}{c_0} \quad (2.12)$$

where:

c_0 = constant concentration at infinite time

The air change efficiency is calculated as follows:

$$\epsilon^a = \frac{\tau_n}{2 \langle \bar{\tau} \rangle} \cdot 100 [\%] \quad (2.13)$$

Finding the air change efficiency for the step up method differs in the way that the area above the curve must be calculated, instead of the area below. A concentration c' is introduced and defined as $c' = c(\infty) - c$. This concentration is substituted in Equation 2.11 and 2.12 the and the equations for the step up response method become the following:

$$\langle \bar{\tau} \rangle = \frac{\sum_{i=1}^n \left[\frac{c'_i + c'_{i-1}}{2} \cdot (t_i - t_{i-1}) \cdot \frac{t_i + t_{i-1}}{2} \right] + \frac{c'_n}{\lambda} \cdot \left[\frac{1}{\lambda} + t_n \right]}{\sum_{i=1}^n \left[\frac{c'_i + c'_{i-1}}{2} \cdot (t_i - t_{i-1}) \right] + \frac{c'_n}{\lambda}} \quad (2.14)$$

$$\tau_n = \frac{\sum_{i=1}^n \left[\frac{c'_i + c'_{i-1}}{2} \cdot (t_i - t_{i-1}) \right] + \frac{c'_n}{\lambda}}{c_\infty} \quad (2.15)$$

where:

$c_\infty =$ constant concentration at infinite time

Due to the logarithmic characteristic of the concentration change, it can take quite some time for the room concentration to reach the supply concentration, especially in large rooms. Therefore, the concentration at infinite time, $c(\infty)$, is set equal to the measured concentration, c_n , at the end of the measuring period. This might not be the true value of the concentration at infinite time, but it should be close if the mixing in the room is adequate and the experiment is allowed to run for a long enough time.

The local mean age is calculated as follows:

$$\bar{\tau}_P = \frac{\sum_{i=1}^n \left[\frac{c_i + c_{i-1}}{2} \cdot (t_i - t_{i-1}) \right] + \frac{c_n}{\lambda}}{c_0} \quad (2.16)$$

where c refers to the concentration at point P in the room.

τ_n is calculated in the same way as for air change efficiency, from the concentration in the exhaust.

2.3 Similarity

A physical model of a real world prototype can be used as a tool for finding optimal technical solutions. This chapter covers theory of similarity and the process of making accurate models of real-world prototypes. The term "prototype" refer to the original real-world object, while the term "model" refer to the scaled physical representation of the object.

2.3.1 The concept of similarity

A model is said to have similitude, or similarity, with the real-world prototype if the two share these three types of similarities ([Zohuri, 2015](#)):

- **Geometric similarity** - The model has the same shape as the prototype, either scaled or not. If the specified physical quantities are geometrical dimensions, the similarity is called geometric similarity.
- **Kinematic similarity** - The fluid flow of both the model and prototype must undergo similar time rates of change motions (the fluid streamlines must be similar). If the quantities are related to motions, the similarity is called kinematic similarity.
- **Dynamic similarity** - Ratios of all forces acting on corresponding fluid particles and boundary surfaces in the two systems are constant. If the quantities refer to forces, then the similarity is called dynamic similarity.

As we change the model to a different size than the prototype, scale effects start to occur. Generally speaking, the scale effects in a fluid flow increase with the scale ratio or scale factor λ , which is as follows ([Heller, 2011](#); [Zohuri, 2015](#)):

$$\frac{L_P}{L_M} = \lambda \quad (2.17)$$

where:

L_P = characteristic length in the real-world prototype

L_M = corresponding length in the model

The inverse of the scale ratio given in Equation (2.17), $1 : \lambda$, is defined as the scale. The scaling between prototype and model for length, area and volume can be seen in Table (2.1) The non-linear behaviour of the scale implies that scale effects will vary depending on what dimension the phenomenas are studied in.

Property	L_M	A_M	V_M
Scale	$1 : \lambda$	$1 : \lambda^2$	$1 : \lambda^3$

Table 2.1: Scale ratios

In practical applications, with for example a building, this means that if the lengths of all walls in the model one half of the prototype, the area of the model becomes one fourth and the volume becomes one eighth.

2.3.2 Similarity Requirements

In order to study and experiment on a model it is important that the model behaves in the same way as the prototype. For this to happen geometric, kinematic and dynamic similarity must be achieved (Zohuri, 2015; Walker et al., 2011; Kalleberg, 1977). There are specific conditions that are required in order for the result from the reduced scale to be transferable to the prototype, such as velocity distribution, air flow patterns, and temperature distributions.

Geometric Similarity

The model and the prototype must share geometric similarity. This is a simple matter of changing the linear dimension parameters by the scale ratio, i.e. sizing the model down or up. The linear dimensions must be reduced by the scaling factor in all three dimensions, x, y, z. This applies to all surfaces, openings and objects within in the model, including walls, floors, windows, furniture and equipment. Lack of geometric similarity can impair the air flow patterns and temperature distribution in the model during experiments, and give inaccurate results.

Kinematic/Dynamic Similarity

To achieve kinematic similarity the ratios the the velocities and acceleration of the fluids must be equal (Walker, 2006). When this is obtained, the streamlines of the flow patterns are similar. Since motion is described by distance and time, it implies similarity in dimensions (geometric similarity) and similarity of time intervals. (Zohuri, 2015). Kinematic similarity is closely related to dynamic similarity which requires that ratios of the forces that create motion in the fluid to be equal in the model and the prototype.

To achieve dynamic similarity, the relation between the forces that are acting on the fluid to cause movement must be the same in the model as in the prototype (Zohuri, 2015; Kalleberg, 1977). An element of air are affected by an inertia force F_i that causes its movement. This force is the sum of all the forces acting on the element, which are: buoyancy force F_ρ , pressure force F_p and viscous friction force F_ν . We get the following equation in equilibrium (Kalleberg, 1977):

$$\vec{F}_i = \vec{F}_\rho + \vec{F}_p + \vec{F}_\nu \quad (2.18)$$

where:

$$F_i = \text{mass} \cdot \text{acceleration} = \rho L^3 \cdot a = \rho u^2 L^2$$

$$F_\rho = \text{density diff.} \cdot \text{gravity} \cdot \text{volume} = \Delta\rho \cdot g L^3 = \beta\Delta T \rho g L^3$$

$$F_p = \text{Pressure diff.} \cdot \text{area} = \Delta p \cdot L^2$$

$$F_\nu = \text{shear stress} \cdot \text{area} = \rho \frac{\nu u}{L} \cdot L^2 = \rho \nu u L$$

The kinematic and dynamic equations for the model are derived by making all the forces in Equation 2.18 dimensionless. The equations that are obtained are a ratio between the inertia force and each of the the other forces (Skistad, 2002; Kalleberg, 1977):

Archimedes' number:

$$Ar = \frac{F_\rho}{F_i} = \frac{\text{bouyancy force}}{\text{inertia force}} = \frac{\Delta\rho g L}{\rho u^2} = \frac{\beta\Delta T g L}{u^2} \quad (2.19)$$

Euler's number:

$$Eu = \frac{F_p}{F_i} = \frac{\text{pressure force}}{\text{inertia force}} = \frac{\Delta p}{\rho u^2} \quad (2.20)$$

Reynold's number:

$$Re = \frac{F_i}{F_v} = \frac{\text{inertia force}}{\text{viscous friction force}} = \frac{uL}{\nu} \quad (2.21)$$

where:

ρ = air density

u = characteristic air velocity

$\Delta\rho$ = density difference between colder and warmer air

g = acceleration of gravity

L = characteristic length

β = thermal expansion coefficient of air

ΔT = temperature difference between colder and warmer air

Δp = pressure difference between colder and warmer air

ν = kinematic viscosity

To obtain complete kinematic and dynamic similarity these three numbers must be equal for the model and the prototype (Zohuri, 2015; Awbi and Nemri, 1990; Kalleberg, 1977)

Archimedes number is a ratio of the relative magnitude of buoyancy forces to inertia forces acting on a fluid. The number is used to evaluate the motion of fluid due to density differences. The parameters in the Archimedes number that are variable is the characteristic air velocity u and the temperature difference ΔT . The thermal expansion coefficient β ($= 1/(\Theta + 273^\circ\text{C})$) varies so little within the temperature range of the current cases that its changes are negligible. The acceleration of gravity is constant. Similarity requirements state that the Archimedes numbers must be equal ($Ar_M = Ar_P$). Equation 2.19 can then be rearranged:

$$\begin{aligned}
Ar_M &= Ar_P \\
\frac{\beta \Delta T_M g L_M}{u_M^2} &= \frac{\beta \Delta T_P g L_P}{u_P^2} \\
\frac{\Delta T_M L_M}{u_M^2} &= \frac{\Delta T_P L_P}{u_P^2} \\
u_M &= u_P \sqrt{\frac{\Delta T_M L_M}{\Delta T_P L_P}} = u_P \sqrt{\frac{\Delta T_M}{\Delta T_P} \frac{1}{\lambda}} \tag{2.22}
\end{aligned}$$

$$\Delta T_M = \Delta T_P \frac{u_M^2}{u_P^2} \frac{L_P}{L_M} = \Delta T_P \frac{u_M^2}{u_P^2} \lambda \tag{2.23}$$

Equation 2.22 and 2.23 represent the relationship between model and prototype for the velocity and temperature difference respectively.

The variable parameters in Euler's number are the characteristic air velocity u and the pressure difference Δp . With the equality condition Equation (2.20) can be rearranged:

$$\begin{aligned}
Eu_M &= Eu_P \\
u_M &= u_P \sqrt{\frac{\Delta p_M}{\Delta p_P}} \tag{2.24}
\end{aligned}$$

$$\Delta p_M = \Delta p_P \frac{u_M^2}{u_P^2} \tag{2.25}$$

Equation 2.24 and 2.25 represent the relationship between the model and the prototype for the velocity and pressure difference respectively.

When a characteristic length are chosen there are no variable parameters in Reynold's number, and the characteristic air velocity u_M for the model with the equality condition is found by rearranging equation 2.21:

$$\begin{aligned}
Re_M &= Re_P \\
u_M L_M &= u_P L_P \\
u_M &= \frac{L_P}{L_M} u_P = \lambda u_P
\end{aligned} \tag{2.26}$$

Equation 2.26 represent the velocity relationship between the model and the prototype. Note that Equation 2.22 and 2.26 will not give the same velocity for $\frac{\Delta T_M}{\Delta T_P} = 1$. This means there will not be correspondence between the Reynolds and the Archimedes number equalities if the temperature difference for the model and the prototype is equal. The condition for the two number equalities to result in the same velocity is found by combining Equation 2.22 and 2.26:

$$\begin{aligned}
u_{M,Re} &= u_{M,Ar} \\
u_P \lambda &= u_P \sqrt{\frac{\Delta T_M}{\Delta T_P} \frac{1}{\lambda}} \\
\Delta T_M &= \lambda^3 \Delta T_P
\end{aligned} \tag{2.27}$$

This means that the temperature difference is not dependent of the velocity, if Reynolds and Archimedes numbers are matched simultaneously.

If Euler's number also is matched with the Reynold's number get an expression for the pressure difference is as follows, by combining Equation 2.24 and 2.26:

$$\begin{aligned}
u_{M,Re} &= u_{M,Eu} \\
u_P \lambda &= u_P \sqrt{\frac{\Delta p_M}{\Delta p_P}} \\
\Delta p_M &= \lambda^2 \Delta p_P
\end{aligned} \tag{2.28}$$

Within the capabilities of the laboratory set up, it is impossible to match all of the

similarity requirements for scaling factors of some magnitude. Reducing the scale by ten would result in a velocity increase by a factor of 10, a pressure difference increase by a factor of 100, and a temperature difference increase by a factor of 1000. Certain compromises and simplifications must therefore be made. [Etheridge and Sandberg \(1996\)](#) states that in such cases the most important is to ensure that the flow stays inside the fully turbulent region, i.e. $Re > 2300$. If the flow stays in the turbulent region the Archimedes number becomes the most important to match between the prototype and the model.

2.4 Traversing an Air Duct to Determine Average Air Velocity and Air Flow Rate

The average air velocity and air flow rate can be calculated by traversing an air duct with an anemometer. In order to get reliable air velocity measurements, it is recommended to measure minimum 7.5 duct diameters downstream and minimum 3 duct diameters upstream from any turns of flow obstructions ([TSI Airflow Instruments, 2015](#)). It is possible to traverse outside of these recommendations, but the accuracy of the measurements will be impaired.

It is also possible to measure the air velocity at a single point in the center of the duct and multiplying the reading by 0.9 to correct for the higher velocity at the center of the duct ([TSI Airflow Instruments, 2015](#)). If conditions are very good it is possible to obtain an accuracy of ± 5 or ± 10 percent. This method is considered unreliable, however, and should only be used where small duct size or other conditions do not permit a full traverse.

2.4.1 Traversing a Round Duct

When traversing a round duct, [TSI Airflow Instruments \(2015\)](#) and [Omega \(2015\)](#) suggest using the log-Tchebycheff method. The duct is split up into concentric circles, each having the same area. An equal number of measurements is read from each circular area, in that way obtaining the best average. Usually, three concentric circles (6 measuring points) per diameter are used for ducts of 250 cm diameter and smaller. Four or five concentric

circles (8 or 10 measuring points per diameter) are used for ducts larger than 250 cm diameter.

It is preferred to perform three traverses, 60 degree angle from each other, and average the readings taken from each measuring.

The average velocity is as follows:

$$\bar{v}_d = \frac{1}{n} \sum_{i=1}^n v_{d,i} \quad (2.29)$$

where:

v_d = velocity at point in duct

The flow rate, Q , is found by multiplying the average velocity for the whole duct by the duct area ([TSI Airflow Instruments, 2015](#); [Omega, 2015](#)):

$$Q = \bar{v}_d \cdot A_d \quad (2.30)$$

where:

\bar{v}_d = average velocity in duct

A_d = area of duct

Figure [2.11](#) show suggested locations the the measuring points. The insertion depth is found by multiplying the numbers in [Table 2.2](#) by the diameter of the duct.

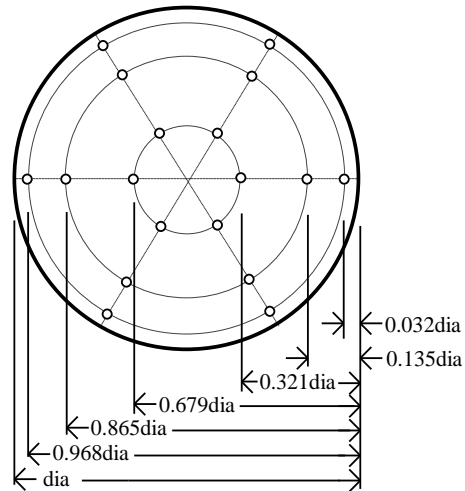


Figure 2.11: Location of measuring points using the log-Tchebycheff method (TSI Airflow Instruments, 2015)

Table 2.2: Anemometer probe insertion depth relative to duct diameter (TSI Airflow Instruments, 2015)

# of measuring points per diameter	Position Relative to Inner Wall									
6	0,032	0,135	0,321	0,679	0,865	0,968				
8	0,021	0,117	0,184	0,345	0,655	0,816	0,883	0,979		
10	0,019	0,077	0,153	0,217	0,361	0,639	0,783	0,847	0,923	0,981

Chapter 3

Fieldwork Methodology

Field work was performed at Powerhouse Kjørbo in order to analyze the ventilation strategy and to establish it as a prototype reference to validate the model against. The field work consisted of several experiments related to the ventilation strategy of the building. An evaluation of the ventilation effectiveness was performed. The air change efficiency and local air change indexes were determined by tracer gas measurements. The adjacent zone of a wall diffuser was examined by velocity mapping. The air flow rate in a duct leading to one of the wall diffusers was measured. Smoke experiments were conducted to visualize air flow patterns. Presence of people in the building was recorded. This chapter presents the methodology of the fieldwork conducted at Powerhouse Kjørbo. This includes descriptions of the principles and methods for tracer gas measurements, air velocity mapping, traversing of an air duct, smoke visualization and registration of the presence of people on a single floor of the building. The results of the fieldwork are presented in Chapter 5. Descriptions of the equipment used in the experiments are given in Appendix E. For limitations in the fieldwork please see Section 1.4

3.1 Tracer Gas Measurements

Tracer gas measurements were performed in the Prototype building Powerhouse Kjørbo. A total of six measurements were performed, three following the step up method and three following the step down method. A step up and step down measurement are conducted consecutively, and called a measurement set. The measurements were performed on March

9 and March 10, between 8 am and 8 pm. People were present in the building during the measurements.

3.1.1 Principle

There are several principles to perform tracer gas measurements by, as described in section 2.2.6. The methods chosen for this work was a step up sequence to a constant concentration followed by a step down sequence. The reason for following both methods of measurement was to acquire more data and gain greater accuracy in the results. Also, because the step up principle of measurement results in the air having a known concentration, C_1 , a step down measurement can be performed directly after a step up, which is time effective. Figure 3.1 show an illustration of the principle of tracer gas measurements.

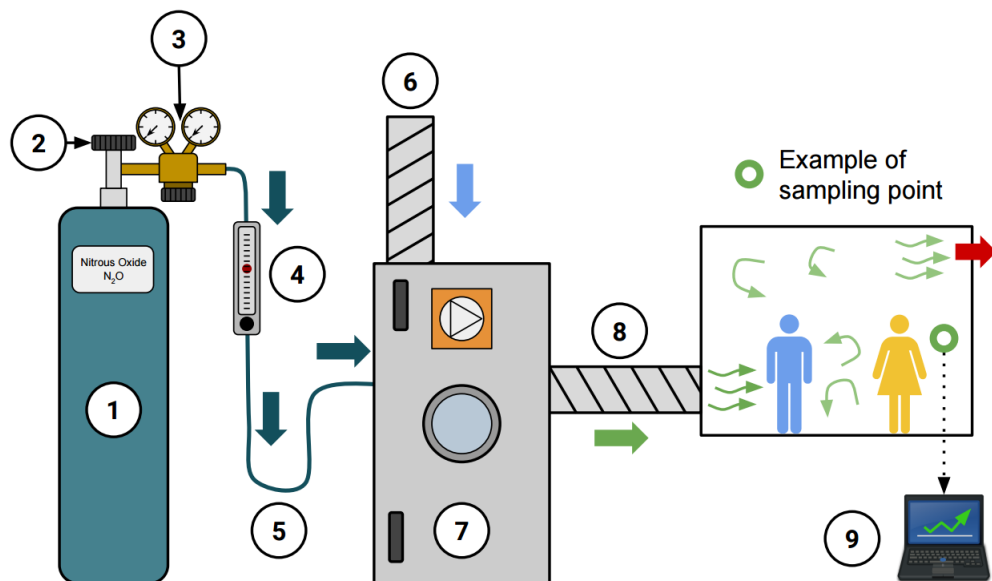


Figure 3.1: Principle illustration of tracer gas measurements. Figure based on illustration by Søgne (2015)

A description of Figure 3.1 is as follows:

1. Gas bottle of industrial nitrous oxide.
2. Main closing valve.
3. Manometers and pressure regulator controlling the output pressure.

4. Rotameter ensuring a steady and constant flow of gas.
5. Plastic tubes supplying gas to the AHU.
6. Outdoor air inlet duct.
7. Air handling unit. The tracer gas is thoroughly mixed with air by the fans in the AHU.
8. Air duct supplying a mixture of air and tracer gas to the room.
9. Computer analyzing the concentration of tracer gas from several sampling points around the room. The concentration is monitored over time.

3.1.2 Method

The tracer gas sampler and monitor equipment was placed in a technical room centrally in second floor of the building. See Appendix E for description of the equipment. Plastic tubes were stretched from the machine along the ceiling to each of the sampling points. Figure 3.2 show the location of the sampling points for the first set of measurements. Please see Appendix A for locations of the sampling points for the second and third set of measurements. Table 3.1 show the heights of the different sampling points. Sampling point 4, named "2nd floor", are located in the central staircase, just above ceiling level of the second floor. The point represent the air extract from floor one and two. The sampling point 5, named "3rd floor" are located in the central staircase, just above ceiling level of the third floor. The point represent the total air extract from floor one, two and three. The fourth floor is sealed off from the other three, and have its own air supply and exhaust. Sampling point 6, "Supply", is located inside of the air duct leading to the south east wall diffuser. The tracer gas, that is injected in the AHU at the fourth floor, is considered to be fully mixed with the air at this point, and give a good representation of the concentration of tracer gas in the supply air.

The tracer gas used for the measurements were Nitrous Oxide (N_2O). Properties for the gas is given in Appendix E. The pressurized gas cylinder along with the injection equipment was placed in the technical ventilation room at the fourth floor. Figure 3.3 show pictures of the setup of the tracer gas injection equipment. A pressure valve and



Figure 3.2: Location of sampling points for tracer gas measurement on March 9, 2016 - first set

Table 3.1: Height of tracer gas sampling points

Measurement # and date								
1			2			3		
09.03.16			09.03.16			10.03.16		
Location	Description	Sampling height (mm)	Location	Description	Sampling height (mm)	Location	Description	Sampling height (mm)
1	East	1500	2a	South	100	1a	East	100
2	South	1500	2b	South	1100	1b	East	1100
3	North	1500	2c	South	2900	1c	East	2000
4	2nd floor	-	3	North	1500	1d	East	2900
5	3rd floor	-	5	3rd floor	-	5	3rd floor	-
6	Supply	-	6	Supply	-	6	Supply	-

rotameter is fitted to the gas cylinder in order control the flow of gas. The rotameter measures the flow rate in litres per minute. A plastic tube was stretched through a small drilled hole into the AHU. The flow rate, V_{tg} , needed to maintain a constant desired concentration, c_{tg} , of tracer gas in the supply air is as follows:

$$\dot{V}_{tg} = c_{tg} \cdot 10^{-6} \cdot q_v \cdot 1000 \frac{L}{m^3} \cdot \frac{1}{60} \frac{h}{min} \quad (3.1)$$

where:

c_{tg} = desired tracer gas concentration

q_v = ventilation air flow rate



(a) The cylinder is tightly secured to prevent it from falling over. (b) A rotameter is used to ensure right gas dosage (c) The gas is injected directly into the air handling unit to ensure proper mixing

Figure 3.3: Tracer gas dosage equipment

The flow rate in the building was set at a constant value of approximately $10\,000\text{ m}^3/h$ for the entire measurement period in order to maintain a constant tracer gas concentration in the supply air. The desired concentration of tracer gas was set to 25 ppm, which gave a flow rate of gas into the AHU of 4.2 l/min. The VAV dampers in the wall diffusers were set to be fully opened in order to avoid fluctuating air flow rates during the experiments.

At time t_0 the flow valve for the gas was opened and the monitoring equipment started logging. The gas concentration was monitored continuously. After approximately two hours the concentration in the room was constant. At this time, the gas dosage was shut of, while the gas monitor was kept running. After another two hours the concentration in the room was close enough to zero to discontinue the monitoring and measuring. The data log files were exported from the gas monitor to a computer for later analysis.

3.2 Air Velocity Mapping in the Adjacent Zone of a Wall Diffuser

The air velocities in the adjacent zone in front of a wall diffuser were measured. The velocity mapping was conducted by following the method suggested by [Chang and Gonzalez](#)

(1989). It consists of measuring the air velocities with anemometers at different heights and distances from the diffuser. A grid was laid down on the floor (see Figure 3.5) in order to measure at right distances in an effective way and keep track of the measurement process. The diffuser chosen for the mapping is highlighted by a red circle in Figure 3.4.

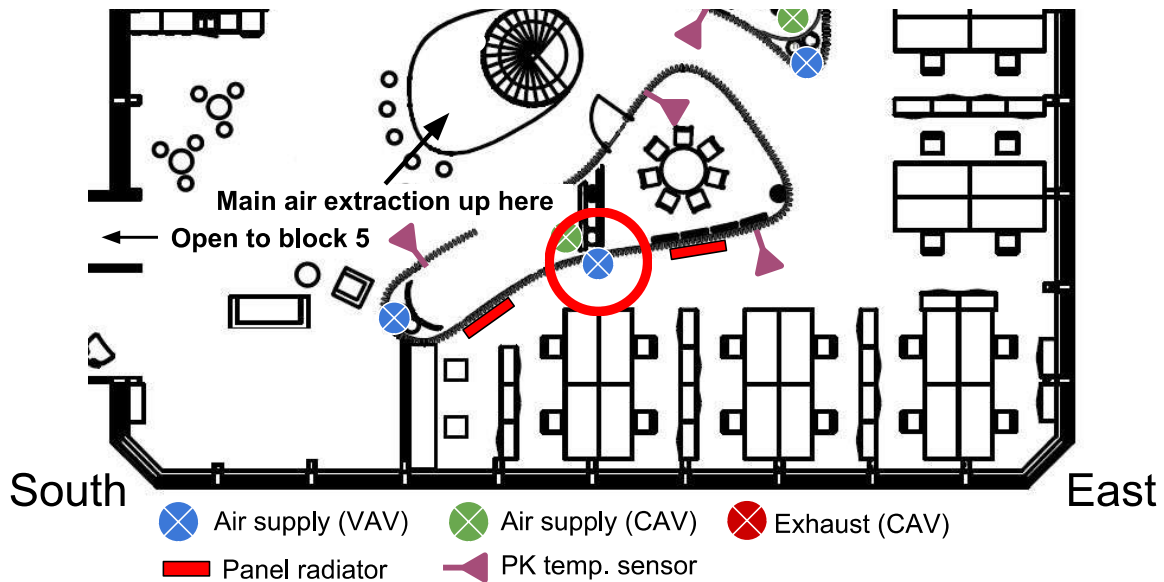


Figure 3.4: Diffuser chosen for air velocity mapping (red circle). Figure based on illustration by Søgne (2015)

3.2.1 Method

The grid consisted of 4 layers with 24 points spread 400mm apart length-wise and 250mm depth-wise. The layers were placed in heights of 30, 100, 400 and 700mm above the floor. The reason for choosing 30mm and not 0mm is that the maximum air velocity from a displacement diffuser discharge is found to be not exactly at floor level, but slightly above (Skistad, 2002). A typical height of the air discharge from a wall diffuser is 200mm (Skistad, 2002), so 100mm was considered to be an appropriate height for measurement inside of the flow.

The anemometer was placed on a stand, enabling the probe to be fixed at a certain height at the chosen location. The red dots in Figure 3.5 indicate the placements of the anemometer stand. The row designation A, B, C, D, E and F and the column number 1, 2, 3, 4, help to identify each stand placement. The stand was first placed at the A1

location and the anemometer probe was set at a height of 30mm. The air flow rate in the diffuser was held at a steady state and the air velocity was measured. The stand was then moved to B1 location, still with a height of 30mm. Another measurement was taken, and the stand was moved to C1. After taking measurements in all locations A1 to F4, the anemometer probe height was set to 100mm, and the stand was placed in A1 to begin a new round of measurements. At each stand location, the anemometer data was collected for five seconds and averaged. In total, ninety-six data points of air velocity in were collected.

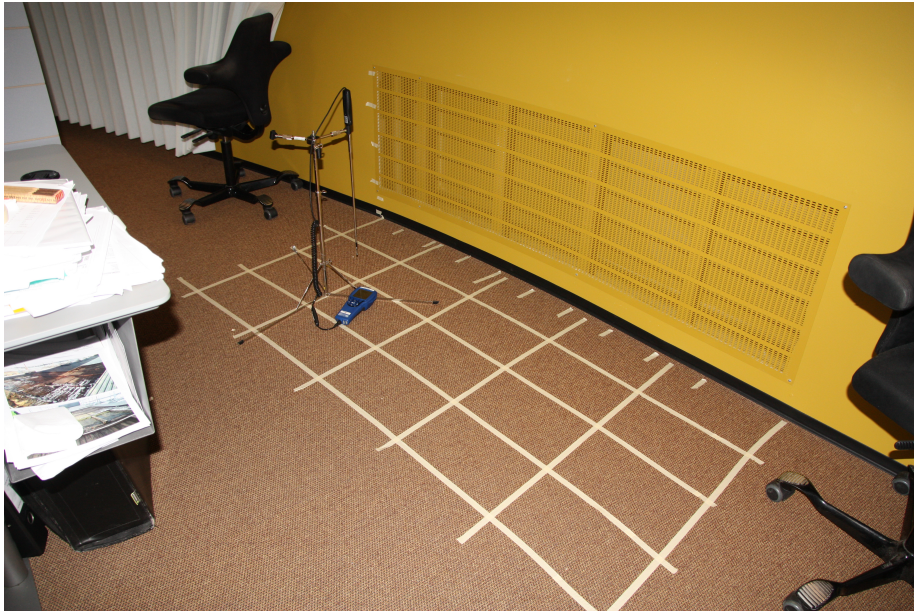
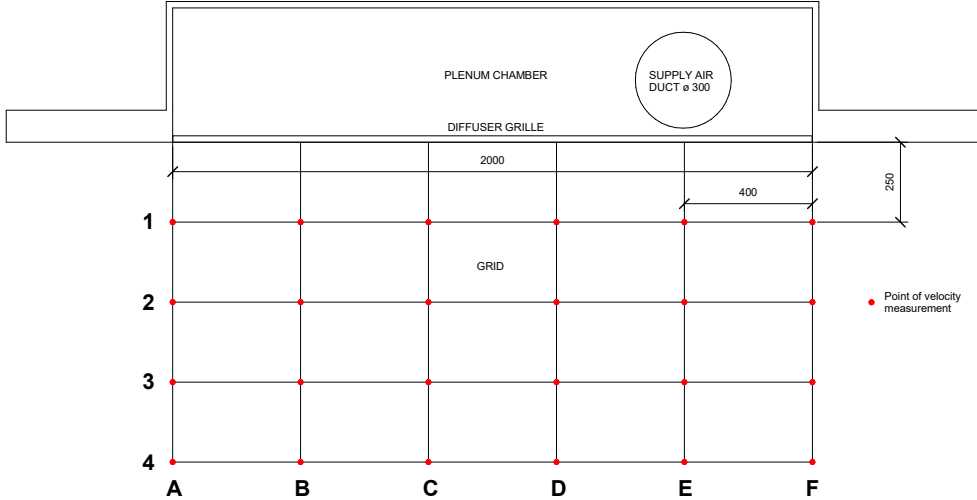


Figure 3.5: Air velocity measurement grid (red dots indicate anemometer location)

3.3 Air Flow Rate in Duct

The airflow rate in the duct leading to one of the wall diffusers was determined by measuring velocities at different points inside of the duct. The log-Tchebycheff method suggested by [TSI Airflow Instruments \(2015\)](#); [Omega \(2015\)](#), and described in Section 2.4 was partially followed. One traverse was performed instead of three, see Section 1.4 for explanation.

3.3.1 Method

Figure 3.6 shows the locations of the anemometer measuring points. The points are placed along a straight line from the duct wall on one side to the other. The anemometer probe was first placed at location 1. The air flow rate in the duct was held at a steady state and the velocity was measured. The probe was then moved to location 2, and another measurement was taken. At each location, the anemometer velocity data was averaged over a time interval of ten seconds. In total, six data points were gathered. The air flow rate was calculated according to Equation 2.30 given in Section 2.4.

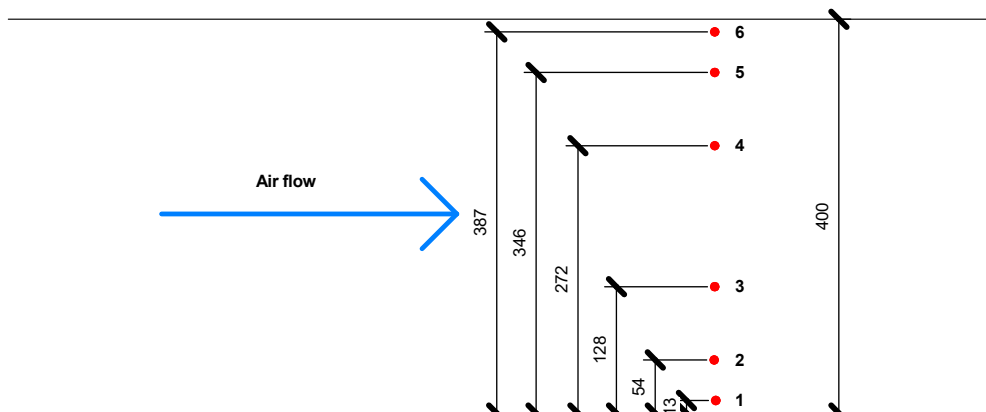


Figure 3.6: Measuring points in duct (red dots indicate anemometer location)

3.4 Smoke Visualization

Directions of the air flows in front of a wall diffuser, in some parts of the office landscape and in the stairwell were visualized by use of smoke. By visualizing the flow patterns, it was possible to gain a better understanding of how the air distributes in the room. The smoke tubes were used to puff small portions of smoke in different locations such as in front of the diffuser, in the stairwell, around the work stations and in openings between the book shelves.

3.5 Presence of People

The presence of people in the building was recorded by simply walking around and counting persons every hour between 09:00 and 13:00, except from the lunch break at 12:00. See Appendix F for details.

3.6 Discussion

The constant concentration of 25ppm in the start of the the step down tracer gas method was measured in the stairwell. If short circuiting between one of the diffusers and the stairwell occurred during the test period, it could result in a faulty measurement of the total concentration of tracer gas in the floor. This can have effects on the results, as it is essential obtain uniform concentration in the whole room, according to [Mathisen et al. \(2004\)](#)

The grid laid down on the floor for air velocity mapping is not perfect. The wall is slightly curved, so the distances from from the grid lines to the wall varies slightly. This, combined with probe misplacement due to human error, can affect the uncertainty in the measurements.

An issue to consider is that the velocity mapping contains no information on the direction of the air flow. Smoke experiments suggested that the air did not discharge evenly and radially from the diffuser. This is assumed to affect the reliability of the velocity mapping.

The sampling/averaging time for the VelociCalc is only five seconds, which mean that bursts of excessive turbulence and air movement can disturb the collected data. This could have been avoided by either setting a longer sampling time, or doing several consecutive mappings. The time constraint of the field work prevented this from being performed.

Instead of using a stack of velocity sensors to cover all heights simultaneously, as suggested by [Chang and Gonzalez \(1989\)](#), a single anemometer mounted on a stand was used. This method is more time consuming, but will most likely produce the same results. During the time it takes to perform the air velocity mapping, the flow from the diffuser may change. The air flow rate may not be constant, or the way the flow behaves may change. [Skistad \(2002\)](#) suggest that the small jets jets from a large perforated plate can create suction between them, and make the discharge flow unstable. This can disturb the flow from the diffuser and make the discharge velocities inconsistent. The cross area of the diffuser in the prototype are above one square meter, and can possibly suffer from these effects.

Chapter 4

Reduced-scale Building Model

A scaled model was built in the laboratory to represent a section of the second floor in building four at Powerhouse Kjørbo. Tracer gas measurements were performed in order to determine the air change efficiency and local air change indexes. Smoke experiments were conducted to visualize air flows. Air velocity mapping in front of a wall diffuser were performed. This chapter will present descriptions of the prototype and the model. It will also present methodology for the experiments performed in the model: tracer gas and temperature measurements, and velocity mapping. The objective of the measurements is to evaluate the model against the prototype. Results and analysis is given in Chapter 5. Description of the equipment is given in Appendix E. Risk assessment report for the tracer gas experiments is given in Appendix J.

4.1 Prototype Building

The prototype building is a four story office building located by the shore at Kjørboparken, Sandvika, Bærum, Akershus, Norway. Figure 4.1 show the building's cross section. Floor two was chosen as the part of the building to be modeled. Figure 4.3 show the floor plan. The floor houses cell offices and an office landscape with room for around 40 employees. According to registration of presence, the normal person load is usually lower than this, at around 20 (see Appendix F for details). The office landscape has work stations separated by bookshelves. Each workstation consist of four desk spaces equipped with computers. Figure 4.2 show views from the office landscape.

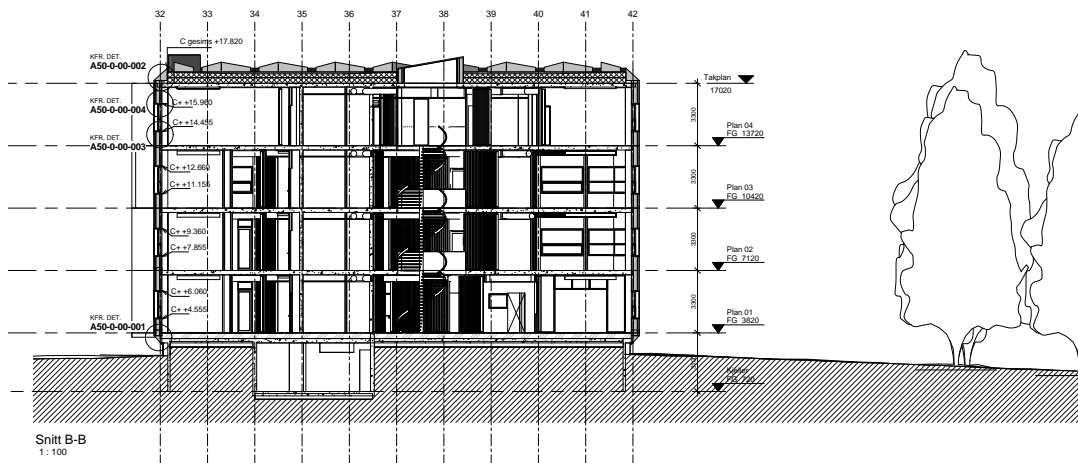


Figure 4.1: Cross section of the prototype building (Projectplace, 2015)



(a) The east corner is almost completely surrounded by bookshelves



(b) View of the office landscape with workstations and bookshelves

Figure 4.2: View of the office landscape in the prototype

4.1.1 Design and Layout of the Ventilation System in the Prototype Building

The building has a displacement ventilation system. Each office cell is fitted with a CAV diffuser but no extract. The air instead overflow into the hallway. The stairwell located in the center is the only air exhaust (except for small extracts in the toilets). The office landscape is ventilated by centrally placed VAV wall diffusers (see Figure 4.3) with a capacity of $800 \text{ m}^3/h$. The office cell diffusers are designed to feed air at a maximum rate of $100 \text{ m}^3/h$ into each office. The air flow rate in these diffusers have been adjusted to $60 \text{ m}^3/h$ (Rådstoga, 2015). For more details of the ventilation system, please see Appendix G. Radiators are also centrally placed, along the walls of the inner structures. It

is unusual to place the radiators away from windows and other surfaces that can experience cold drafts, but the building are designed after very high standards of insulation and air tightness of the envelope and windows, so unacceptable drafts should not occur (Powerhouse, 2015).

4.2 Reduced-scale Building Model Description

A scaled building model was designed and built at one fourth scale ($\lambda = 4$). Figure 4.3 show the portion of the second floor in the prototype building that was modelled. Air was used as working fluid for the experiments. Figure 4.4 show a simple floor plan of the model, with the diffusers and exhausts indicated. For detailed floor plans and 3D sketch of the diffuser placement in the model, please see Appendix G. Figure 4.5 and 4.6 show pictures of the model inside and outside.

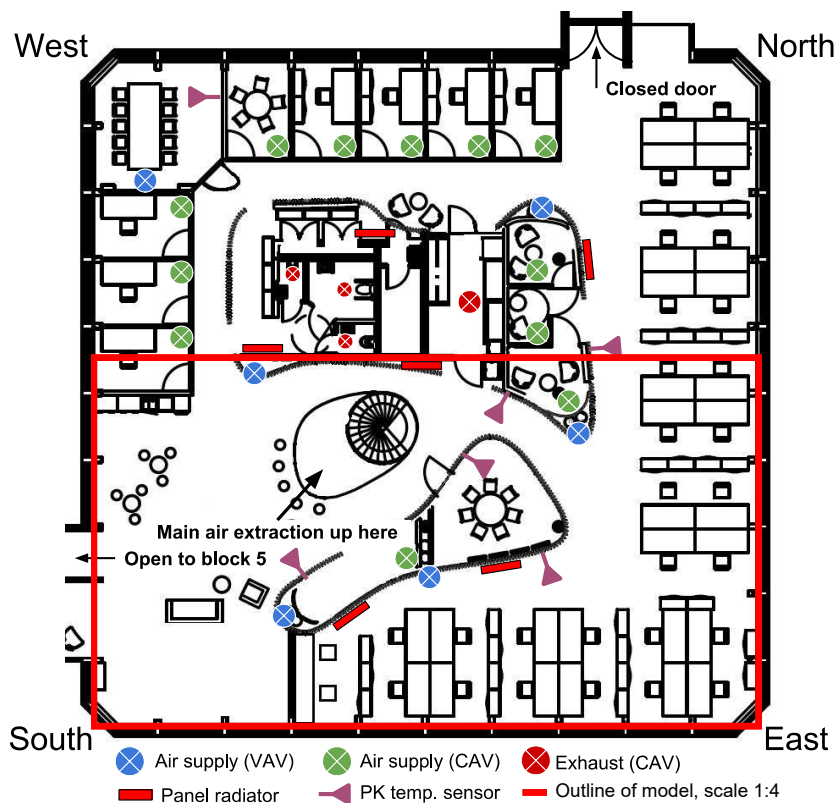


Figure 4.3: Overview of 2nd floor with air supplies, exhaust and radiators highlighted (red line indicate the modeled area). Based on illustration by Søgne (2015)

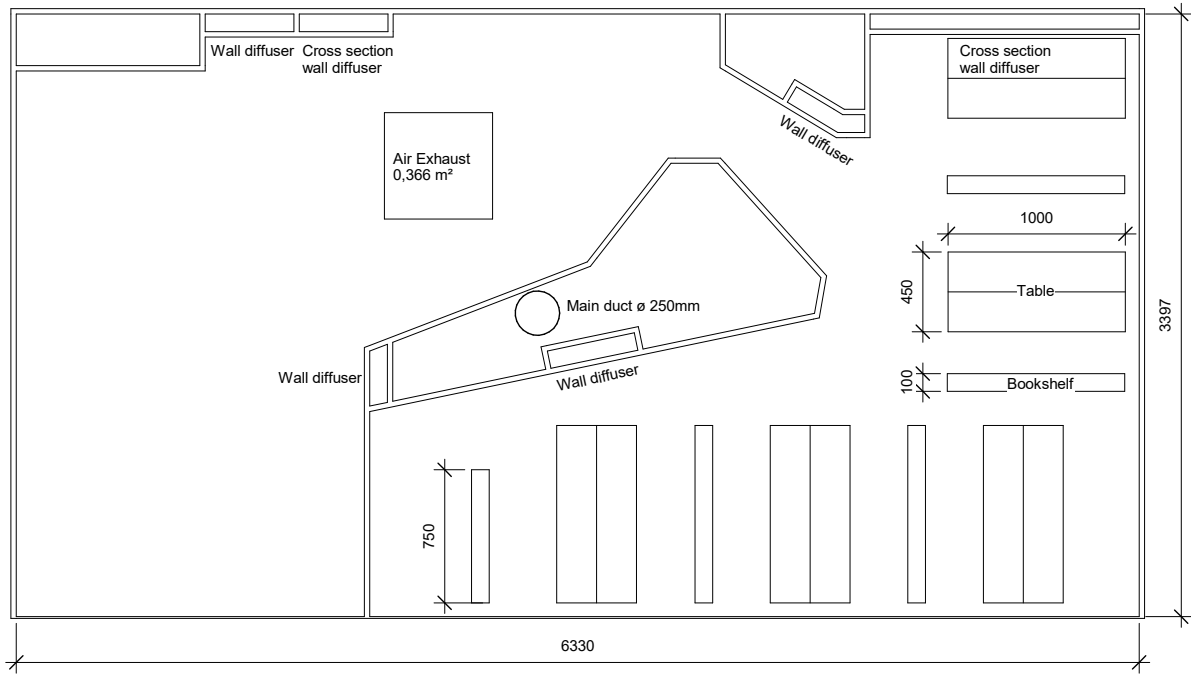


Figure 4.4: Floor plan of model. The height of the model is 750mm.



Figure 4.5: Outside view of the model

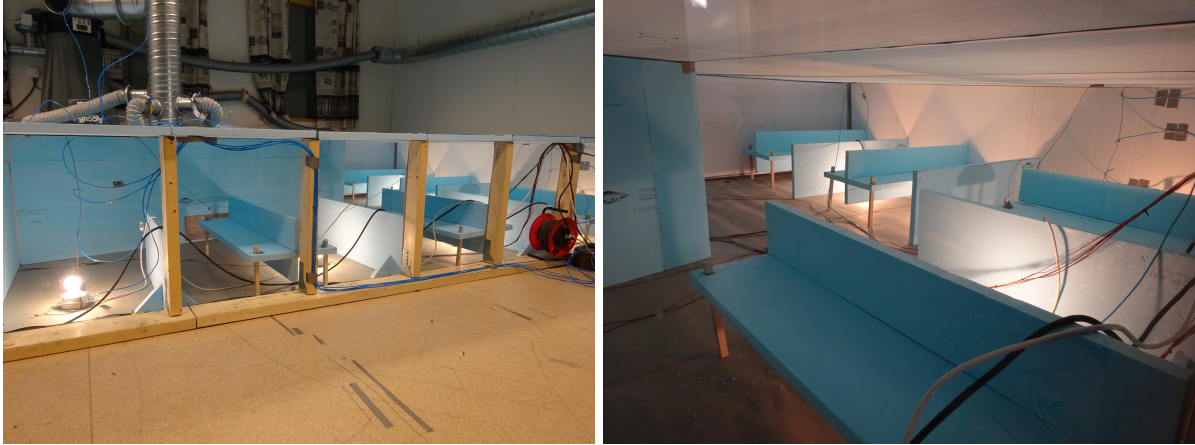


Figure 4.6: Inside view of the model office landscape

4.2.1 Building Materials

The walls in the model was made out of extruded polystyrene foam (Styrofoam), due to its insulation capabilities, light weight and ease to work with. The wall facing down (southeast) in Figure 4.4 was made from wood and Polymethyl methacrylate (Plexiglas) to allow for smoke visualisation and general overview inside the model. The roof was made from Styrofoam supported by lightweight metal girders. The furniture consisted of five reduced-scale tables and five bookshelves (see pictures in Figure 4.4 and 4.6), also made by polystyrene.

4.2.2 Internal Heat Gains

According to the presence map in Appendix F, an average of approximately ten people were present over the course of of the tracer-gas measurement day, in the area that was chosen for modeling . An approximate value of the dry heat emitted from a person performing office work is given by SINTEF Energiforskning (2007) to be 100 W. The corresponding heat gain in the model becomes 25 W per person. The simulation of persons in the model was reduced from ten to eight since it represented the average presence during one of the step down tests. The technical equipment in the prototype consisted of a laptop and an LCD screen and was set to 40 W per work-space/person. This corresponded to 10 W per workplace in the model. The total scaled heat gain from persons and equipment combined became 35W per workplace. The person and the equipment heat gains was

decided to be joined together and represented by a single heat source. To achieve the same air flow rate from a single heat source the heat output must be larger than the sum of the two original separated heat sources. By reviewing Equation 2.1 from section 2.1.1, a formula for the heat source output power was derived:

$$\begin{aligned}
 q_{v,z,1} &= q_{v,z,2} + q_{v,z,3} \\
 5 \Phi_1^{1/3} z^{5/3} &= 5 \Phi_2^{1/3} z^{5/3} + 5 \Phi_3^{1/3} z^{5/3} \\
 \Phi_1^{1/3} &= \Phi_2^{1/3} + \Phi_3^{1/3} \\
 \Phi_1 &= 3 \Phi_2^{2/3} \Phi_3^{1/3} + 3 \Phi_2^{1/3} \Phi_3^{2/3} + \Phi_2 + \Phi_3
 \end{aligned} \tag{4.1}$$

If the heat output from the two sources are equal, we get the special case were $\Phi_1 = 8\Phi_2 = 8\Phi_3$. This means that the heat output of a source must be eight times as high as two other equal sources to produce the same total vertical air flow rate, assuming that the heat sources are placed adequate distance apart from each other to avoid disturbance and ensure individuality of the plumes.

The heat output in the model from one person and with corresponding technical equipment is found by applying Equation 4.1 to be 131 W per workplace. A 100 W light bulb was decided to represent this heat source (see Section 4.7 for reasoning).

The heat gain from lighting was set to 8 W/m^2 , according to approximate values given in SINTEF Energiforskning (2007). The heat gain was simulated in the model as heated floor mats, evenly spread across the office landscape. Figure 4.7 illustrate the location of the heated area of the floor. Heat gain by solar radiation is also simulated by the floor heating.

Table 4.1 show a summary of the internal heat gains in the prototype and how they are represented in the model. Note that the scaled model heat gain must be sized to four times the prototype heat gain, in order to provide the buoyancy flux ratio the same as the the geometric ratio. The floor heating was controlled to the desired 412 W by adjusting the voltage output to the floor heat to around 100V using a auto-transformer (Variac).

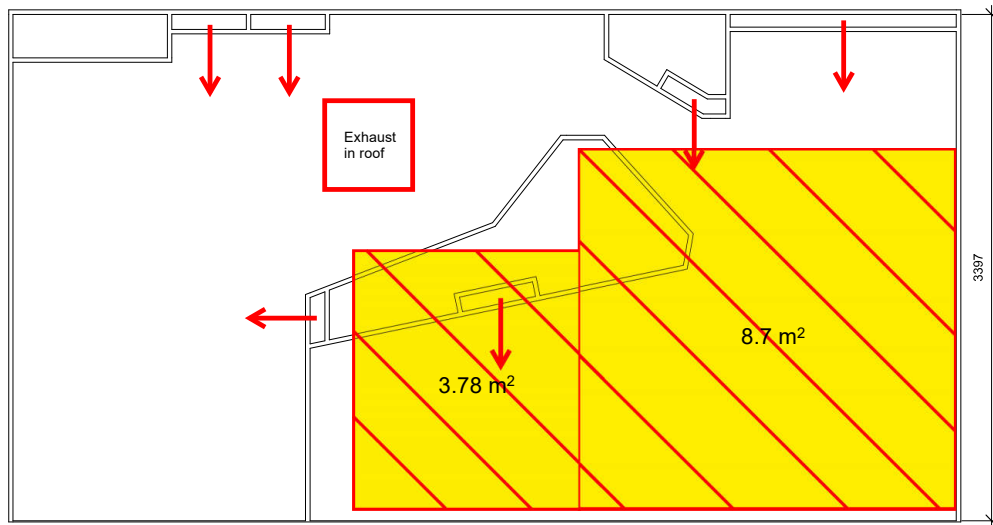


Figure 4.7: Area of the model with electric Floor heating (the yellow area indicate the floor heating, and the red arrows indicate the air flow from the diffusers)

Table 4.1: Summary of the internal heat gains in the prototype and the equivalent representation in the model

Prototype				
Heat gains	#	Area (m²)	Output (W)	Heat gain (W/m²)
Radiators	6	304	-	2
Solar radiation	-	-	-	2
Persons	8	304	100	2,63
Equipment	10	304	40	1,32
Light	-	304	-	8
Total				15,95

Model				
Heat gain	#	Area (m²)	Output (W)	Heat gain (W/m²)
Light bulbs	8	19	100	42,11
Floor heating	-	12,48	412	21,68
Total				63,79

4.2.3 Design of the Ventilation System in the Model

The ventilation system in the model was made to resemble the prototype. Figure 4.5 show pictures of the model with its ventilation system. It consist of four wall diffusers with geometric resemblance to the prototype. The dimensions of the diffusers are 137.3 x 500 mm. A vertical air duct is extended from the original ventilation ducts in the roof of the laboratory down to the model. Flexible ducts with Iris-dampers are connected to the

main duct, and run to each of the four wall diffuser. A duct with a damper are fitted to the main duct above the model in order to bleed of an adequate amount of air in order to avoid excessive heating of the air in the ducts on the way from the AHU to the model. The dampers were used to control the scaled air flow to each diffuser according according to the value found in Section 3.3 by adjusting the opening inside the dampers.

The main air exhaust for the whole model consist of an opening in the ceiling. This is the only exhaust and it extracts air from the entire model, in the same way that the staircase extracts the air in the prototype.

The air from the part of the prototype excluded from the model (see Figure 4.3) flows into the modeled part and towards the exhaust. To simulate this flow of air in the model, two diffusers with dimensions 750 x 500 mm and 750 x 1500 mm were placed along the top wall (northeast) of the model (see Figure 4.4) They were designed to blow air evenly over the whole cross area from floor to roof and between the walls. A channel fan with two outlets and Iris-dampers were mounted on the back wall and connected through flexible ducts to the two larger cross section diffusers.

Table 4.2: Summary of the air flow sources in the prototype and the equivalent representation in the model

Prototype (m3/h)			
Source of air	# of diffusers	Air flow rate	Total air flow rate
VAV wall diffuser	5	696,68	3483,40
CAV diffuser office	8	60,00	480,00
CAV diffuser large meeting room	1	450,00	450,00
CAV diffuser small meeting room	4	60,00	240,00
Total	18		4653,40

Model (m3/h)			
Source of air	# of diffusers	Air flow rate	Total air flow rate
CAV wall diffuser	4	10,89	43,54
West cross section diffuser	1	14,64	14,64
South cross section diffuser	1	14,53	14,53
Total	6		72,71

The air flow rates in the model along with the prototype are presented in Table 4.2. The air flow rate from each of the wall diffusers was controlled by Iris-dampers. The flow rate from the cross section diffusers was controlled by a variable speed channel fan and iris-dampers. For balancing methodology and documentation see Appendix I). Skistad (2002)

states that all plumes encountered in practical ventilation are turbulent flows, so it is safe to assume that the plumes from the heat sources fall within the turbulent regime.

4.3 Model Parameters

As mentioned in the theory, it is not possible to match all the dimensionless number to achieve complete similarity. The main similarity requirements to focus on in displacement ventilation is to match the Archimedes number, while at the same time making sure that the flow stays within the turbulent regime.

Table 4.3 present a summary of the values and dimensionless parameters of the prototype and the model. Since displacement ventilation mainly are driven by the convection flows (plumes) in the room, the velocity term in the Archimedes and Reynolds number are the plume center line velocity at ceiling height. With the given velocities in the prototype and model, the temperature difference in the model of 16 °C is needed for the Archimedes numbers to match. This temperature difference is not possible to achieve in the model. The difference is therefore set to a achievable value of 8 °C. The flow stays turbulent in both the prototype and the model ($Re > 2300$). The working fluid is air for both the prototype and model, so the Prandtl number is equal.

Table 4.3: Summary of values and dimensionless parameters for full scale prototype and reduced-scale model

Parameter	Prototype	Model
Scale (λ)	1	4
$g(m/s^2)$	9,81	9,81
$\rho(kg/m^3)$	1,2	1,2
$\beta(1/K)$	0,0033	0,0033
$\nu(m^2/s)$	$1,477 \cdot 10^{-5}$	$1,477 \cdot 10^{-5}$
$\Delta T(K)$	4	8
$A = \text{area of the room } (m^2)$	304	19
$H = \text{height of room } (m)$	3	0,75
$q(m^3/h)$	4653,40	72,71
$v(m/s)$	0,33	0,33
Ar	3,63	1,82
Pr	0,7	0,7
Re	$6,64 \cdot 10^4$	$1,66 \cdot 10^4$

4.4 Tracer Gas Measurements in the Model

Tracer gas measurements was conducted in the reduced-scale model. The measurements were performed after the same method as the measurements in the prototype (see Section 3.1.2 for methodology).

4.4.1 Method

Four step up and four step down measurements were conducted in the model, to give a total of eight measurements. The locations of the sampling points in were held equal to the locations in the prototype. Figure 4.8 show the sampling point locations for the measurements conducted on June 2 and June 4. For the locations in the the other measurements, please see Appendix A. The height of the points were scaled to match the prototype. Table 4.4 give a summary of the point heights.

At the prototype, both second and third floor staircase was sampled. In i model there is only one floor, so this leaves one unused sampling point. This point was placed in between the south and east corner, represented by number 4 in Figure 4.8. This point holds no relevance to the validation of the prototype against the model, it merely act as another data point in determining the distribution of the local air change indexes throughout the office landscape. The same can be said for point 3, as the original point of the prototype is placed in the north corner while this point is placed approximately in the center of the northeast facing wall.

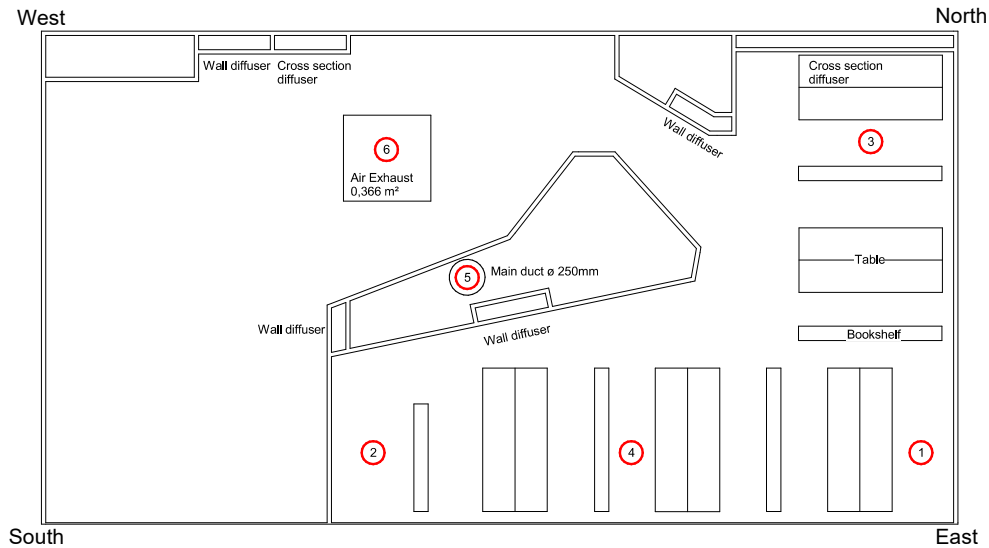


Figure 4.8: Location of sampling points for tracer gas measurement on June 2, 2016 and June 4, 2016

Table 4.4: Sampling point heights

Measurement # and date					
1			2		
01.06.2016			01.06.2016		
Location	Description	Sampling height (mm)	Location	Description	Sampling height (mm)
1a	East	25	1a	East	25
1b	East	275	1b	East	275
1c	East	500	1c	East	500
1d	East	725	1d	East	725
5	Supply	-	5	Supply	-
6	Exhaust	-	6	Exhaust	-
3			4		
02.06.2016			04.06.2016		
Location	Description	Sampling height (mm)	Location	Description	Sampling height (mm)
2a	South	375	1	East	375
2b	South	375	2	South	375
2c	South	375	3	North	375
2d	South	375	4	Southeast	375
5	Supply	-	5	Supply	-
6	Exhaust	-	6	Exhaust	-

4.5 Air Velocity Mapping in the Adjacent Zone of a Wall Diffuser in the Model

The air velocity mapping in the model was performed by the same method as used for the mapping in the prototype, described in Section 3.2. Figure 4.9 show the layout of the measurement grid. For description of the equipment for the air velocity mapping, please refer to Appendix E

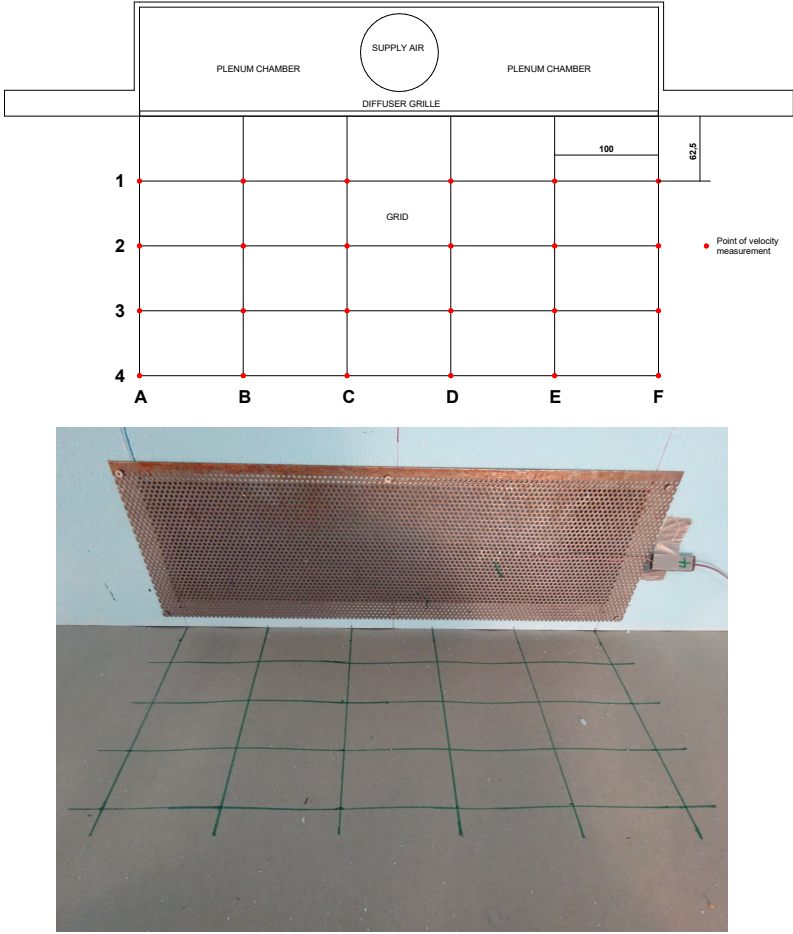


Figure 4.9: Air velocity measurement grid (red dots indicate anemometer locations)

4.6 Temperature Measurements in the Model

Temperature measurements was performed in the model in order to monitor the supply and exhaust air temperatures and the temperature differences in the room.

4.6.1 Method

A total of 15 thermocouples were placed in the model. Figure 4.10 show the locations of the thermocouples. Thermocouple 1 is broken and is therefore omitted from the measurements. The heights of the thermocouple measuring points are presented in Table 4.5. The thermocouple at location 4 was placed inside of the wall diffuser plenum chamber in order to measure air supply temperature. Location 5 is inside the Cross section diffuser, and measure the temperature of the air coming from the channel fan. Location 16 is in the middle of the air exhaust hood in order to measure the exhaust temperature. The cluster locations at (2, 3), (6, 7), (8, 9, 10), and (13, 14, 15) are located on top of each other, at different heights. The measurement sets were taken simultaneously with the tracer gas measurements. The signal from the thermocouples were sent to the data logging system, and recorded on a computer for later analysis.

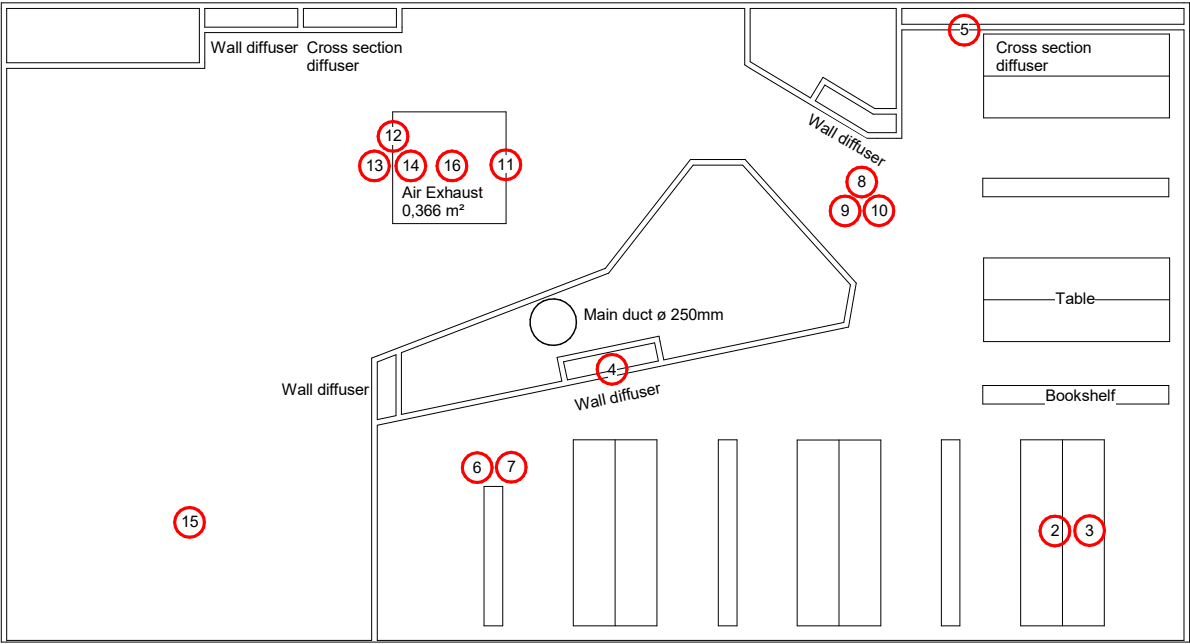


Figure 4.10: Location of thermocouples

Table 4.5: Thermocouple height

Thermocouple Type T			
Location	Height (mm)	Location	Height (mm)
2	25	10	725
3	725	11	725
4	-	12	375
5	-	13	725
6	25	14	25
7	725	15	725
8	25	16	-
9	375		

4.7 Discussion

The pressure drop in the iris dampers are in the range of $3 - 5 Pa$. Considering that the accuracy of the pressure measuring equipment are $\pm 1 Pa$, the uncertainty in the measured flow rate is quite large. The balancing of the model's ventilation system is therefore not very accurate.

There are visible gaps in the model construction, especially between the ceiling panels, and between the ceiling panels and the walls. Despite attempts of closing the gaps with sealant and duct tape, the air leakage in the model is suspected of being quite high.

At maximum cooling during warm days, the AHU can maintain an air supply temperature of no lower than 14 degrees. Since there is no insulation on the ducts in the model, the supply temperature into the model was quite high, in the range of $20 - 22^\circ C$. This is assumed to have an influence temperature difference in the model, and affect the similarity.

Although calculations suggest 131 W output of the heat sources, 100 W light bulbs was used. This was decided to be adequate, and the rest of the heat gain was simulated by the floor heating. It is also possible that the heat sources are too close to each other to avoid them affecting each other. In the case that they affect each other, the combined output is becomes lower.

Chapter 5

Experimental Results

Experiments and measurements were carried out in the prototype during the fieldwork, and later on in the reduced-scale model. This chapter present and discuss the results of the measurements. The results of tracer gas measurements and velocity mapping in both prototype and model are presented and discussed. The results from the duct traversing, smoke visualization and registration of presence are presented and discussed. The temperature measurement results from the model are presented and discussed. In the last section the results from the prototype and model are compared to evaluate the similarity.

5.1 Tracer Gas Measurements

Tracer gas measurement were performed in the prototype building (Powerhose Kjørbo), and later in the reduced-scale model. Linear and logarithmic charts describing the time lapse of the tracer gas concentration are presented. The air change efficiency for the prototype/model and the local air change indexes for each sampling point in the measurement sets are presented.

It was observed that the tracer gas concentration in the supply air was not constant during the step up period. This is due to inaccuracy of the gas injection equipment and inaccuracy in the total air flow rate of the ventilation system. Although the air flow rate was set to a value of approximately $10\,000\text{ m}^3/h$, it might not have been totally constant. The

unstable supply air gas concentration can be observed in all of the measurements in both the prototype and the model. This reduces the reliability of the step up measurements considerably, and therefore it was decided to omit the step up results completely, and focus on the step down, which was considered more accurate.

The channel fan installed to simulate the air from the parts of the prototype excluded from the model were turned off during all tracer gas measurement. The reason for this decision is that it was not possible to predict and simulate the development of the additional tracer gas flowing into the model from the non-modelled part. If the channel fan was turned on, the options were to either supply air with zero tracer gas concentration into the model, or to supply air with concentration equal to the supply air. Neither of these options were considered to be realistic to the prototype. It was decided to turn the fan off and concentrate on analysing the part of the prototype represented by the model. Focus was put on studying the air quality in the south and east corner, and since the air from the non-modelled part does unlikely flow into these parts, it was assumed that turning of the fan does not affect the air movement in these areas at a significant degree.

5.1.1 Results from Fieldwork

The results from the tracer gas experiment are presented for Wednesday March 9 and Thursday March 10. During the whole experiment period the ventilation system was set to provide a constant air flow of approximately $10\ 000\ m^3/h$, and the VAV-dampers in the wall diffusers were fully opened. A step up measurement followed by a step down are called a measurement set. Two sets were performed on March 9, one in the morning and one in the afternoon. One measurements set was conducted on March 10.

March 9 - First Set

The first set of tracer gas measurements, conducted at March 9, had sampling locations at a height of 1,5 m in the east, south, and north corner, in the supply duct and in the staircase above 2nd and 3rd floor (exhausts). This represent an overall measurement of the ventilation efficiency for the whole building. The concentration time lapse is presented linearly and logarithmic in Figure 5.1. In the logarithmic chart, the decay for the South,

East and North point present themselves mainly as a straight line, which implies that the decay is stable and undisturbed, and free of influences by other air streams. It was not expected to observe a completely straight line, however, as this indicate fully mixed flow, which is unwanted in displacement ventilation.

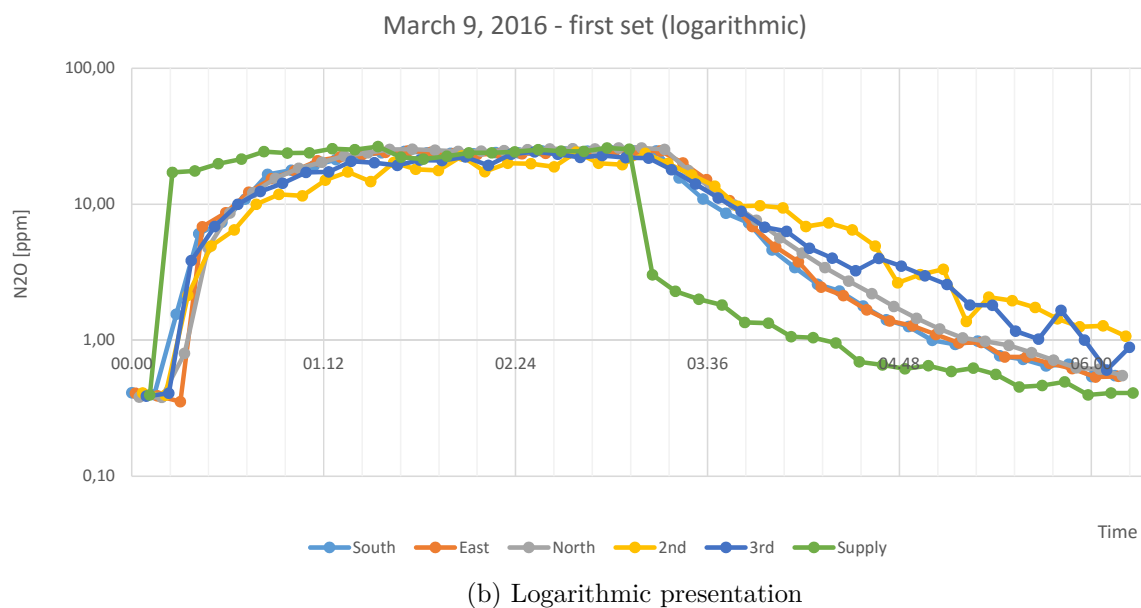
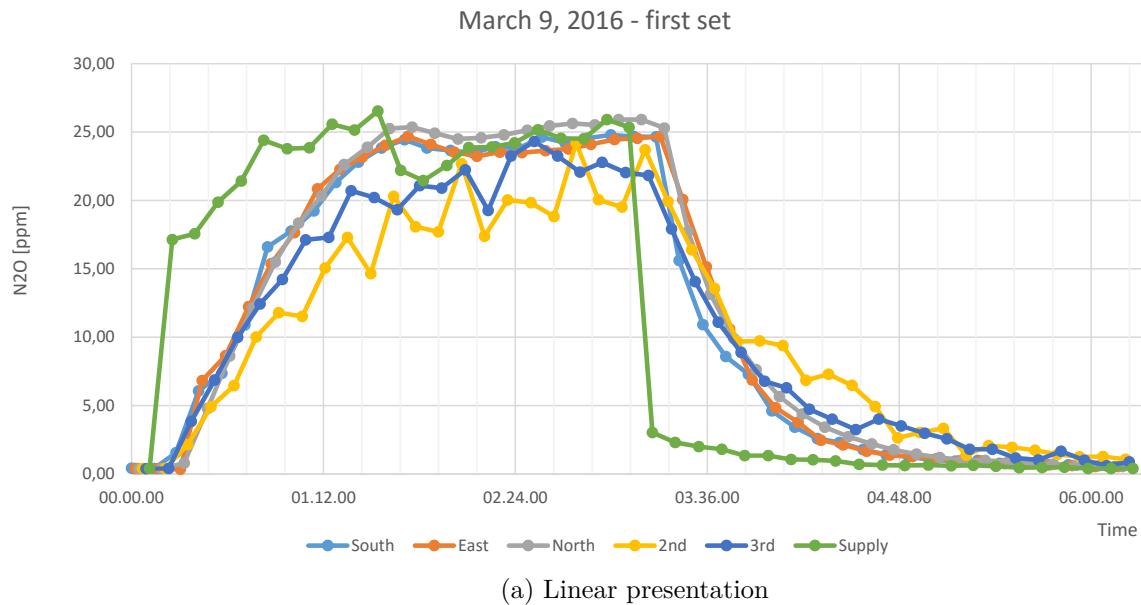


Figure 5.1: Tracer gas measurement on March 9, 2016 - first set

The logarithmic decay lines of the 2nd and 3rd staircase points are jagged, and it was observed in both charts that the concentrations does not decrease evenly. The most likely reason for this is that the air in the adjacent building interact with the prototype through the walkway connecting the two buildings. The other building was not injected

with tracer gas, so it might push clean air into the prototype building a certain times. Previous studies made by [Søgnen \(2015\)](#) also support this hypothesis.

After the gas dosage is stopped, the concentration of tracer gas in the supply air does not decrease to zero immediately. Shortly after turning off the gas injection, the concentration in the supply air is measured to around 3 ppm, and there is a lag of about one and an half hour before the concentration decrease to zero. [Søgnen \(2015\)](#) saw the same situation in his measurements, however more prominent. He found that the reason for this was an air leakage within the heat exchanger, causing contaminated exhaust air to mix with the fresh inlet air. This problem was reported and improvements were made to make the heat exchanger more airtight. The lag was considerably larger in Søgnen's measurements, so it is fair to assume that the improvements of the heat exchanger were successful, although some leakage still occur. Other reasons for the concentration lag effect could be leakage of indoor air into the main ventilation shaft in the center of the building. The sampling point of the supply air measurement were placed in a duct in the second floor, so leakage the gas into the main shaft could occur prior to this location. The driving pressure of the ventilation system is quite low (maximum 20 Pa in main shaft), so there is a possibility that tracer gas can diffuse into the supply air at some point. If the outdoor air inlet are placed in some proximity of the air outlet it is a possibility that some of the tracer gas may travel between the two terminals.

Table 5.1: Summary of tracer gas measurement at March 9, 2016 - first set

	Step down				
Date	09.03.2016				
Sample point	South 1500	East 1500	North 1500	2nd	3rd (Exhaust)
Mean age of air					45,03
Local mean age of air	25,35	29,39	28,75	48,57	41,67
Nominal time constant	41,67	41,67	41,67	41,67	41,67
Air change efficiency, %					46,27
Local air change index, %	164,36	141,77	144,93	85,80	100,00

Table 5.1 show the air change efficiency and local air change indexes at the sampling points in the first measurement. The air change efficiency is 46,27 %. This is lower than expected for displacement ventilation, which should be in the 50 - 100 % range. Efficiencies below 50 % suggest mixed or short-circuit flow characteristics, or stagnant zones ([Mathisen et al., 2004](#)). The local air change indexes are above 100 % however,

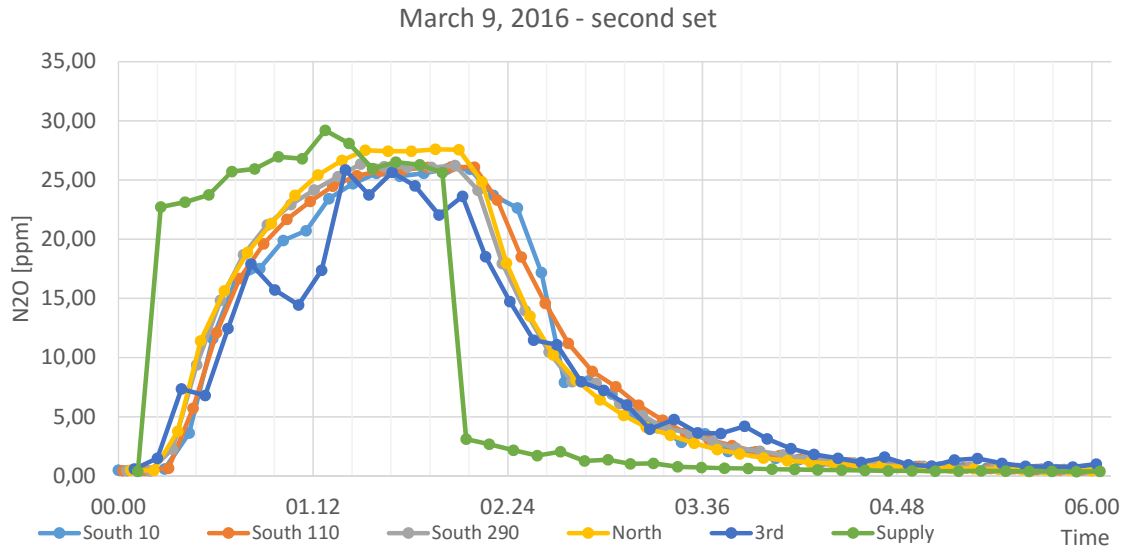
indicating displacement ventilation in each of the zones. The values suggest that the air exchange in these zones are satisfactory. The sampling point in the staircase above second floor, named "2nd", has a much lower air change index. This point gather air from the entire first and second floor. The low value might suggest that air from other parts of the building than the office landscape suffer from short-circuiting and stagnant zones. The issues may be present in the kitchen area, which has a wall diffuser very close to the stairwell.

March 9 - Second Set

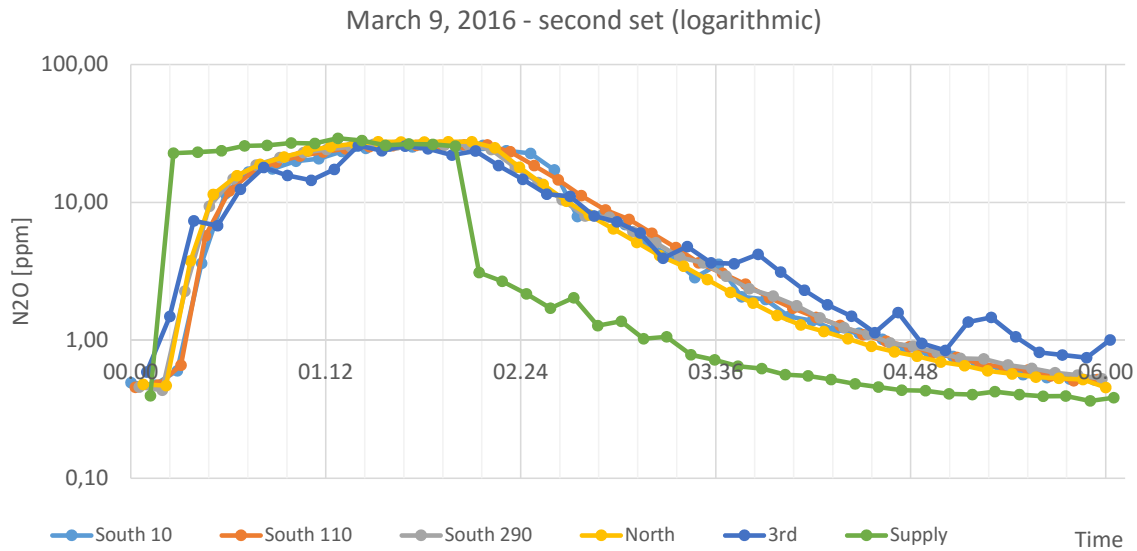
In the second tracer gas measurement set, at March 9, three sampling point where placed at different heights in the south corner. The other points are in the north corner, supply and in the staircase above 3rd floor (exhaust). Figure 5.2 show the time lapse of the concentration in the sampling points.

In a displacement ventilated zone, the fresh air distributed along the floor. It was therefore expected to observe a quicker concentration increase and decrease in the sampling point located 10 cm above floor level, named "South 10". The point, "South 110", located 110 cm above floor level should be the second one to record the increase or decrease, and the point at the roof, "South 290" should respond last. As seen by Figure 5.2, this was not the case. The three sampling points follow each other quite closely, and if anything, the lowest point react slowest in both the step up and step down period. This suggest that the air may not enter the zone at floor level and rise upwards to create the wanted stratification. Rather, the fresh air is mixed with the old contaminated air, and give the room air flow characteristics of mixing ventilation.

Table 5.2 show the air change efficiency and the local indexes at the sampling points in the second measurement. The efficiency is relatively equal to the first measurement, as expected. The local indexes in the different heights in the south corner are similar. The initial expectation was that the efficiencies would decrease as the height above the floor increased. This relationship does not seem to exist though, as the efficiency at 10cm is not any higher than at 110 cm or 290 cm. Ideal mixing ventilation has a local air change index of 100 %, but displacement ventilation can also have values down to 100 %, so it is hard to conclude which characteristic that dominates in this corner.



(a) Linear presentation



(b) Logarithmic presentation

Figure 5.2: Tracer gas measurement on March 9, 2016 - second set

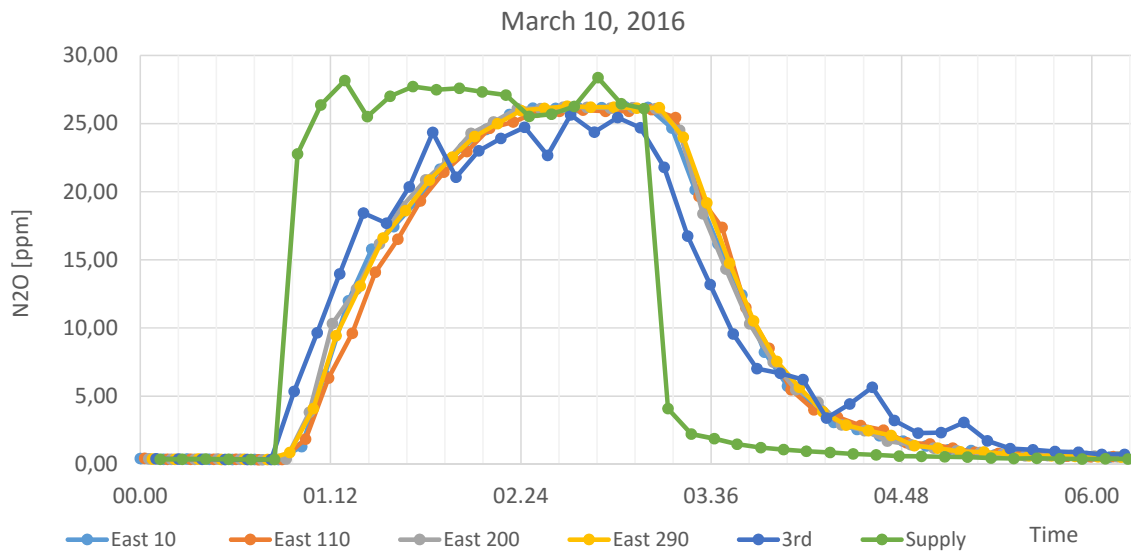
Table 5.2: Summary of tracer gas measurement at March 9, 2016 - second set

	Step down				
Date	09.03.2016				
Sample point	South 100	South 1100	South 2900	North 1500	3rd (Exhaust)
Mean age of air					42,36
Local mean age of air	41,06	40,54	41,16	31,69	41,38
Nominal time constant	41,38	41,38	41,38	41,38	41,38
Air change efficiency, %					48,84
Local air change index, %	100,77	102,06	100,52	130,57	100,00

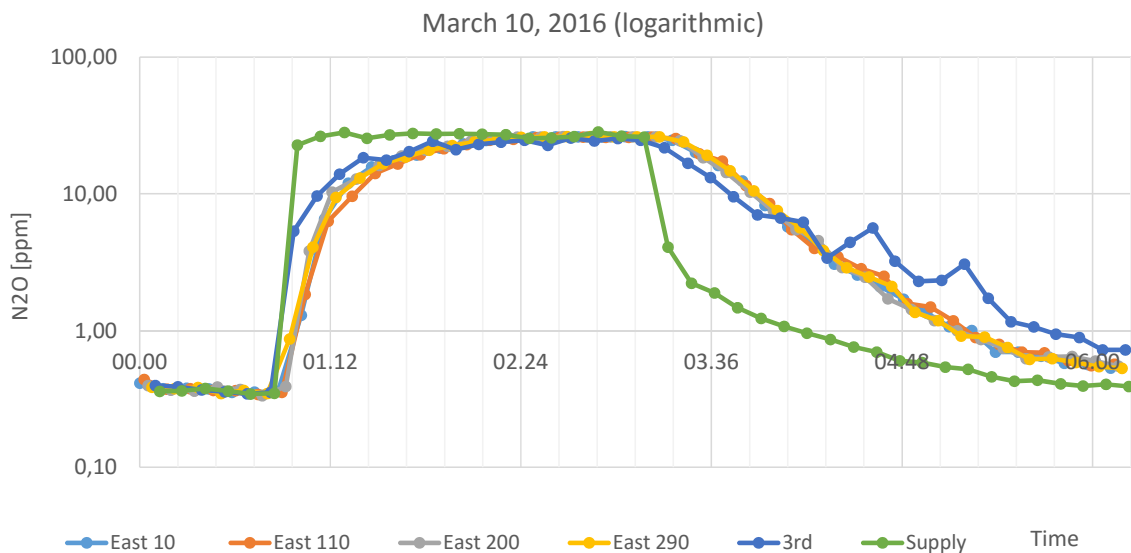
March 10

The third measurement, at March 10, consisted of four sampling points at various heights in the east corner, in addition to the fixed points in the supply duct and the staircase above 3rd floor. The east corner is the location with the most concerns about the air quality, so it was decided to do a thorough measurement in this zone. The zone is almost completely surrounded by bookshelves, and down by the floor there is a gap only about one meter wide for the air to flow through into the zone (see Figure 1.2). Figure 5.3 show the time lapse of the concentration in the sampling points. Similar to the measurements in the south corner presented previously, it was expected to observe a quicker response in the tracer gas increase and decrease for the low level sampling points. This is not the case in this measurement either. The concentration curves follow each other very closely, and indicate mixing tendencies in this corner as well.

Table 5.3 show the calculated air change efficiency and local indexes at the different sampling points. The efficiency is relatively similar to the other measurement, as expected. The local indexes are slightly higher in the points closer to the ceiling, suggesting that the air in the higher levels are ventilated quicker. Lower air change indexes close to the floor in the east corner suggest that the bookshelves placed around the corner may work as obstructions to the air flow.



(a) Linear presentation



(b) Logarithmic presentation

Figure 5.3: Tracer gas measurement on March 10, 2016

Table 5.3: Summary of tracer gas measurement at March 10, 2016

	Step down				
Date	10.03.2016				
Sample point	East 100	East 1100	East 2000	East 2900	3rd (Exhaust)
Mean age of air					45,51
Local mean age of air	39,11	40,01	36,58	36,59	43,26
Nominal time constant	43,26	43,26	43,26	43,26	43,26
Air change efficiency, %					47,53
Local air change index, %	110,62	108,11	118,25	118,22	100,00

5.1.2 Results from Model

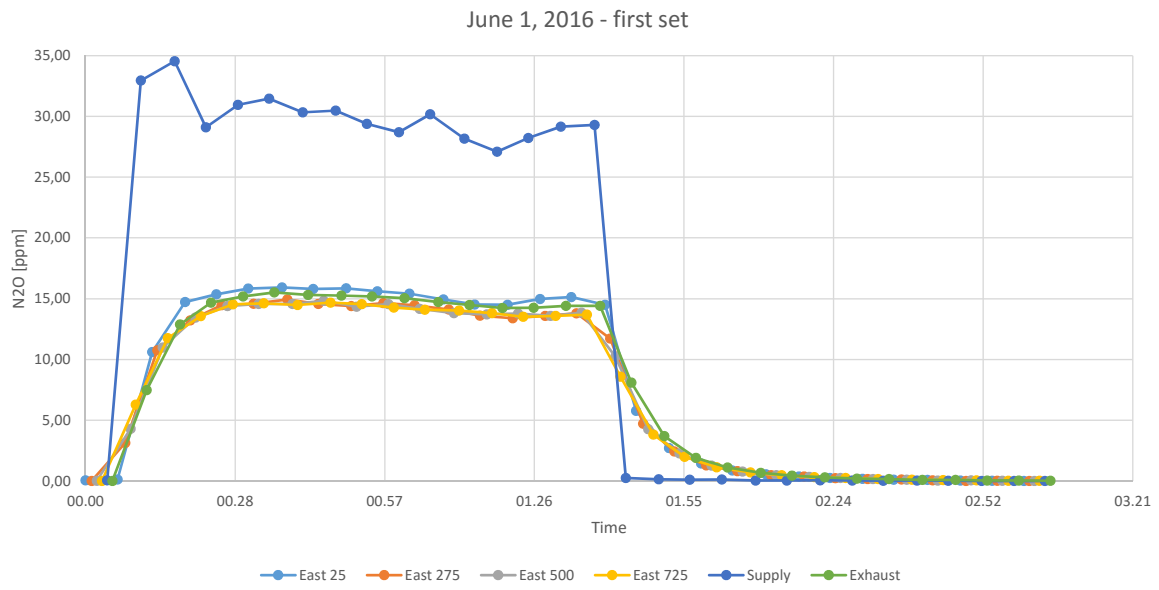
The results from the tracer gas experiment are presented for June 1, June 2 and June 4. During the whole experiment period the ventilation system was set to provide a constant air flow. Two sets were performed on June 1, one on June 2 and one on June 4. Focus was placed on performing the measurements in the model following the same method as for the prototype, in order to see if the two behaved similarly. This implies that the sampling locations were equal (see Section 4.4.1 for specifications and exceptions), and the airflow rate and temperature gradient were scaled appropriately (see Section 4.2).

June 1 - First Set

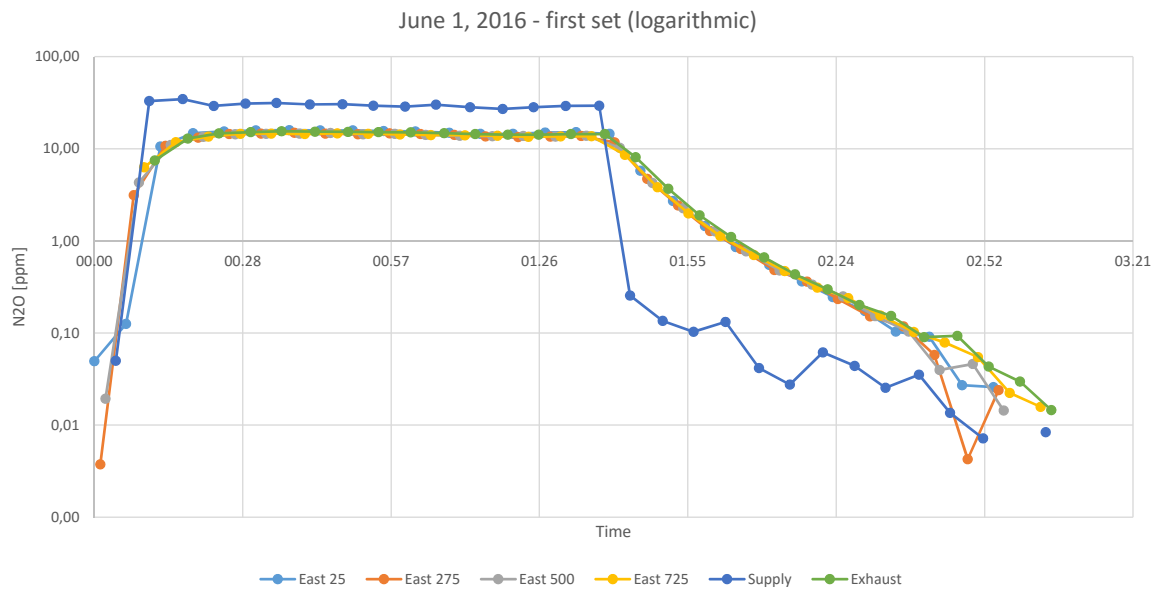
The first measurement in the model, at June 1, had four sampling point located at different heights in the east corner, equal to the prototype measurement at March 10. The time lapse of the concentrations are presented in Figure 5.4. An obvious observation was that the concentrations at the sampling points stabilize way below the supply air concentration. While the supply air concentration is held at approximately 30 ppm, the sampling points never reach more than about 15 ppm. The reason for this is excessive air leakage in the model. As discussed in Section 4.7, the model have gaps in the construction and is not airtight. This caused air to flow into the model at various places and dilute the tracer gas concentration. Theory in Section 2.2.6 states that tracer gas measurements do not give reliable result and therefore should not be performed in rooms that exchange air with other parts of the building. The larger laboratory test chamber in which the model is built in can be considered as other parts. The large difference between the sampling point and the supply concentration is unfavorable for producing accurate results.

Although the model exchange air with the outside, this does not necessarily mean that the results of the measurements are useless. If the air leakage flow rate are constant and somewhat uniform throughout the model, it is still possible to detect variations in the air change indexes at different locations in the model. Figure 5.4 show the logarithmic presentation the the measurement. Although there was disturbance from air leakage, the decay for the sampling point except for the supply present themselves as relatively straight lines, suggesting that the decay was stable and the air leakage was relatively

constant.



(a) Linear presentation



(b) Logarithmic presentation

Figure 5.4: Tracer gas measurement on June 1, 2016 - first set

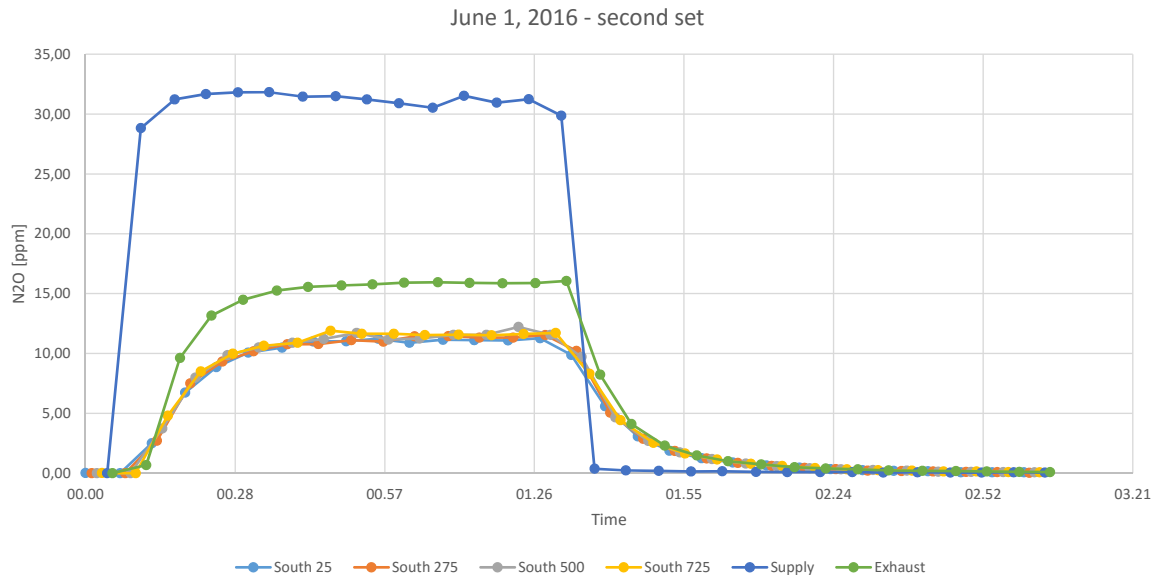
Table 5.4: Summary of tracer gas measurement at June 1, 2016 - first set

Step down					
Date	01.06.2016				
Sample point	East 25	East 275	East 500	East 725	Exhaust
Mean age of air	11,56				45,51
Local mean age of air	14,31	13,50	12,48	11,41	10,25
Nominal time constant	10,25	10,25	10,25	10,25	10,25
Air change efficiency, %					44,34
Local air change index, %	71,65	75,95	82,18	89,90	100,00

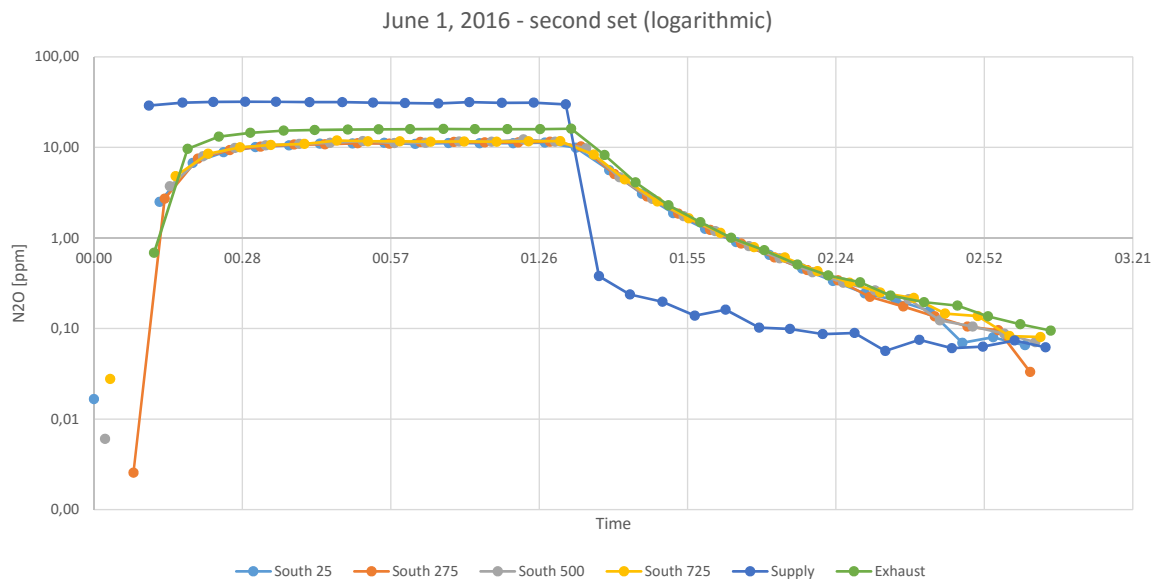
Table 5.4 show the calculated air change efficiency for the model and the air change indexes at the different sampling points. The air change efficiency is 44,34 %. This is low for displacement ventilation, which should have values above 50 %, and indicate short circuiting or stagnant zones. The air change indexes are all under 100 %, which indicate mixed flow in the east corner. The indexes are lower at floor level than at ceiling level. This indicate that the air is more quickly exchanged in the higher parts of the corner, and suggest that the the air does not flow correctly into the corner along the floor, but rather enter the area over the whole height of the room, in a mixed fashion. The cause for this may be the obstructions made by the bookshelves.

June 1 - Second Set

The second measurement set, also performed on June 1, had four sampling point located at different heights in the south office landscape corner. The time lapse of the concentrations at the points are presented in Figure 5.5. From the figure, an observation is made. The concentration in the exhaust sampling point stabilizes at a higher level than the the points in the south corner. The concentration in the exhaust is approximately 15 ppm, while the concentration in the south corner is about 11 ppm. The concentration in the supply air is still at around 30 ppm. This observation indicate that the air leakage in the south corner is higher than in the east corner, where it stabilized at around 15ppm. The south landscape corner is in the middle of the model, and is exposed to air leakage through three surrounding walls in addition to the ceiling (please see Appendix A for clarity of the sample point locations). In comparison, the east corner is only exposed to air leakage through the wall facing southeast. The wall facing northeast are part of the original test chamber, and is airtight.



(a) Linear presentation



(b) Logarithmic presentation

Figure 5.5: Tracer gas measurement on June 1, 2016 - second set

Table 5.5: Summary of tracer gas measurement at June 1, 2016 - second set

Step down					
Date	01.06.2016				
Sample point	South 25	South 275	South 500	South 725	Exhaust
Mean age of air					14,69
Local mean age of air	16,90	16,21	20,82	20,81	11,08
Nominal time constant	11,08	11,08	11,08	11,08	11,08
Air change efficiency, %					37,71
Local air change index, %	65,60	68,37	53,23	53,27	100,00

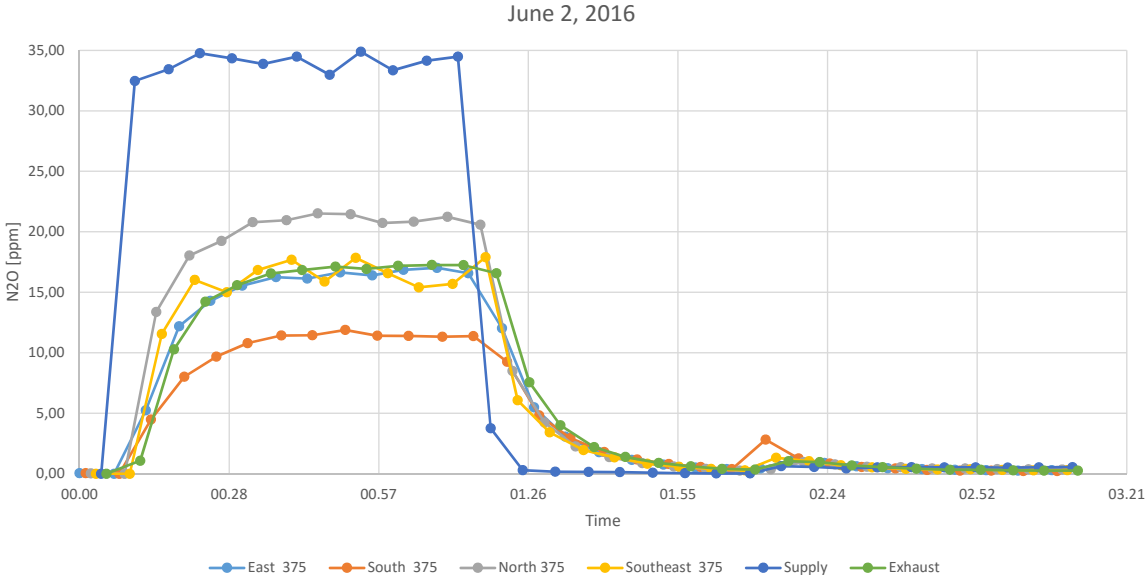
Table 5.5 show the air change efficiency and local indexes at the different sampling points. The air change efficiency of 37,71 % are lower than in the previous measurement. This is peculiar, considering that the parameters and conditions of the model should be equal to the previous measurement. Possible reasons can be be that the air leakage flow rate has changed, or that the supply flow rate or temperature gradient in the room have changed slightly. The local air change indexes are quite low, suggesting that the south corner is a stagnant zone. In contradiction to the first measurement in the east corner however, the efficiencies on the south corner show an increase as the height above the floor decrease. This suggest that there is somewhat more stratification of the air layers in this corner.

June 2

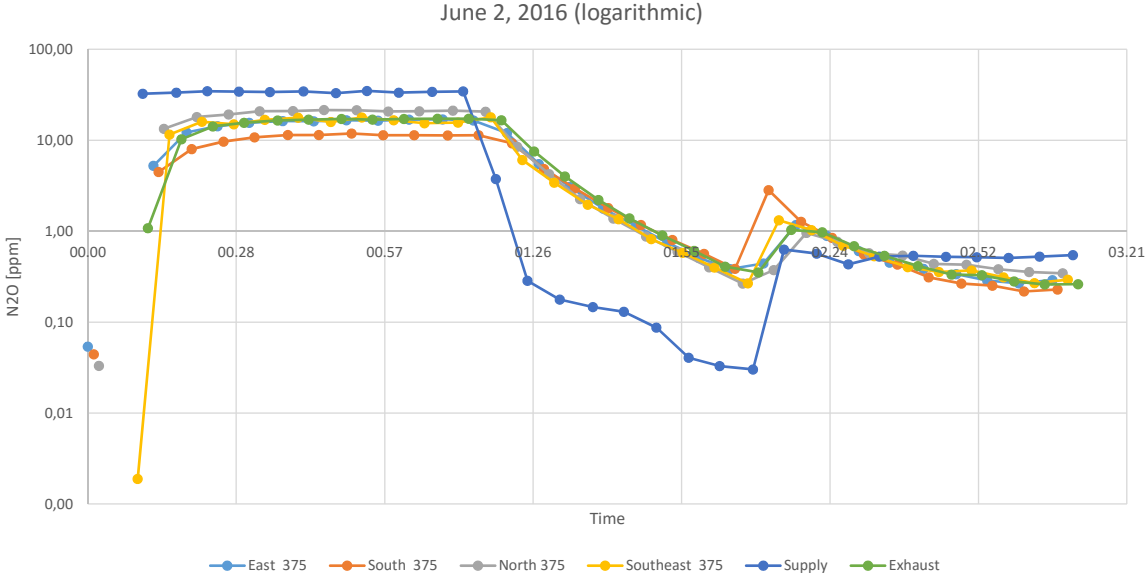
The measurement set performed on June 2, had sampling point located around the office landscape at at height of half the model height (375mm). The time lapse of the concentrations at the points are presented in Figure 5.6. By observing the figures, the air leakage issue becomes clearly visible. The north corner has the highest equilibrium concentration, and therefore the lowest air leakage (please see Figure 4.8 in Section 4.4.1 for clarity in sampling point locations). This corresponds well with the fact that the corner is surrounded in the northwest and northeast by two walls from the original test chamber, which are airtight. The east and southeast sampling points both have air leakage through one wall, and therefore have approximately the same equilibrium concentration. The south corner has the highest air leakage, as suggested previously, and therefor has the lowest equilibrium concentration.

The sudden unexpected spike in concentration at around 2 hours into the measurement is caused by human intervention of the tracer gas injection equipment. The equipment is placed in proximity to the south corner sampling point. Handling of the equipment caused an unexpected release of tracer gas. The gas was not released into the model but into the test chamber room surrounding the model. Because of the air leakage issue an unknown amount of the released gas diffused into the model at the south office landscape corner. Although not favourable, the spike occurred at a time were the concentration was close to zero, so this incident is not critical for the calculation of the efficiency. The analysis

of the concentrations were stopped at this point in time, and the decay from thereon and out (the tail) were extrapolated, as described in the theory in Section 2.2.6.



(a) Linear presentation



(b) Logarithmic presentation

Figure 5.6: Tracer gas measurement on June 2, 2016

Table 5.6: Summary of tracer gas measurement at June 2, 2016

Step down					
Date	02.06.2016				
Sample point	East 375	South 375	North 375	Southeast 375	Exhaust
Mean age of air					12,46
Local mean age of air	12,99	15,60	8,79	8,43	9,94
Nominal time constant	9,94	9,94	9,94	9,94	9,94
Air change efficiency, %					39,89
Local air change index, %	76,51	63,69	113,03	117,87	100,00

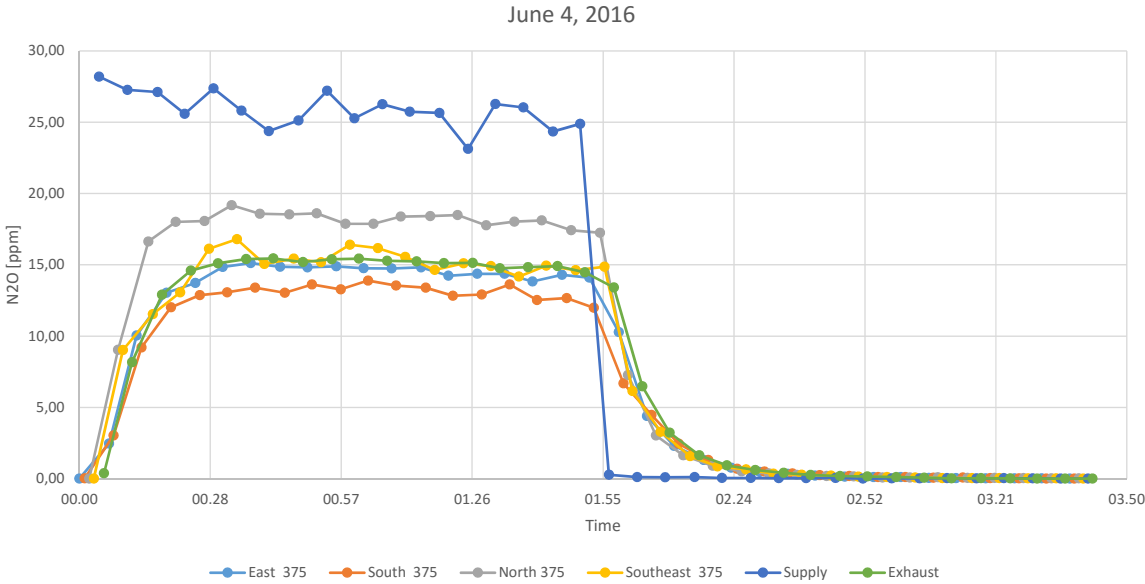
Table 5.6 show the calculated air change efficiency and local indexes at the different sampling points. The air change efficiency of 39,89 are approximately equal to the measurement at June 1, which is expected. The local air change indexes for the east corner fall in between the indexes of the measurement at June 1, East 275 and East 500, as expected. The same applies to the South measurement. The north sampling point has an index of 113,03, which is considerably higher than the east and south point. This is most likely because the the sampling point is quite close to the diffuser, and is therefore well ventilated. The same can be observed for the southeast point, as it is also located close to a diffuser. Displacement ventilation characteristic seem to be present here.

June 4

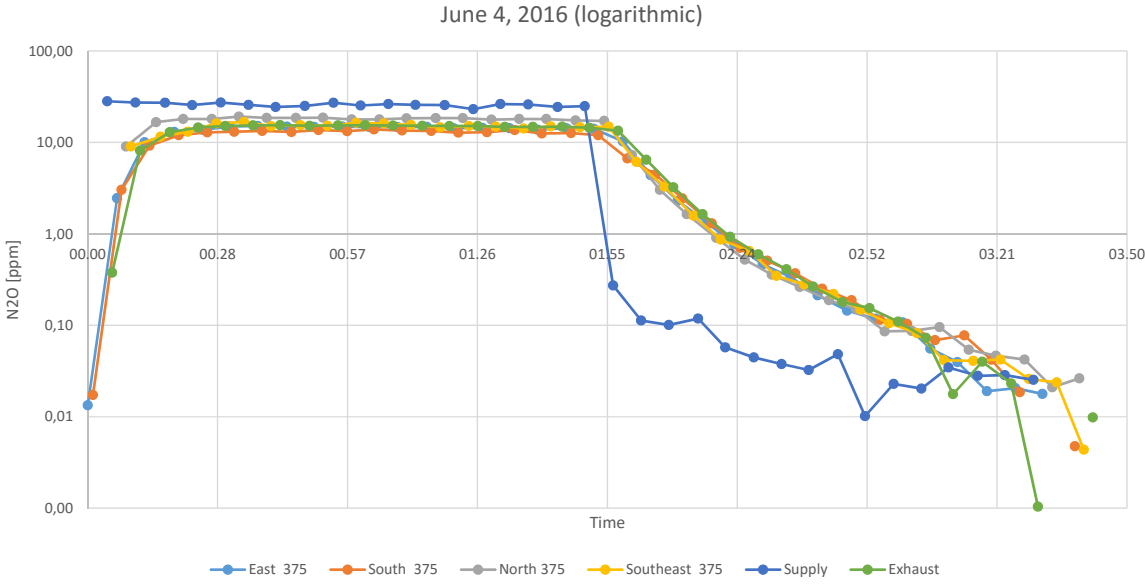
The measurement set performed on June 4 had the same sampling point location as the measurement on June 2. Between the measurement on June 2 and the one on June 4, improvements where made to the model to make it more airtight and thus reduce the air leakage. The improvements consisted of closing the gaps between the walls and the ceiling using sealant, and sealing smaller holes and gaps with duct tape. Figure 5.7 show the concentration time lapse. It is apparent that the improvements to the air-tightness of the model had an effect. The average concentration of the supply gas is around 25 ppm, while the average concentration of the exhaust air is approximately 15 ppm. This represent a 40 % difference, as opposed to the 50% difference before the improvements. This means the air leakage is reduced by 20 %. The model is still quite far from being completely airtight, and further improvements should be the made to reduce the air leakage.

Table 5.6 show the calculated air change efficiency of the model and the local indexes at the different sampling points. The air change efficiency of 41,9 does not differ very much

from the previous measurements, but is slightly higher than before the improvements were made. The same can be said for the local index in the east corner. The index in the south are significantly higher here than before the improvements. This could be because the air leakage prior to the improvements created extra mixing of the air in the south corner, possibly disturbing and stagnating the flow in the area.



(a) Linear presentation



(b) Logarithmic presentation

Figure 5.7: Tracer gas measurement on June 4, 2016

Table 5.7: Summary of tracer gas measurement at June 4, 2016

Step down					
Date	04.06.2016				
Sample point	East 375	South 375	North 375	Southeast 375	Exhaust
Mean age of air					11,55
Local mean age of air	12,30	12,26	8,31	8,88	9,68
Nominal time constant	9,68	9,68	9,68	9,68	9,68
Air change efficiency, %					41,90
Local air change index, %	78,69	78,92	116,42	108,98	100,00

5.2 Temperature Measurements

Fifteen thermocouples were placed in the model to measure temperatures at various locations in the room. The specific locations are given in Figure 4.10 in Section 4.6. Three sets of measurement were conducted in total, the first lasting approximately six hours and the others about three. The measurements were performed at the same time as the tracer gas measurement in order to monitor the temperatures in the model during the experiments.

5.2.1 Results from Model

As derived in Section 2.3, the temperature gradient in the reduced-scale model must be significantly larger than in the prototype in order for the two to behave similar. Practically, it is not possible to achieve a temperature difference to fully satisfy Archimedes number similarity requirement, which for this model would have been 16 °C. Due to the cooling capacity of the ventilation system supplying the model, the temperature difference was set to 8 °C. The thermocouples were placed in the the same locations for all measurement sets. Specific locations of the thermocouples are presented in Figure 4.10 in Section 4.6. The sampling interval for all sets were 2 minutes. The results are presented as tables and charts containing all the measurements and selected temperature differences.

June 1

The temperature measurement set on June 1 cover the time period of both tracer gas measurements that were conducted that day. Figure 5.8 show the time lapse of the temperatures. It can be observed that the temperatures are not fully stabilized during the measurement period. A few reasons for this was discovered. The most important one was that the outdoor temperature increased during the day, making the temperature of the supply air rise despite attempts of the AHU to control it to a constant temperature. T4 is the thermocouple measuring the supply temperature. At the start of the day, in order to achieve the desired temperature gradient in the model, the supply air set-point temperature in the AHU was set to the lowest temperature that could be achieved. When the outside temperature increased later in the day, the cooling unit in the AHU was not able to remove enough heat to maintain the set-point temperature. The value at T4 rose from 19,16 °C in the morning to 21,49 °C in the afternoon. This also causes the temperatures in the room to rise.

The distinct dip in the temperature between 14:30 and 15:30 are caused by an unexpected failure of the tracer gas sampling set-up. The rack holding the plastic tubes at the specified sampling heights in the south corner fell down. In order to repair this the model had to be opened, which made colder air flow into the model from the surrounding test chamber and resulted in a disturbance of the temperatures. The incident affected all of the measurements except for the supply air, naturally. Although the model was opened only for a few minutes, it took nearly one hour for the temperatures in the model to reach equilibrium again. Fortunately, this incident happened in between the two tracer gas measurement of that day, so it should not affect the results.

Table 5.8 show a summary of the measurement set. The standard deviation of the T4 thermocouple located in the wall diffuser is quite large, indicating that the temperature is not stable. This applies to all the thermocouples. T6 and T7 are located in the south corner, at floor and ceiling level respectively. They have the largest deviation in the set, as a result of the failure of the tracer gas rack, as described earlier.

Figure 5.9 show the temperature difference between selected points in the model. Table 5.9 give a summary of the temperature differences, along with a description of which thermocouples the difference are between. T16 - T4 represent are the difference between

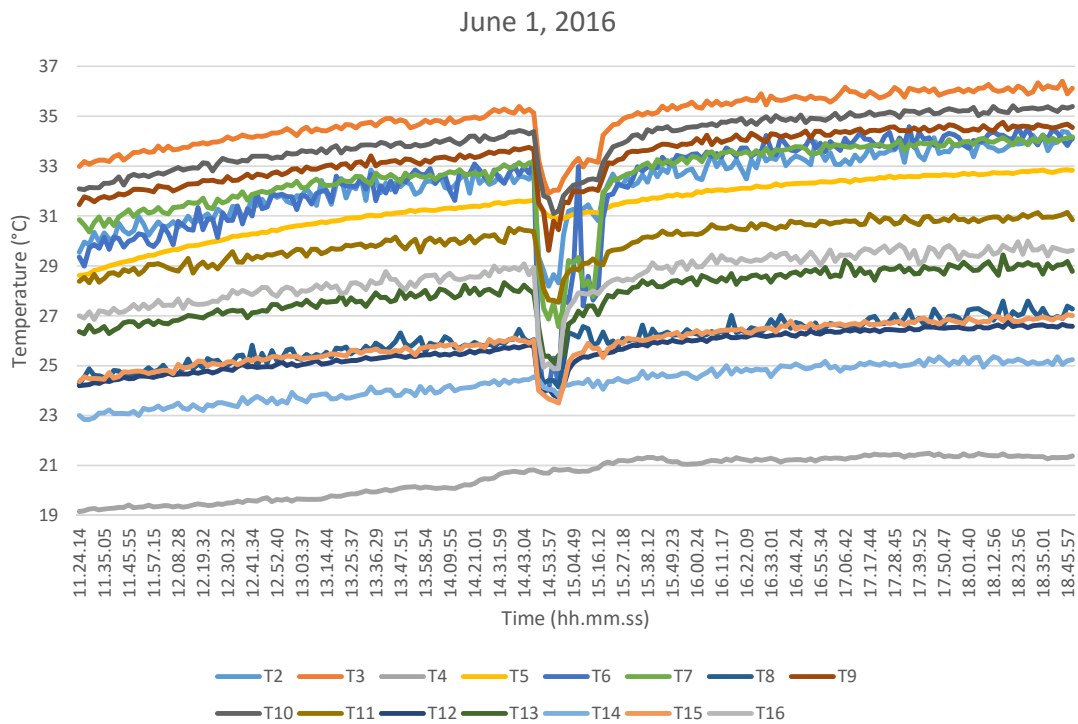


Figure 5.8: Temperature measurements at June 1, 2016

the supply and exhaust air temperature. The mean is $7,98^{\circ}\text{C}$, with a relatively low deviation of $0,27^{\circ}\text{C}$. This is about two degrees short of the desired 8°C degree temperature difference that was the aim for the model to achieve decent similarity.

T7 - T6 represent the temperature difference between the the ceiling and the floor in the south corner. The mean of this is $0,27^{\circ}\text{C}$ and the deviation is $0,44^{\circ}\text{C}$. The reason that this difference is close to zero is most likely the excessive air leakage into this area. Colder air from the test chamber enters the model in the joint between the ceiling and the walls and mix with the air in the top layers of the model, causing the temperature close to the ceiling to drop.

As stated earlier, the temperatures in the model was not stable. However, study of the the slope of the trend lines from the linear regression in Figure 5.9 implies that the temperature differences are relatively stable. This implication is supported by the low standard deviation in Table 5.9. A stable temperature difference is more important than a stable temperature in terms of model similarity and behavior, so this is beneficial considering the reliability of the tracer gas experiments. The spikes in the figure are caused by the failure in the tracer gas rack, as mentioned earlier.

Table 5.8: Summary of measurement set on June 1, 2016 (°C)

June 1, 2016				
Thermocouple	Minimum	Maximum	Mean	Standard Deviation
T2	28,19	34,39	32,32	1,28
T3	31,90	36,40	34,88	1,02
T4	19,16	21,49	20,57	0,79
T5	28,61	32,85	31,38	1,11
T6	23,95	34,58	32,27	2,02
T7	26,57	34,23	32,54	1,52
T8	24,15	27,59	26,00	0,80
T9	29,63	34,75	33,37	1,02
T10	31,10	35,41	34,02	1,03
T11	27,54	31,14	29,97	0,82
T12	23,72	26,72	25,62	0,75
T13	25,11	29,44	27,92	0,89
T14	22,84	25,36	24,31	0,69
T15	23,50	27,05	25,87	0,80
T16	24,87	29,99	28,55	0,98

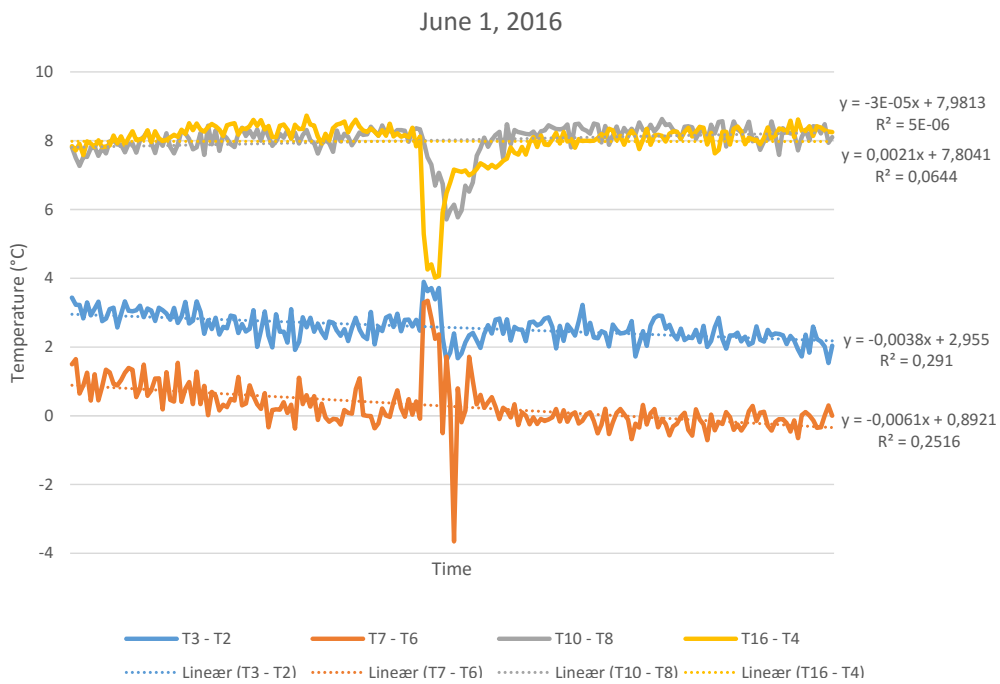


Figure 5.9: Temperature difference between floor and ceiling at four different locations in the model at June 1, 2016

Table 5.9: Temperature differences in the model ($^{\circ}\text{C}$)

Description	Temperature difference between floor and ceiling in east corner	Temperature difference between floor and ceiling in south corner	Temperature difference between floor and ceiling in narrow passage	Temperature difference between supply and exhaust air
Measurement	T3 - T2	T7 - T6	T10 - T8	T16 - T4
June 1, 2016				
Minimum	1,54	-3,65	5,71	4,02
Maximum	3,89	3,34	8,63	8,73
Mean	2,57	0,27	8,02	7,98
Standard deviation	0,28	0,44	0,23	0,27
June 2, 2016				
Minimum	2,01	-1,45	7,70	6,71
Maximum	3,39	0,78	8,84	7,96
Mean	2,72	-0,31	8,41	7,41
Standard deviation	0,28	0,44	0,23	0,27
June 4, 2016				
Minimum	3,37	2,95	6,83	7,61
Maximum	4,63	4,13	7,74	8,53
Mean	4,16	3,63	7,34	7,98
Standard deviation	0,23	0,24	0,18	0,20

June 2

Figure 5.10 show the time lapse of the temperatures. Table 5.9 give a summary of the temperature differences. The deviations of the supply temperature are lower, indicating a more stable temperature than on June 1. This gives more stable temperatures throughout the model. There is still a significant gap between the minimum and maximum temperatures, so overall the the model is not at steady state.

Figure 5.11 show the temperature difference between selected points in the model. Three of the curves are relatively straight, indicating a stable difference. T10-T8 was the difference between the ceiling and the floor in the narrow passage from the office landscape towards the exhaust. At this location the mean is 8.41°C with a deviation of $0,23^{\circ}\text{C}$. This is the largest measured difference in the model, and is larger than the difference between the supply and exhaust. The reason for this is that the thermocouples are placed close to one of the diffusers.

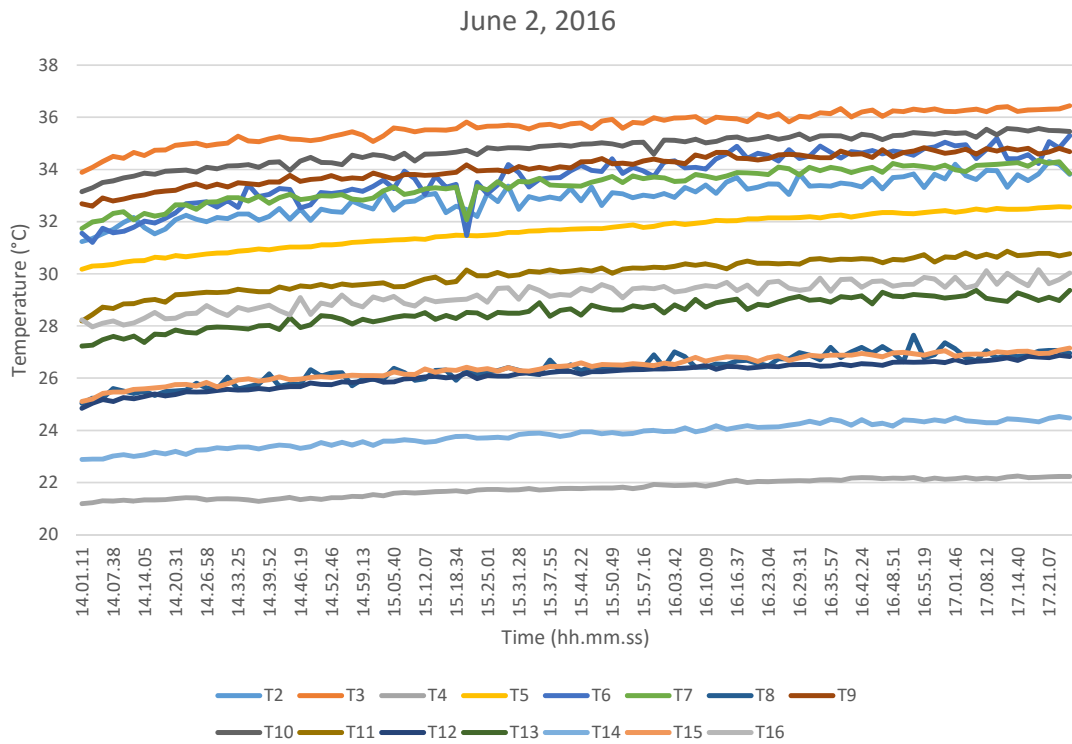


Figure 5.10: Temperature measurements at June 2, 2016

Table 5.10: Summary of measurement set on June 2, 2016 (°C)

June 2, 2016					
Thermocouple	Minimum	Maximum	Mean	Standard Deviation	
T2	31,24	34,30	32,92	0,70	
T3	33,89	36,44	35,64	0,58	
T4	21,19	22,25	21,77	0,33	
T5	30,18	32,57	31,63	0,66	
T6	31,21	35,30	33,71	0,99	
T7	31,74	34,35	33,40	0,64	
T8	25,04	27,64	26,35	0,56	
T9	32,60	34,83	34,06	0,58	
T10	33,15	35,57	34,77	0,59	
T11	28,19	30,87	29,98	0,62	
T12	24,84	26,87	26,12	0,49	
T13	27,23	29,36	28,53	0,54	
T14	22,88	24,53	23,82	0,46	
T15	25,10	27,15	26,40	0,49	
T16	27,97	30,15	29,18	0,53	

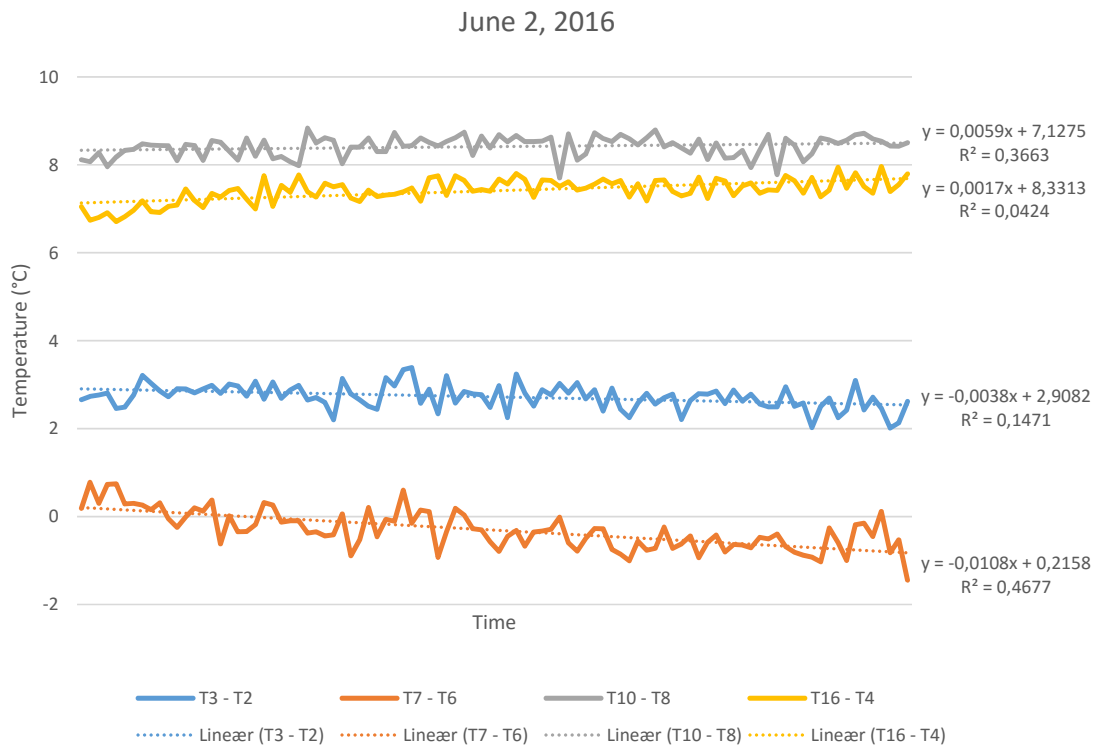


Figure 5.11: Temperature difference between floor and ceiling at four different locations in the model at June 2, 2016

June 4

Figure 5.8 show the time lapse of the temperatures. Table 5.9 give a summary of the temperature differences. The deviation in the measurements are smaller and it can also be observed in the figure that the temperatures are more stable. More stable supply air temperature and improvements to the model air-tightness are the most likely reasons for the increased stability.

Figure 5.11 show the temperature difference between selected points. The differences are more stable than on the two other days. Compared to the measurement on June 2, the deviation of the T3 - T2 is reduced from 0,28 to 0,23, which equals a 18 % reduction. This compares quite well with the 20 % reduced air leakage found from the analysis of the tracer gas results.

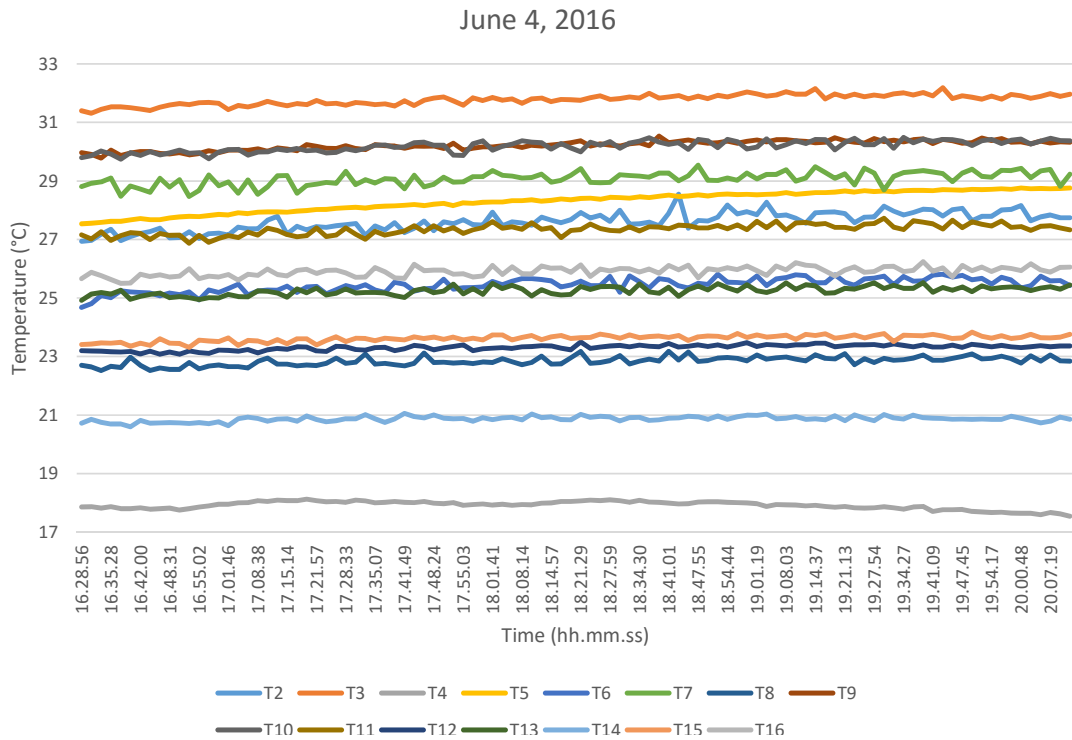


Figure 5.12: Temperature measurements at June 4, 2016

Table 5.11: Summary of measurement set on June 4, 2016 (°C)

June 4, 2016					
Thermocouple	Minimum	Maximum	Mean	Standard Deviation	
T2	26,94	28,55	27,62	0,32	
T3	31,31	32,19	31,78	0,17	
T4	17,54	18,12	17,92	0,14	
T5	27,54	28,76	28,30	0,35	
T6	24,68	25,81	25,44	0,23	
T7	28,47	29,54	29,07	0,23	
T8	22,52	23,18	22,84	0,15	
T9	29,78	30,53	30,22	0,16	
T10	29,75	30,49	30,19	0,19	
T11	26,87	27,73	27,34	0,18	
T12	23,08	23,50	23,31	0,09	
T13	24,92	25,52	25,25	0,15	
T14	20,60	21,06	20,87	0,09	
T15	23,31	23,83	23,62	0,11	
T16	25,50	26,24	25,91	0,16	

After the improvements of the air leakage, the temperature difference in the south corner is at 3,63 (°C), with a deviation of 0,24. This is a significant improvement from the two previous measurements, and indicate that the extra sealing of the model has a positive effect. The T3 - T2 difference also show an improvement.

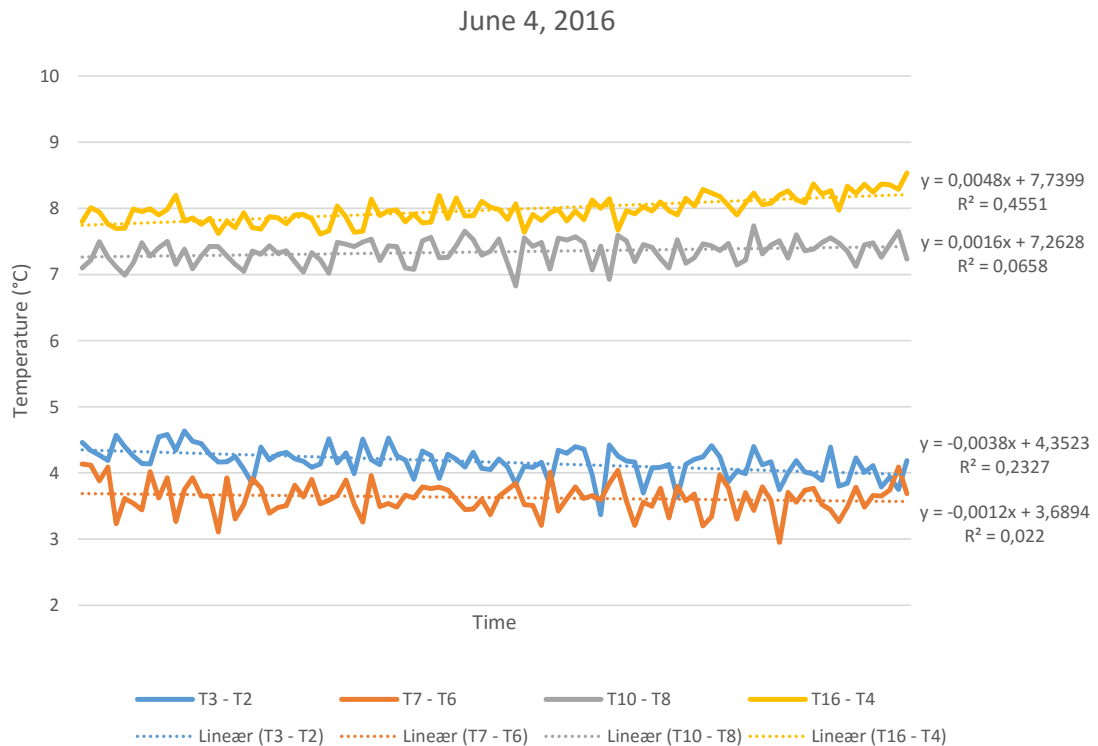


Figure 5.13: Temperature difference between floor and ceiling at four different locations in the model at June 4, 2016

5.3 Diffuser Air Velocity Mapping

The velocities in the adjacent zone of a wall diffuser were mapped in both the prototype and the model. The mapping was conducted in the same diffuser location for the prototype and the model.

5.3.1 Results from Fieldwork

The results from the air velocity mapping in the prototype are presented for Wednesday March 9. The velocity was mapped in a grid pattern at four different heights. Please see Section 3.2 methodology. Figure 5.14 show a 3D shaded surface plot of the the velocity mapping results at a height of 100mm above the floor. The other mapping charts are given in Appendix C.

Skistad (2002) suggest that large diffuser units with a large discharge area are prone to instability in the discharge flow (see Section 2.1.5). The diffuser at the prototype has

an area of over one square meter, so instability effects may occur. The velocity in the middle of the diffuser are significantly lower than on the sides, so there seem to be some irregularities in the discharge, which may be caused by the combination of a large area and velocity.

As expected, the velocities decrease proportional to the the distance from the diffuser. The velocity is maintained at a higher level on the left side as the distance increase, which suggest that there is a larger air flow rate in that direction. The south corner lays to the left of the diffuser, so the result indicate that air flow more towards that area.

Except from one value, all velocity measurements at a distance of 1 meter for all four measurement heights are below 0,2 m/s. On this basis it is reasonable to assume that the adjacent zone stretches for no more than 1 meter from the diffuser. No occupants or obstructions are found within this zone, which is important to avoid draft problems and air distribution issues.

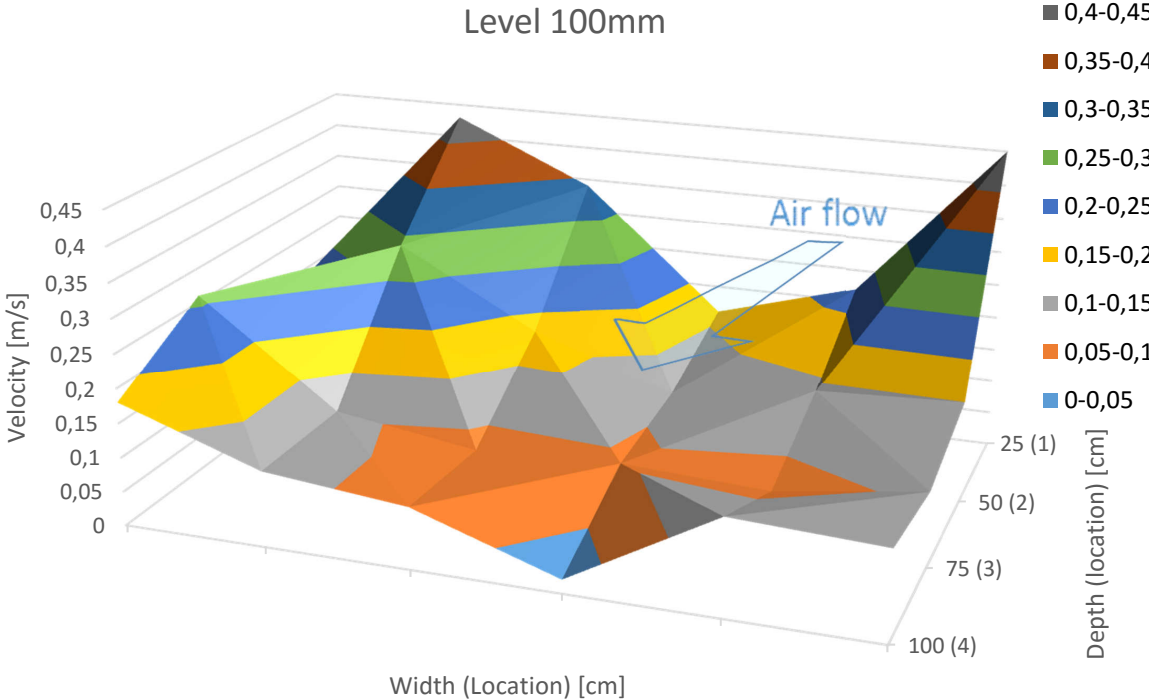


Figure 5.14: Air velocities at a height of 100mm - prototype

5.3.2 Results from Model

The results of the air velocity mapping in the model are presented for May 27. The velocity were measured at four different heights, corresponding på the heights in the prototype.

Figure 5.14 show a 3D shaded surface plot of the the velocity mapping results at 25mm, which correspond to 100mm in the prototype. The other mapping charts are given in Appendix C.

The highest velocities in this measurement are found on the right side. This indicates that the air flow rate is highest in that direction, which is towards the east corner. This is contrary to the prototype measurement, where the air flow was indicated to flow in the opposite direction, towards the south diffuser. This is assumed to affect the similarity, and further investigation into this should be performed.

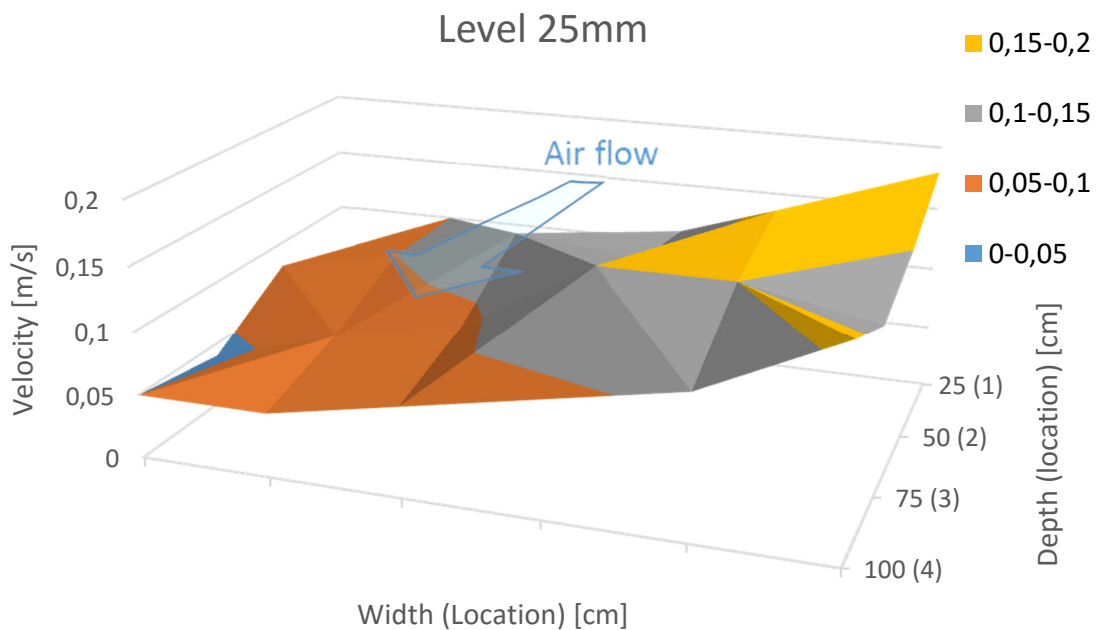


Figure 5.15: Air velocities at a height of 25mm - model

5.4 Traversing of Duct

Traversing of a duct to find average air velocity and flow rate was performed on March 9, in the prototype building. The air velocities in the duct leading to the south east diffuser were measured (see Figure 3.6 in Section 3.2 for locations). Figure 5.16 show the air velocity profile in the duct. The average air velocity was 1.54 m/s and the flow rate was $697 \text{ m}^3/h$. The results are used for balancing the diffusers in the model to achieve appropriately scaled flow rate.

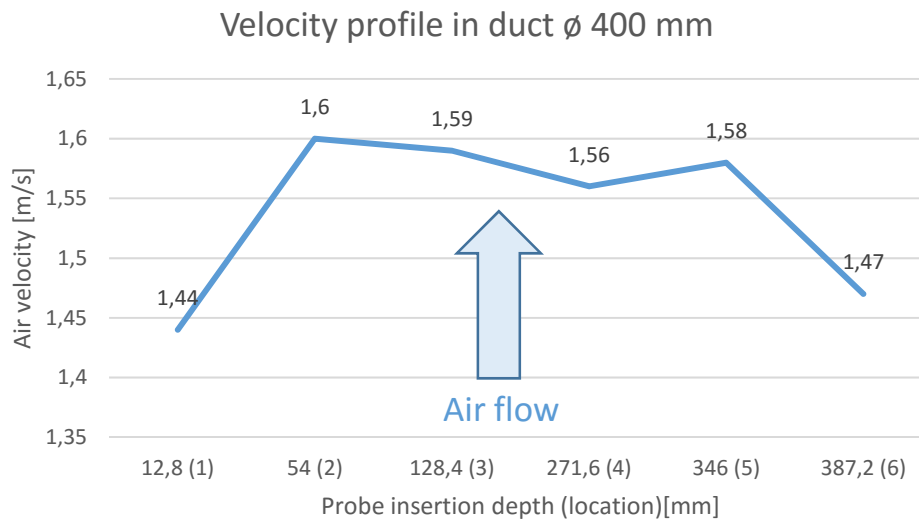


Figure 5.16: Air velocities in duct with diameter of 400 mm

5.5 Smoke Visualization

Smoke visualization were carried out at various locations in the prototype on March 9. The visualization showed that the air did not spread evenly and radially from the diffuser. On the contrary, in some parts of the adjacent zone, the air flowed in towards the diffuser, and then upwards towards the roof or to a higher air layer. This is an effect that can cause unwanted mixing of the stratified air layers and short-circuiting.

The visualization showed that air flowed toward the south corner of the office landscape, as also suggested from the velocity mapping in Section 5.3.2. It was also confirmed that air was flowing along the floor between the to bookshelves and into the east corner of the office landscape. The flow rate of this air in unknown.

Figure 5.17 show smoke rising upwards through the center stairwell, confirming that the air flow from the second floor into the stairwell and up into the exhaust fans at the top of the stairwell.

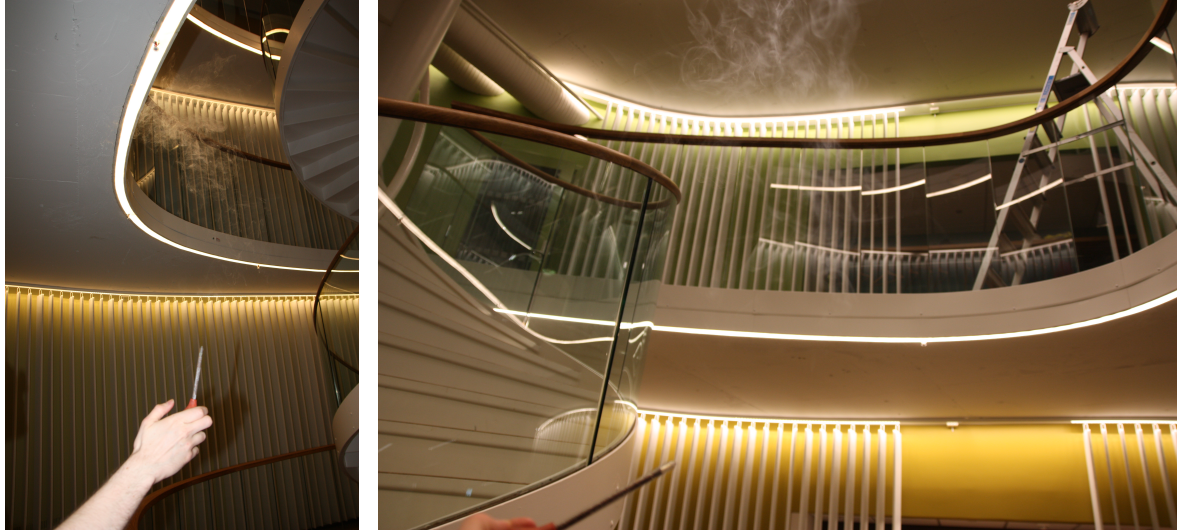


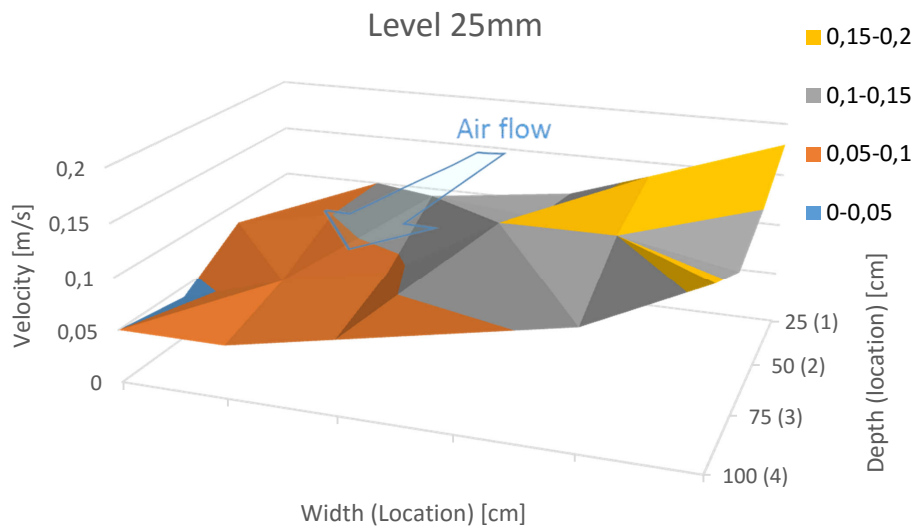
Figure 5.17: Smoke rises up through in the center stairwell

5.6 Comparison of Prototype and Model Results

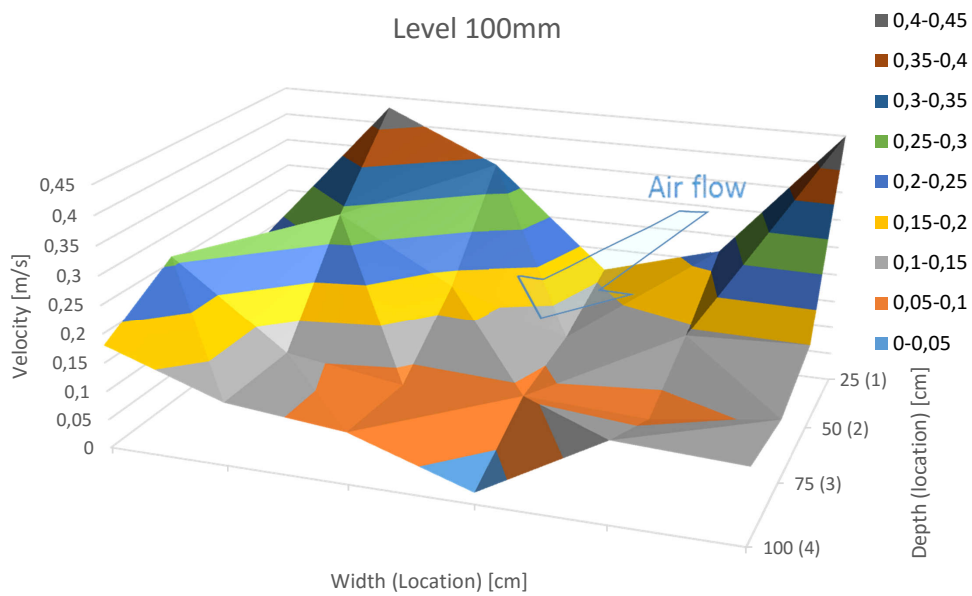
The tracer gas and air velocity mapping results have been compared in order to determine at which degree the reduced-scale model share similarity with the prototype. Observations from the comparison are presented and discussed in this section.

The air leakage seem to effect the air flow patterns in the model. A trend was discovered from studying Figure 5.18, along with the rest of the charts from the velocity mappings (see Appendix C). It was observed that the highest velocity in the model was in the east part of the diffuser discharge, which make most of the air flow towards the east part of the office landscape. This does not match the prototype, where the mapping indicated that most of the air flowed towards the south corner. The reason that the air seem to flow in the opposite direction in the model could be that the excessive air leakage in the south corner push the air and drive it northeast instead of towards the south corner.

The equilibrium concentration in the south corner were considerably lower than in the rest of the room prior to the air leakage improvements. After the improvements were made the concentration was more similar to the rest. There are still differences, however, and the concentrations in all of the sampling point far from reaching the supply concentration. Before the model can share similarity with the prototype, the air leakage must be taken care of.

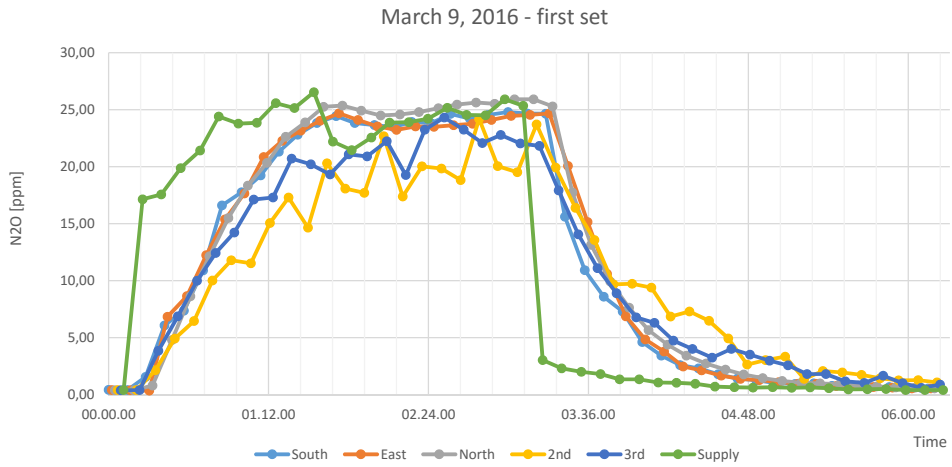


(a) Air velocities at height of 25mm - prototype

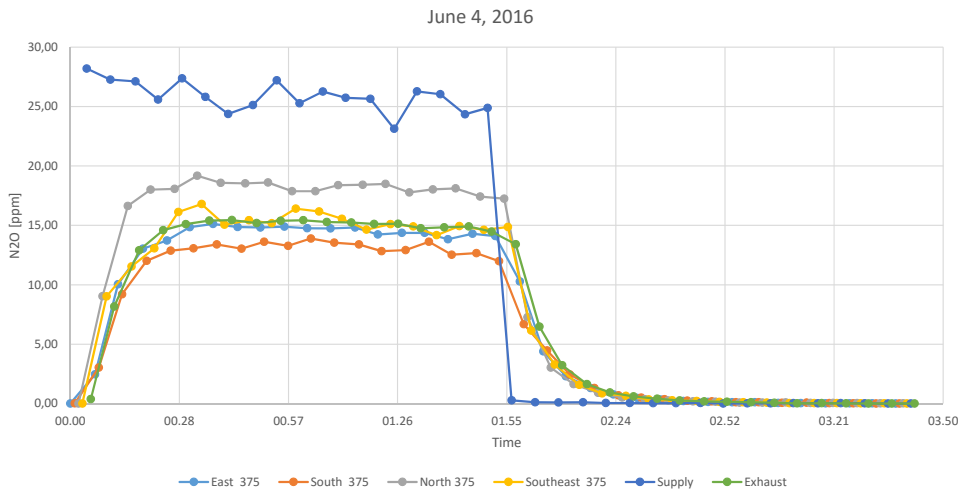


(b) Air velocities at height of 100mm - prototype

Figure 5.18: Comparison of air velocities at similar heights in prototype and model



(a) Tracer gas measurement on March 9, 2016 - prototype



(b) Tracer gas measurement on June 4, 2016 - model

Figure 5.19: Comparison of tracer gas measurement in prototype and model

Figure 5.19 show a comparison of tracer gas measurement in the prototype and the model. The sampling points South, East, Supply and 3rd in the prototype correspond to the points South, East, Supply and Exhaust in the model. The response in the model is quicker than in the prototype.

Table 5.12 show a comparison of the air change efficiencies and local indexes for the prototype and the model for the whole building. The air change efficiencies match fairly good between the prototype and model, although the efficiency in the model is slightly lower. This is most likely because of the non-ideal temperature difference. There are considerably greater inequalities in the local air change indexes. The index in the south corner of the prototype are more than twice the value of the model. There are probably multiple reasons for this deviation. The air leakage, temperature difference and the unequal air flow patterns are considered to have the most most influence over the similarity, and make the model behave different from the prototype.

Table 5.12: Comparison of air change efficiencies prototype and model

Prototype				
Date	09.03.2016			
Sample point	South 1500	East 1500	North 1500	Exhaust
Mean age of air				45,03
Local mean age of air	25,35	29,39	28,75	41,67
Nominal time constant	41,67	41,67	41,67	41,67
Air change efficiency, %				46,27
Local air change index, %	164,36	141,77	144,93	100,00
Model				
Date	04.06.2016			
Sample point	East 375	South 375	North 375	Exhaust
Mean age of air				11,55
Local mean age of air	12,30	12,26	8,31	9,68
Nominal time constant	9,68	9,68	9,68	9,68
Air change efficiency, %				41,90
Local air change index, %	78,69	78,92	116,42	100,00

Table 5.13 show a comparison of the air change efficiencies and local indexes in the east corner. The air change efficiencies are quite equal. Similar to the previous comparison, the local indexes differ significantly. However, they seem to show the same trend of increasing as the height above the floor increases. This might indicate that the air flows in this area of the model are somewhat similar to the prototype.

Table 5.13: Comparison of air change efficiencies prototype and model

Prototype					
Date	10.03.2016				
Sample point	East 100	East 1100	East 2000	East 2900	Exhaust
Mean age of air					45,51
Local mean age of air	39,11	40,01	36,58	36,59	43,26
Nominal time constant	43,26	43,26	43,26	43,26	43,26
Air change efficiency, %					47,53
Local air change index, %	110,62	108,11	118,25	118,22	100,00
Model					
Date	01.06.2016				
Sample point	East 25	East 275	East 500	East 725	Exhaust
Mean age of air	11,56				45,51
Local mean age of air	14,31	13,50	12,48	11,41	10,25
Nominal time constant	10,25	10,25	10,25	10,25	10,25
Air change efficiency, %					44,34
Local air change index, %	71,65	75,95	82,18	89,90	100,00

The model reached a temperature difference of approximately eight degrees Celsius. This gave a lower Archimedes number in the model than in the the prototype. It is hard to predict exactly how this affect the similarity, but considering that the model ideally should have a difference of 16 degrees Celsius to match the Archimedes numbers, it is assumed it is going to affect the air flow significantly.

Overall, the model and the prototype do not share satisfactory similarity yet. Although the air change efficiencies match reasonably well, the local air change indexes differs extremely, the air flow patterns are not equal, and the air leakage in the model is unacceptably high. It is believed, however, that the model and prototype can share similarity after improvements have been made to the air leakage, temperature difference and control of the extra air coming from the part of the floor excluded from the model.

5.7 Discussion

There is an open walkway between the prototype building and another building. The tracer gas measurements performed in this thesis and previous measurements by [Søgnen \(2015\)](#) indicate air movement between the two buildings. This is not considered in the

model, and might have an effect on the similarity. The pressure in each building is supposed to be equal, so it is not supposed to be exchange of air between them. The measurements although, suggest there are some interference between the buildings.

As mentioned in the background theory in Chapter 2, in order to measure air change efficiency, the room must exchange air only with the outside, and can not have any inflow of air from other parts of the building. When the air leakage in the model is this high, it has the same affect as inflow from another part/room. This impairs the results from the tracer gas and temperature measurements.

The extra air from part of the floor in the prototype excluded from the model may have an effect on the air flow in the office landscape. This is not considered in the thesis.

Although the air change efficiency is low, this does not necessarily mean poor air quality for the occupants. Plumes along the body causes air in the breathing zone to be considerably better than in the surrounding air. This requires the displacement ventilation strategy to work however, as there can not be excessive mixing for this effect to be present.

Complete steady state temperatures in the model was not achieved during the experiments. This can likely be achieved by leaving the heat sources in the model on for longer periods of time, and setting the supply temperature at a set-point where it can maintain a constant temperature for the whole period of the experiment, regardless of the outside conditions.

The velocity mapping hold no information about the direction of the flow at each measurement location. The air was assumed to flow radially form the diffuser. However, smoke experiments indicated that the air in some part actually flowed in towards the diffuser. This effects the accuracy of the measurements. Places where the air velocities are high are assumed to have flow radially from the diffuser, and the analysis regarding those results should hold certain credibility.

Chapter 6

Conclusion

A reduced-scale model was designed, built and outfitted with experimental equipment. The model was validated against the prototype building Powerhouse Kjørbo.

The tracer gas measurements in the prototype show that the air change efficiency is below 50 %, which is lower than what is expected for displacement ventilation. This indicate existence of short-circuiting and stagnant zones in the building. The local air change indexes were above 100 %, but only marginally. This indicate displacement characteristic of the air flows in the measured zones, but also suggest that some mixing between the air stratified layers occur. Similar air change indexes at the floor and ceiling indicate the same issue, that the air stratification in certain areas of the office landscape are suboptimal. Comparison of the air change indexes for the office landscape and for the whole floor suggest that short-circuiting and stagnant zones may occur in in other parts of the building than the office landscape. Minor air leakage within the exchanger still occurs. Lower air change indexes close to the floor in the east corner suggest that the bookshelves placed around the corner may work as obstructions to the air flow.

The tracer gas measurements in the model show that the air change efficiency is similar to the prototype. However, the local air change indexes differs extremely. Excessive air leakage and suboptimal temperature differences in the model are concluded to be the main causes for this. The improvements made to the air-tightness were confirmed by the tracer gas measurements. Similar to the results in the prototype, the lower air change indexes close to the floor in the east corner suggest that the bookshelves placed around

the corner may work as obstructions to the air flow.

The temperature measurements in the model reveal a temperature difference which is relatively stable, but nonetheless insufficient to match the Archimedes number to the prototype. The cooling capacity of the air handling unit, air leakage, and uninsulated ducts are identified as the main causes. The improvements of the air-tightness were confirmed by the measurements, as it reduced the deviation in the temperature difference.

The diffuser velocity mapping in the prototype show that velocities in the center of the discharge are lower than on the sides, indicating that the isovel of the diffuser are indistinct and unstable. Smoke visualization show that the discharge was not even and radial. These results suggest instability in the discharge caused by a large diffuser area. The issue affect the air distribution into the room and can cause short circuiting. The adjacent zone of the mapped diffuser are approximately one meter. No occupants or obstructions are found within this zone.

The diffuser velocity mapping in the model reveal that the velocities and flow rates of the discharge was largest on the opposite side of the diffuser compared to the prototype. This directs the air flow from the diffuser in the model towards different parts of the office landscape than in the prototype.

The comparison of results conclude that the model and the prototype do not share satisfactory similarity yet. The local air change indexes differs too much, the air flow patterns are not equal and the air leakage in the model are unacceptably high. However, there are indications that the air flows in some of the zones are behaving similarly, It is believed that the model and prototype can share similarity after improvements have been made to the air leakage, temperature difference and control of the simulation of the extra air coming from the part of the floor excluded from the model (controlled by the channel fan).

6.1 Recommendations for Further Work

The design, construction and validation of a reduced-scale model is a time consuming task, and is only the beginning of the project and possibilities that surround a building

model. There are still a lot of aspects left to study with the constructed model. The important part of utilizing the model in order to gain more knowledge of and improve ventilation strategies are still unexplored. It is highly recommended to continue working on the model until similarity is achieved and the model can provide results that relate to the prototype building.

Some recommendations for further work are:

- Improve the air-tightness of the model envelope. Perform tests to determine the air leakage number of the model.
- Increase the temperature difference in the model, by insulating the ducts, achieve colder air from the AHU, bleed of more more air to reduce air heating in the ducts.
- Perform experiments to determine the contaminant removal effectiveness (CRE) and local air quality index.
- Further improve the similarity by experimenting with changing air velocities and flow rates in the model.
- Perform temperature and velocity mapping to further validate and improve the similarity.
- Experiment with heat source placement and distribution. Experiment with different set ups, such as different number of heat sources, placement and heat outputs.
- Perform more extensive and detailed smoke experiments in the model and prototype.
- Experiment with ways of using the channel fan in a way that can improve the similarity.

Bibliography

- AGA. Nitrous oxide safety data sheet. http://www.aga.no/internet.lg.lg.nor/no/images/Nitrous_oxide_EN_N0639_170966.pdf, 2016.
- Asplan Viak. Kravspesifikasjon vvs-anlegg. *RIV*, 2012.
- H. B. Awbi and M. M. Nemri. Scale effect in room airflow studies. *Energy and Buildings*, 14(3):207–210, 1990.
- E. Bjørn and P. V. Nielsen. Dispersal of exhaled air and personal exposure in displacement ventilated rooms. *Indoor Air*, 12(3):147–164, 2002.
- Corine Brouns, Bob Waters, IEA Energy Conservation in Buildings, Community Systems Programme, Air Infiltration, and Ventilation Centre. *A guide to contaminant removal effectiveness*. Coventry,[Eng.] : Air Infiltration and Ventilation Centre, 1991. ISBN 0946075573 (pbk.).
- Stephen K. Chang and Richard R. Gonzalez. Air velocity mapping of environmental test chambers. In *ASHRAE Transactions*, volume 97, pages 31–37, New York, NY, 1989.
- T.M.Ø. Danielsen. Ventilation for a zero energy building. Project work, 2014.
- D.W. Etheridge and M. Sandberg. *Building ventilation: theory and measurement*. John Wiley & Sons, 1996.
- V. Heller. Scale effects in physical hydraulic engineering models. *Journal of Hydraulic Research*, 49(3):293–306, 2011.
- S. Ingebrigtsen. *Ventilasjonsteknikk Del I*. Skarland Press AS, 2015.
- K. Kalleberg. *Ventilasjon av ovnshus for silisiumkarbidproduksjon*. VHL rapport, 1977.

- Brüel & Kjær. *Technical Review 1990-2: Optical Filters and their Use with the Type 1302 & Type 1306 Photoacoustic Gas Monitors*. Brüel & Kjær, 1990.
- Hans Martin Mathisen, Elisabeth Mundt, Peter V. Nielsen, and Alfred Moser. *Ventilation Effectiveness*. Federation for European Heating and Air Conditioning Associations (REHVA), 2004.
- Hiroshi Matsumoto and Yusaku Ohba. The influence of a moving object on air distribution in displacement ventilated rooms. *Journal of Asian Architecture and Building Engineering*, 3(1):71–75, 2004.
- Mads Mysen and Peter Schild. *Behovsstyrt ventilasjon, DCV – forutsetninger og utforming: Veileder for et energioptimalt og velfungerende anlegg*. SINTEF akademisk forlag, 2014.
- P.E. Nilsson. *Achieving the Desired Indoor Climate: Energy Efficiency Aspects of System Design*. Studentlitteratur AB, 2003.
- Omega. Measuring air flow in ducts, pipes, hoods and stacks. http://www.omega.com/Green/pdf/AIRFLOW_MEAS_REF.pdf, 2015.
- Powerhouse. Powerhouse kjørbo. <http://www.powerhouse.no/prosjekter/kjorbo/>, 2015.
- Price Industries. *Price Engineer's HVAC Handbook: A Comprehensive Guide to HVAC Fundamentals*. Price Industries Limited, 2011.
- Projectplace. Projectplace powerhouse kjørbo, 2015.
- Olav Rådstoga. Personal conversation march 8, 2015.
- SINTEF Energiforskning. *Enøk i bygninger: Effektiv energibruk*. Gyldendal undervisning, 2007.
- H. Skistad. *Displacement ventilation in non-industrial premises*. REHVA, 2002.
- Helen Sutcliffe. *A guide to air change efficiency*. Coventry [England] : Air Infiltration and Ventilation Centre, 1990. ISBN 0946075433. "Document AIC-TN-29-90".
- O.B Søgne. Indoor climate in a zero energy building. Master's thesis, NTNU, 2015.

- Lumasense Technologies. *User Manual for Application Software 7620*. Lumasense Technologies A/S, 2008.
- TSI Airflow Instruments. Traversing a duct to determine average air velocity or volume. http://www.tsi.com/uploadedFiles/_Site_Root/Products/Literature/Application_Notes/AF-106%20Traversing%20a%20Duct.pdf, 2015.
- C.E. Walker. *Methodology for the evaluation of natural ventilation in buildings using a reduced-scale air model*. Ph. d., Massachusetts Institute of Technology, 2006.
- Christine Walker, Gang Tan, and Leon Glicksman. Reduced-scale building model and numerical investigations to buoyancy-driven natural ventilation. *Energy and Buildings*, 43(9):2404–2413, 2011.
- Bahman Zohuri. Similitude theory and applications. In *Dimensional Analysis and Self-Similarity Methods for Engineers and Scientists*, pages 93–193. Springer International Publishing, 2015.

Appendices

Appendix A

Location of Tracer Gas Sampling Points



Figure A.1: Location of sampling points for tracer gas measurement on March 9, 2016 - second set

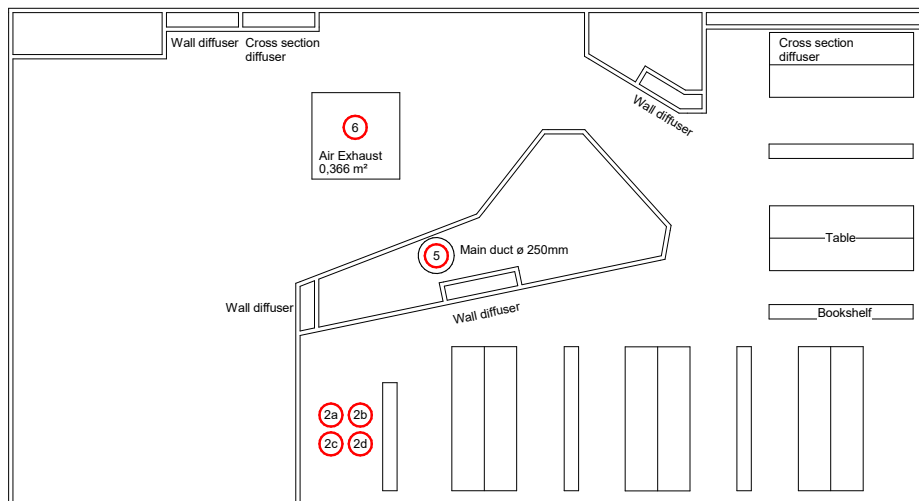


Figure A.4: Location of sampling points for tracer gas measurement on June 1, 2016-second set

Appendix B

Air Velocity Data

Table B.1: Air velocity data prototype duct \varnothing 400 (m/s)

Anemometer probe insertion depth (mm)	Air velocity (m/s)	Anemometer Location
12,8	1,44	1
54	1,6	2
128,4	1,59	3
271,6	1,56	4
346	1,58	5
387,2	1,47	6

Table B.2: Air velocity data for the prototype (m/s)

<u>Anemometer probe height</u>				Anemometer location
30mm	100mm	400mm	700mm	
0,21	0,12	0,15	0,11	A1
0,28	0,13	0,17	0,28	A2
0,25	0,27	0,26	0,3	A3
0,23	0,16	0,18	0,22	A4
0,21	0,17	0,43	0,34	B1
0,25	0,26	0,29	0,3	B2
0,27	0,24	0,11	0,17	B3
0,2	0,22	0,11	0,12	B4
0,25	0,24	0,34	0,16	C1
0,23	0,22	0,18	0,25	C2
0,2	0,22	0,08	0,16	C3
0,16	0,12	0,09	0,23	C4
0,18	0,24	0,16	0,09	D1
0,13	0,11	0,11	0,24	D2
0,16	0,11	0,09	0,16	D3
0,1	0,12	0,02	0,13	D4
0,15	0,15	0,22	0,36	E1
0,09	0,06	0,14	0,19	E2
0,16	0,13	0,08	0,17	E3
0,13	0,11	0,14	0,16	E4
0,13	0,11	0,45	0,35	F1
0,15	0,13	0,15	0,24	F2
0,12	0,12	0,11	0,18	F3
0,15	0,14	0,13	0,14	F4

Table B.3: Air velocity data for the model (m/s)

<u>Anemometer probe height</u>				Anemometer location
7,5 mm	25 mm	100 mm	175 mm	
0,15	0,1	0,05	0,02	A1
0,17	0,13	0,08	0,03	A2
0,17	0,12	0,04	0,11	A3
0,16	0,14	0,05	0,08	A4
0,05	0,04	0,1	0,1	B1
0,16	0,16	0,1	0,03	B2
0,17	0,1	0,07	0,08	B3
0,16	0,16	0,05	0,12	B4
0,04	0,13	0,08	0,13	C1
0,15	0,12	0,13	0,03	C2
0,19	0,17	0,09	0,06	C3
0,19	0,18	0,07	0,03	C4
0,05	0,16	0,11	0,11	D1
0,18	0,15	0,12	0,08	D2
0,18	0,17	0,15	0,04	D3
0,18	0,18	0,09	0,05	D4
0,1	0,12	0,14	0,17	E1
0,18	0,14	0,17	0,14	E2
0,19	0,18	0,15	0,02	E3
0,22	0,16	0,11	0,04	E4
0,13	0,15	0,18	0,15	F1
0,2	0,17	0,15	0,09	F2
0,23	0,14	0,13	0,13	F3
0,2	0,2	0,16	0,02	F4

Appendix C

Charts of Diffuser Air Velocity Mapping

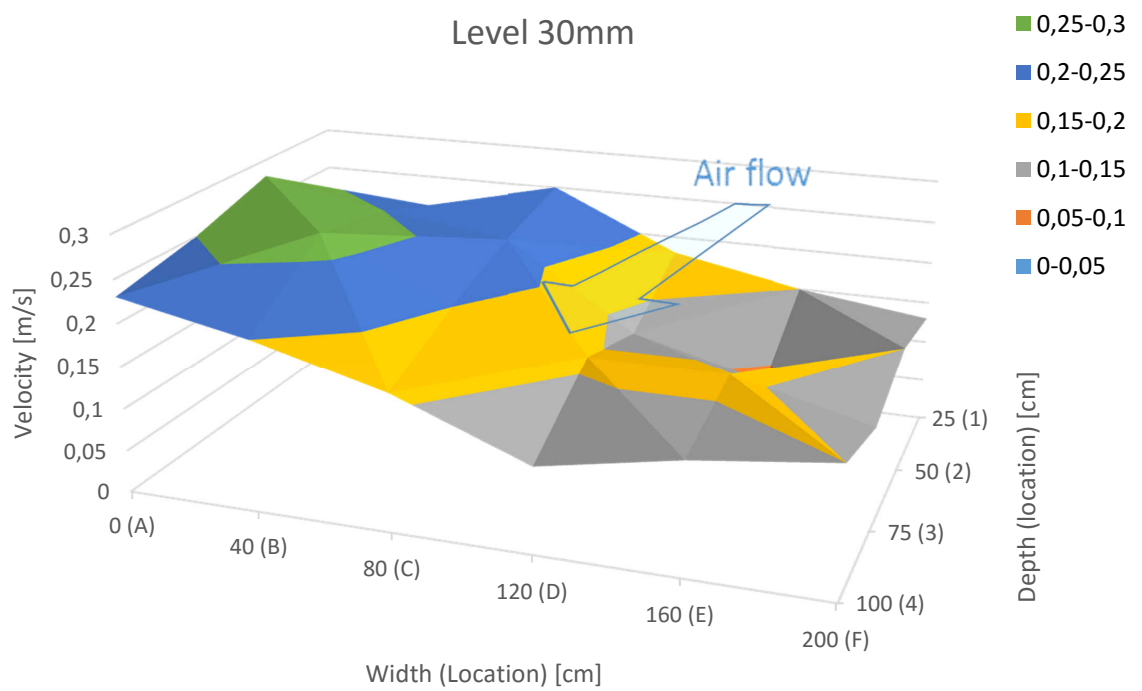


Figure C.1: Air velocities at height of 30mm- prototype

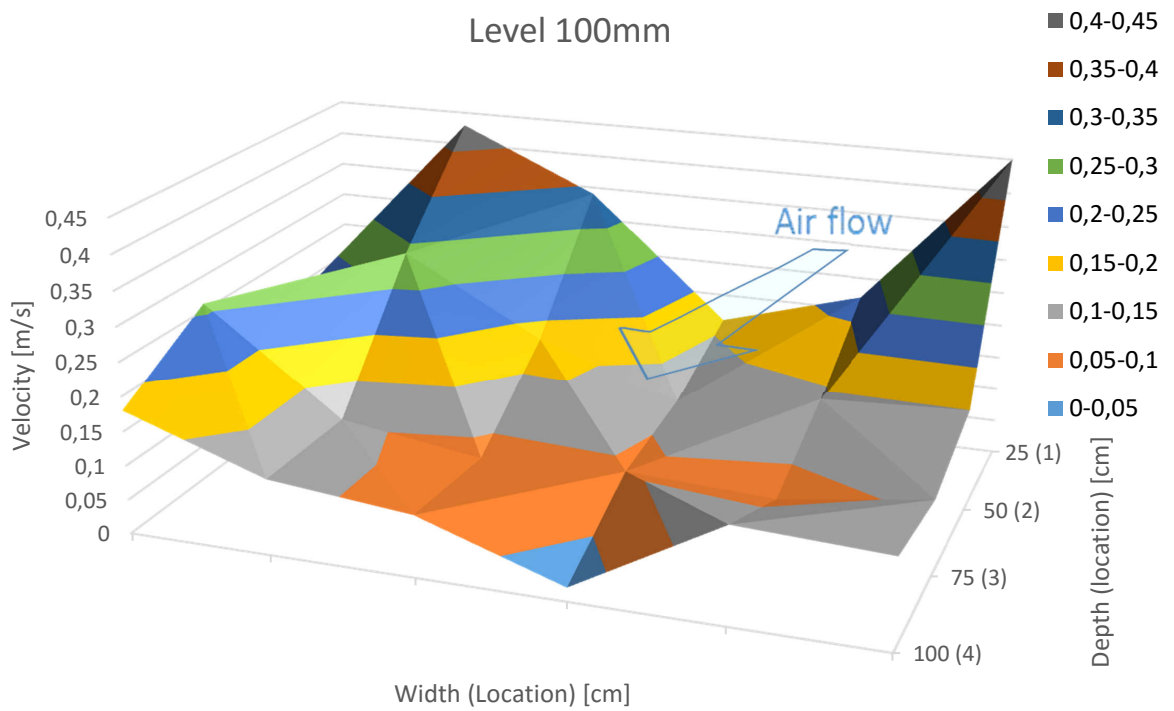


Figure C.2: Air velocities at height of 100mm - prototype

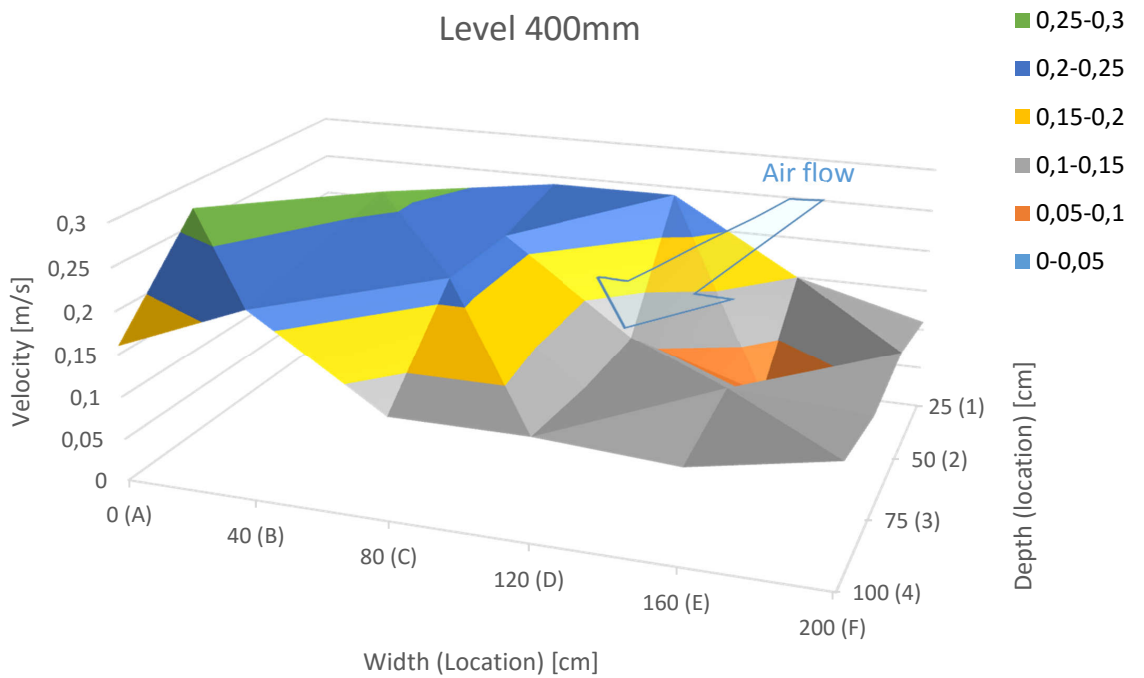


Figure C.3: Air velocities at height of 400mm- prototype

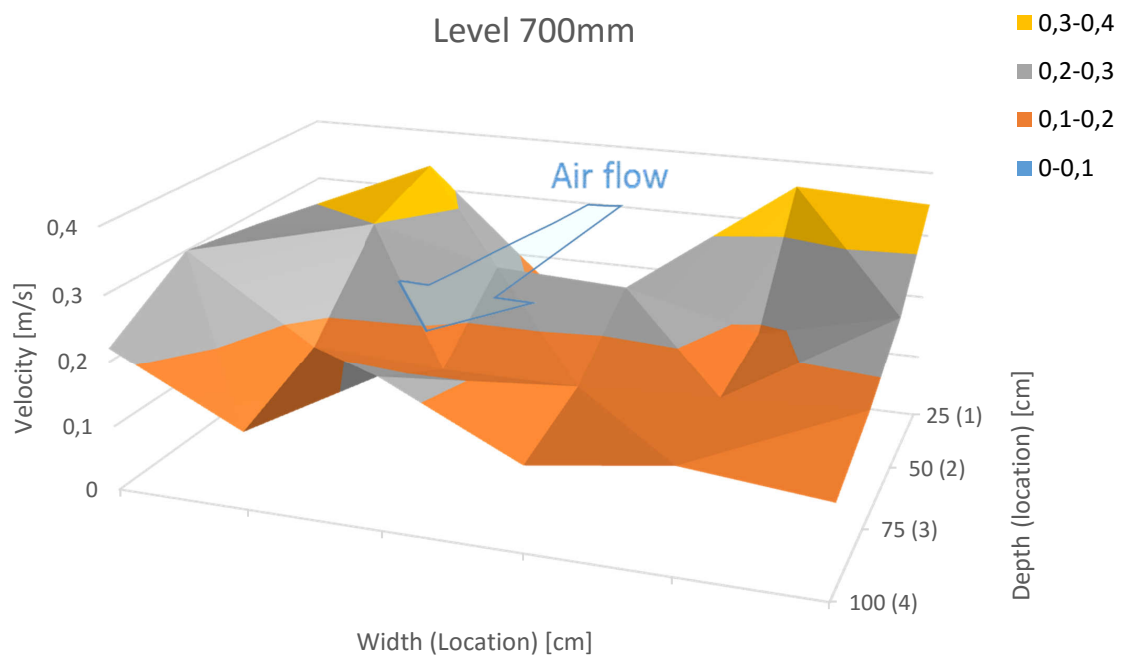


Figure C.4: Air velocities at height of 700mm - prototype

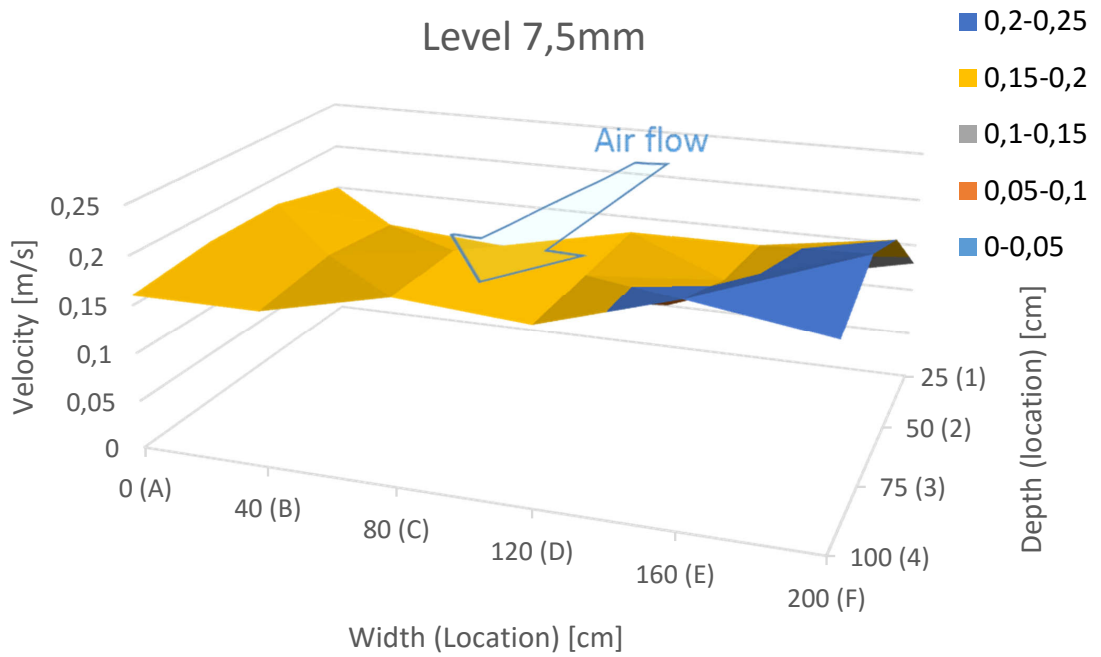


Figure C.5: Air velocities at height of 7.5mm - model

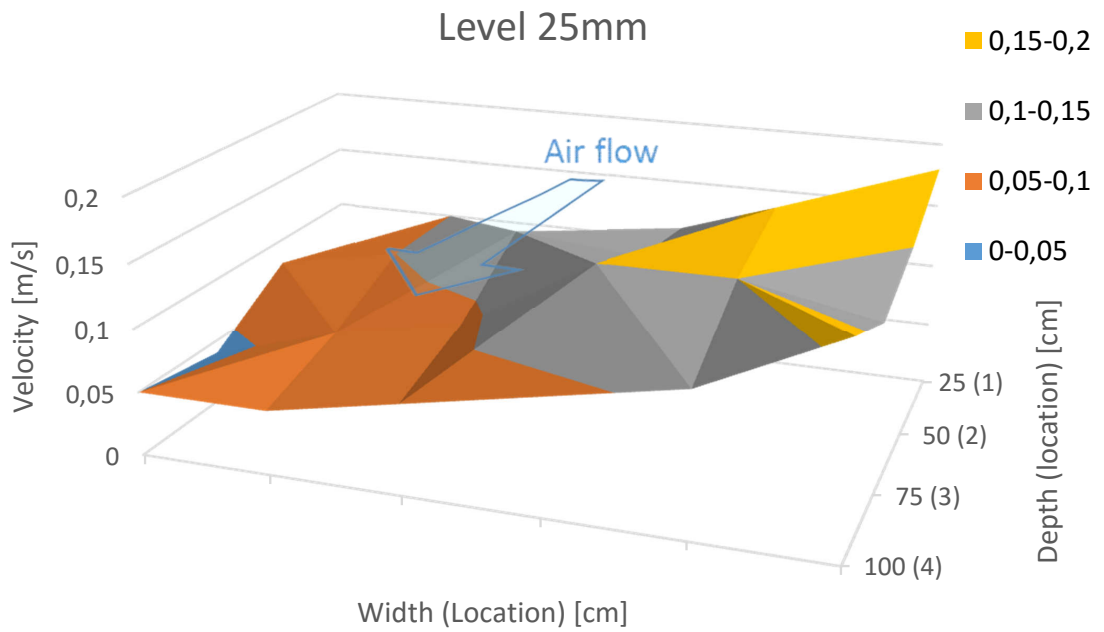


Figure C.6: Air velocities at height of 25mm - model

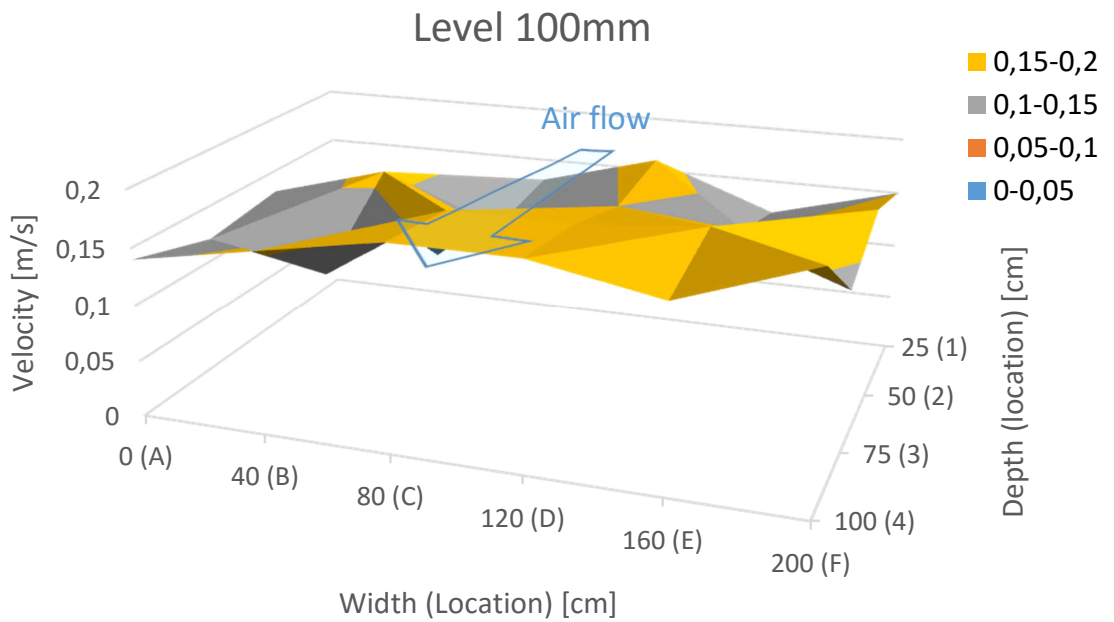


Figure C.7: Air velocities at height of 100mm - model

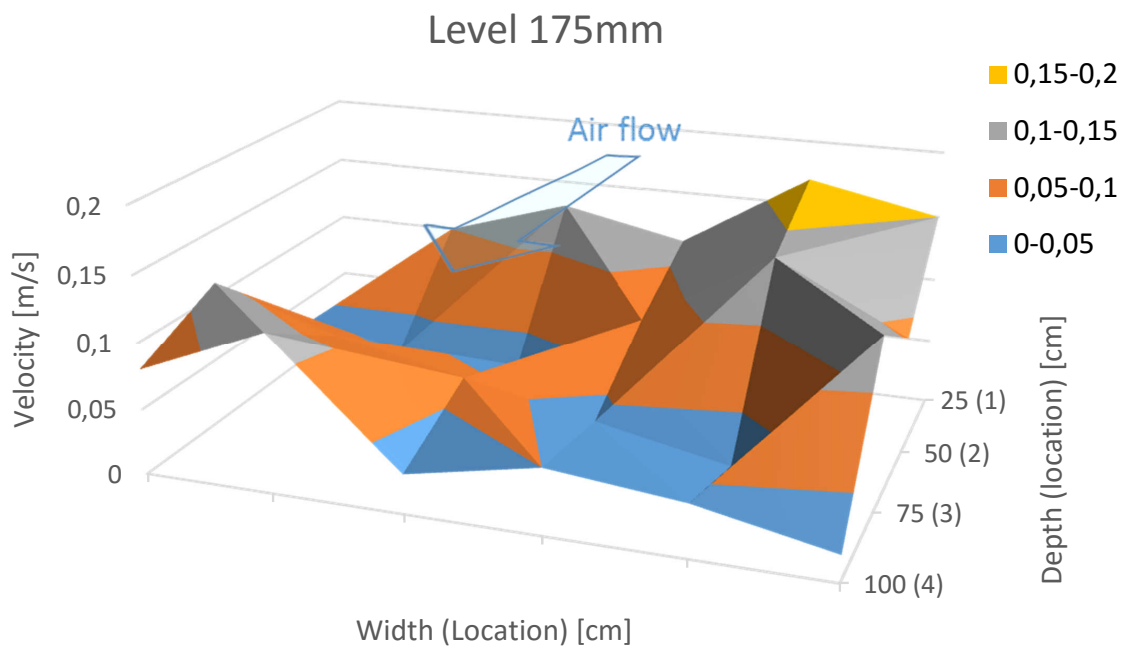


Figure C.8: Air velocities at height of 175mm - model

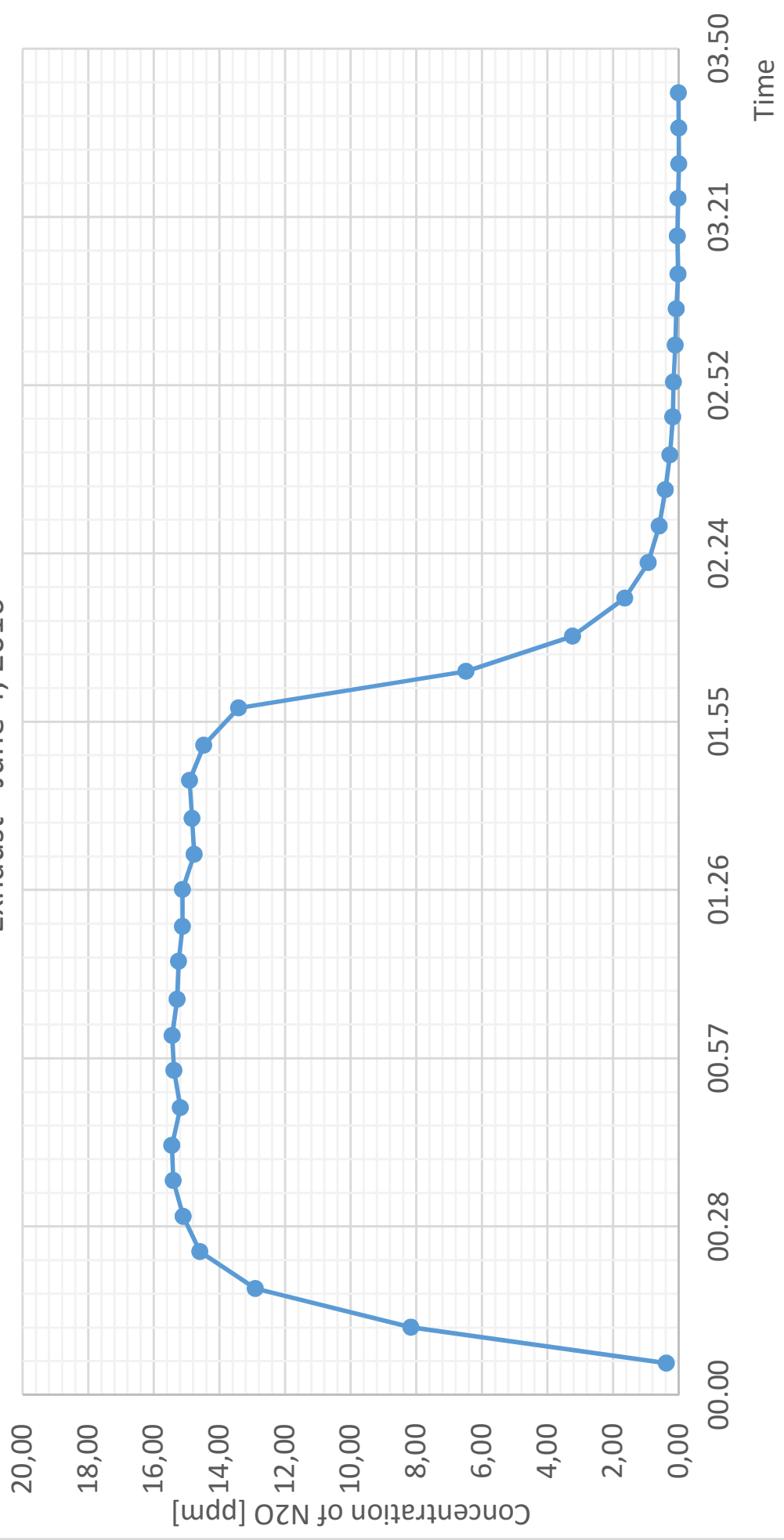
Appendix D

Excel Worksheet for Tracer Gas Calculations

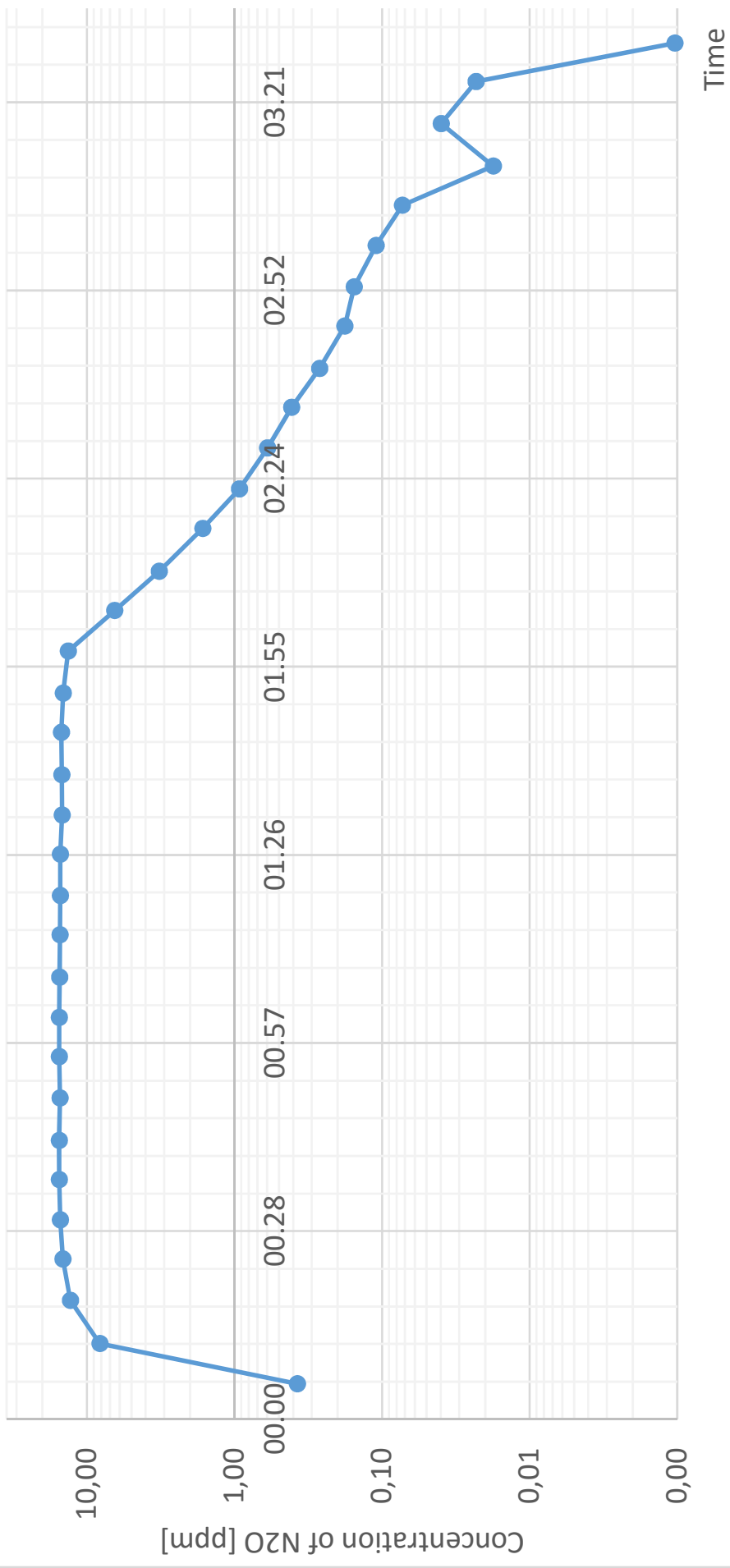
This appendix present the Excel data sheet for calculating the air change efficiency and local air change index from one single sampling point. A total of 42 data sheets equal to the one presented here make up the entire tracer gas calculation. The following sheet are the sampling point in the exhaust from the measurement in the model on June 4, 2016.

Exhaust		0,55
Time	N2O	REG N2O
00.05.25	0,92	0,38
00.11.35	8,72	8,17
00.18.10	13,46	12,91
00.24.30	15,15	14,60
00.30.30	15,65	15,11
00.36.40	15,96	15,41
00.42.40	16,00	15,45
00.49.10	15,74	15,19
00.55.30	15,93	15,38
01.01.30	15,99	15,44
01.07.40	15,83	15,29
01.14.10	15,79	15,25
01.20.10	15,67	15,13
01.26.30	15,68	15,13
01.32.30	15,31	14,76
01.38.40	15,38	14,83
01.45.10	15,46	14,91
01.51.10	15,02	14,47
01.57.35	13,97	13,42
02.03.50	7,03	6,48
02.09.50	3,78	3,23
02.16.20	2,19	1,64
02.22.25	1,48	0,93
02.28.40	1,15	0,60
02.34.55	0,96	0,41
02.40.50	0,81	0,27
02.47.20	0,73	0,18
02.53.20	0,70	0,15
02.59.40	0,66	0,11
03.05.50	0,62	0,07
03.11.50	0,57	0,02
03.18.20	0,59	0,04
03.24.45	0,57	0,02
03.30.40	0,55	0,00
03.36.50	0,55	0,00
03.42.50	0,56	0,01

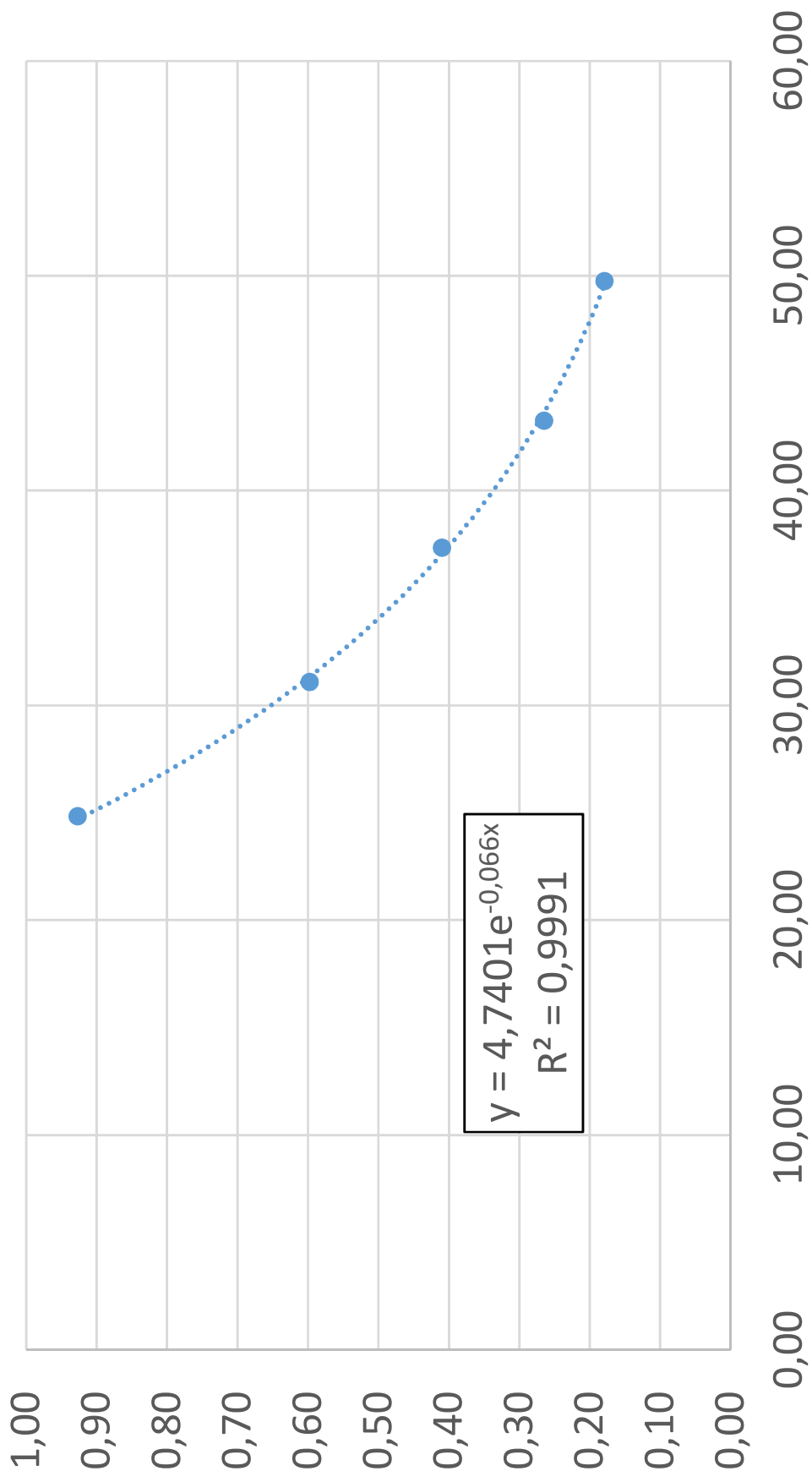
Exhaust - June 4, 2016



Exhaust - June 4, 2016



Step down trendline - Exhaust, June 4, 2016



Appendix E

Equipment

E.1 Tracer Gas Measurement Equipment and Apparatus



(a) Multi-gas monitor Type 1302

(b) Multi-point sampler Type 1303

Figure E.1: Tracer gas sampler and monitor equipment

To measure gas concentration, a sampler and monitor system from Brüel & Kjær were used. The Multi-point sampler and doser Type 1303 has six channels for sampling of tracer gas, and six channels for dosing. The sampling and dosing is done at regular time intervals. The instrument also has six inputs for temperature sensors. For the experiments in this thesis, only the sampling inputs are used. The samples are collected by suction through plastic tubes up to 50 meters long. The collected sample is delivered through another tube to the Multi-gas monitor Type 1302 to be analyzed. Both the sampler

Table E.1: Tracer gas properties

Chemical name	Nitrous oxide
Chemical formula N ₂ O	<i>N₂O</i>
Physical state at 20 °C and 1 atm	Gas
Color Colorless	Colorless
Smell Slightly sweet-scented	Slightly sweet-scented
Molar weight 44 g/mol	<i>44g/mol</i>
Melting point -90,81	-90.81
Boiling point -88,5	-88.5
Critical temperature 36,4	36.4
Relative density, gas (air=1) 1,5	1.5
Relative density, liquid (water=1) 1,2	1.5
Density 1.98 kg/m ³ or g/L	<i>19 kg/m³</i>
Conversion (ppm = mg/m ³)	<i>1 ppm = 1.8 mg/m³</i>
) 1 ppm = 1,8 mg/m ³	No know toxicity

and monitor is controlled remotely from a computer running the LumaSense Technologies Application Software - Innova 7620. The software is capable of activating the desired gas filters and sample channels, where each channel correspond to a specific location in the room. The locations can be named for organization, and the computer then logs the concentration of gas for each location ([Technologies, 2008](#)). All data is saved to a database and can be viewed graphically or numerically. The active gas filters for the experiments in this thesis was nitrous oxide (n₂o). For a more in-depth technical review of the the Type 1302 gas monitor, please refer to [Kjær \(1990\)](#).

The tracer gas used in the experiments were nitrous oxide (N₂O) from a pressurized cylinder of 10 liters at 50 bar, or 7.5 kg. At room temperature, it is a colorless, non-flammable gas, with a slightly sweet odor and taste. One of its uses apart from tracer gas experiments are in surgery and dentistry for its anaesthetic and analgesic effects. At elevated temperatures, nitrous oxide is a powerful oxidizer similar to molecular oxygen ([AGA, 2016](#)).

E.2 Air Velocity Measurements

To measure air velocities the TSI VelociCalc 9555-P probe anemometer was used. The device averages each air velocity sample over a user defined sampling period between 1 and 60 seconds. The samples are be saved to a database within the device and can be

exported for later analysis.

E.3 Air Flow Rate Measurements

To measure air flow rates the TSI VelociCalc 9555-P was used. The VelociCalc can measure flow by either entering the k-factor into the machine and measure pressure drop over the dampers, or entering duct size and measuring the average velocity in the duct.

E.4 Smoke visualization

To visualize air movement with smoke Dräger air current tubes was used. Once breaking the seal on a tube, it emits smoke for a certain amount of time. A small rubber bladder is attached to the smoke tube in order to push out a desired amount of smoke.

E.5 Temperature Measurements

Type T thermocouples were used to measure temperature at different heights and locations in the model. The thermocouples are connected to a data logger system by National Instruments. The data are sent to a computer running a custom made National Instruments LabVIEW program. The data are logged at desired time intervals, and written to a text file on the computer and stored for later analysis.

E.6 Sampling Intervals of Equipment

The Brüel & Kjær tracer gas equipment runs in intervals of about 1 minute per sampling point. When utilizing all six sampler points, this results in one full measuring sequence taking approximately six minutes to finish, and again means that information from each specific point are acquired every six minutes.

The VelociCalc anemometer data logger averages the velocity over a given time interval. At each stand location, the anemometer data was collected at five seconds. For the duct

traversing, it was set to ten seconds.

The data logger gathered information from all thermocouples simultaneously every two minutes.

Appendix F

Presence of People During a Work Day

The presence of people was measured during the course of one work day. Figure [F.1](#) show an overview at different times of the day. The average presence of people on the whole floor during the day is 20.75 while the average presence for the area modelled in this thesis is 10.25.

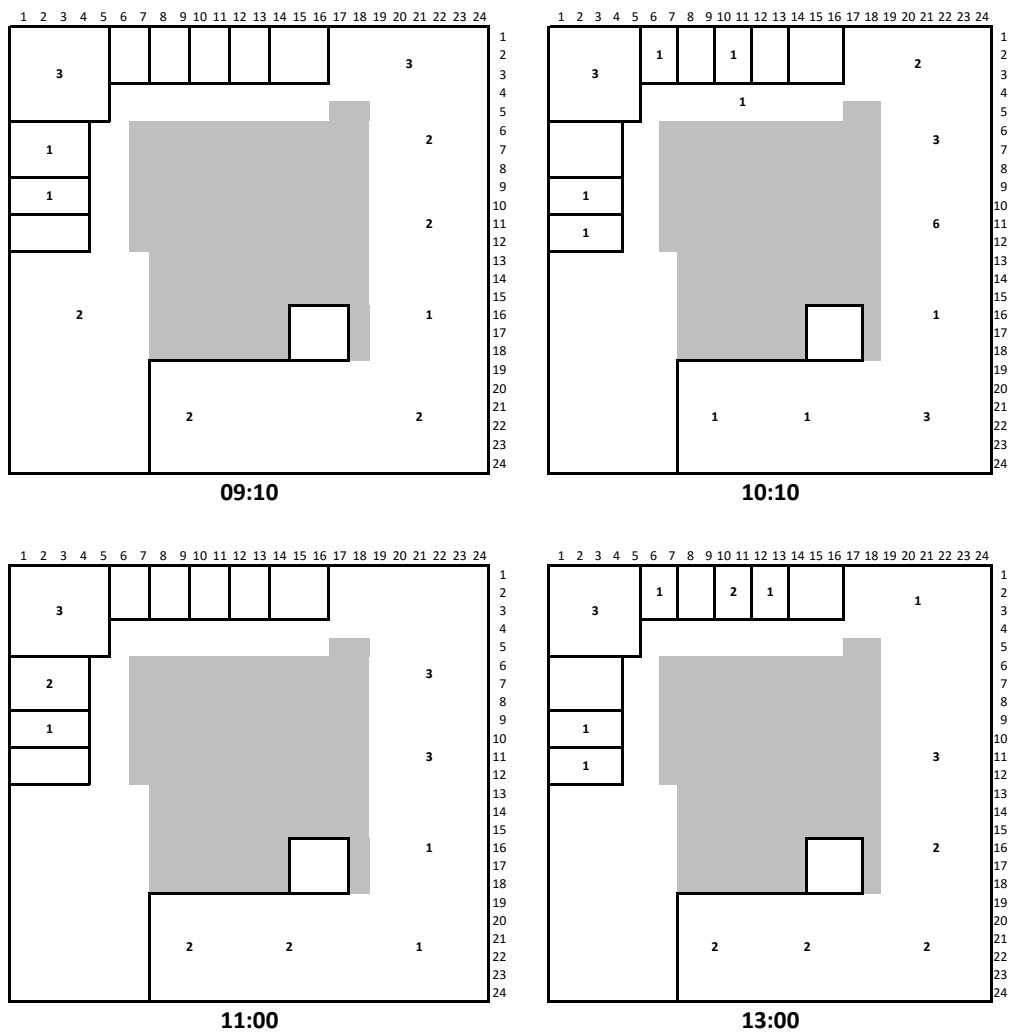
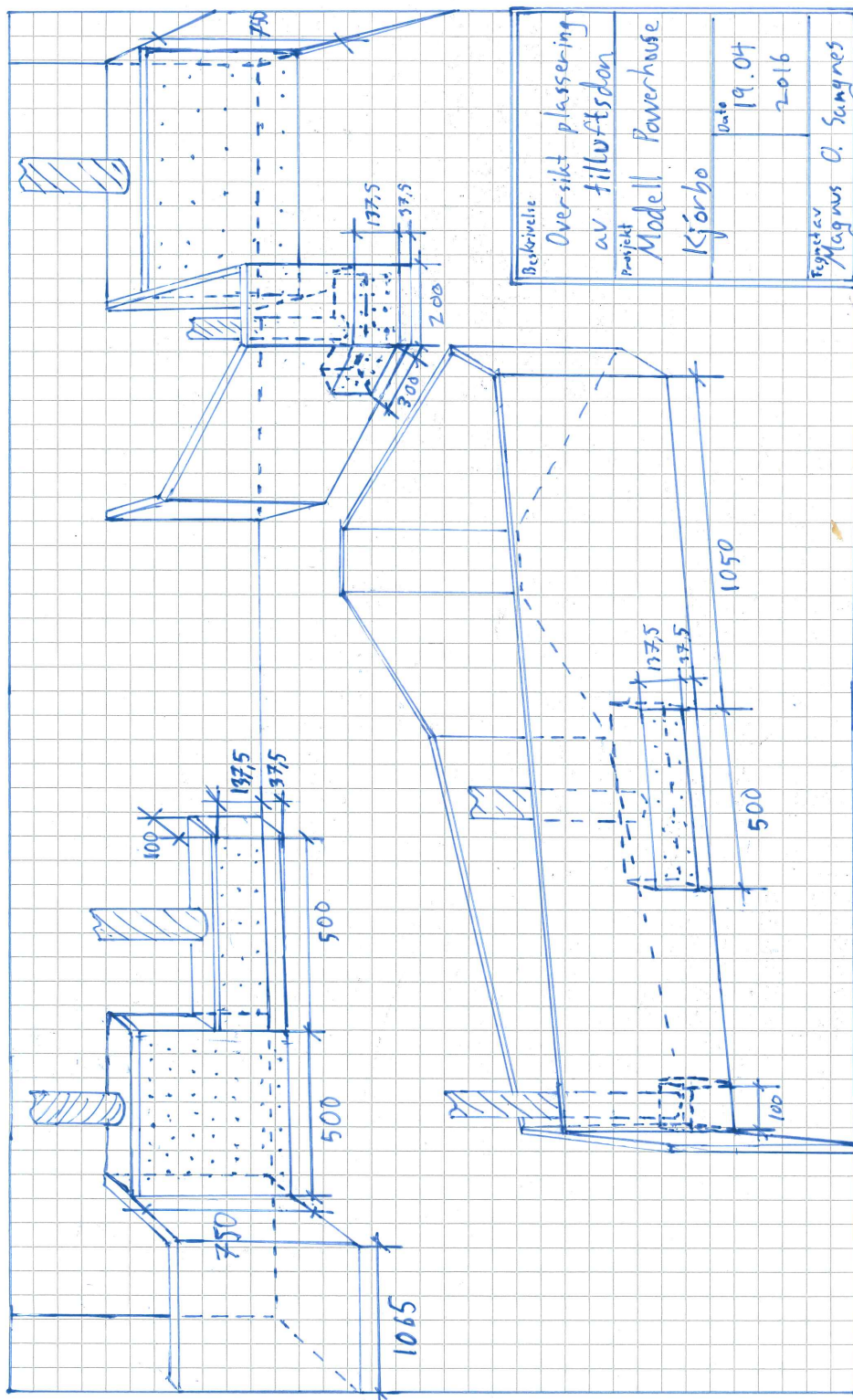


Figure F.1: Presence of people on 2nd floor at different times on March 10. The numbers indicate the number of people in the specified area

Appendix G

Floor Plans and Drawings of the Model and Prototype



Appendix H

Calibration of Equipment

It is crucial to have as accurate equipment as possible to get reliable results from experiments. This is achieved by calibration. The Brüel & Kjær Multi-gas monitor Type1302 and the TSI comes with a calibration card, see Figures [H.1](#), [H.2](#) and [H.3](#)

The thermocouples were calibrated manually. The thermocouples were put into an insulated cup of heavily iced water, and a set of zero point temperature measurements were taken. Table [H.1](#) show each thermocouple's mean error from zero degrees Celsius, and the standard deviation of the measurement samples. The mean error for each thermocouple is subtracted from its respective measurement data value.

H.1 Errors in Calibration Methodology

The ice-water may not be exactly zero degrees. The thermocouples all show a temperature above zero degrees, which rises the question if the water is exactly at freezing point. The thermocouples may also touch the edges of the cup, which is not necessarily at zero degrees.



Calibration Chart for Multi-gas Monitor Type 1302

Serial No. : 1846864

Installed Optical Filter: UA 0985 to
measure: Dinitrogen oxide with
Detection Limit: 0.03 ppm.
Filter Installed in Position: D
Filter Bank: I

Calibration Data for Filter :

Gas name: Dinitrogen oxide
Molecular weight: 44.01
Concentration offset factor¹: 3.096E-06
Humidity gain factor¹: 2.365E-02
Conc. conversion factor: 1.9000E+05
Cross interference on filter A: 3.667E+08
Cross interference on filter B: 1.096E+06
Cross interference on filter C: 1.401E+06
Cross interference on filter D: 1
Cross interference on filter E: 0.0000E+00

¹ Coefficients copied to bank 2 to 5.

Calibration Data :

Average zero level, (Dry zero gas): -2.19E-03 ppm
Standard deviation, (Dry zero gas): 1.50E-02 ppm
Average zero level, (Wet zero gas): -1.34E-02 ppm
Standard deviation, (Wet zero gas): 7.89E-03 ppm
Average gas concentration level: 5.14 ppm
Standard deviation: 0.017 ppm

Ambient temperature: 25.6 °C
Ambient pressure: 1000.0 mBar
Nafion tubing used? Yes

The Gas Monitor was calibrated mounted on a
non-vibrating surface during calibration.

This Calibration is covered by a warranty for a
period of 3 months.

Gas used during calibration:

Specific gas: Dinitrogen oxide
Substitute gas: 1
Calibration Gas Concentration: 5.05 ppm

Span Gas Specifications :

Span Gas: *Data from the "Analysis Certificate":*
Certificate no.: 040005508995
Contents: Dinitrogen oxide
Concentration: 5.05 ppm ± 2% rel.
Date of gas analysis: 141014
Valid after gas analysis date: 60 months
Manufactured by: Air Products

Zero Gas:

Contents: 1
Quality: 1 %
Manufactured by: 1
Zero Gas used (Quality > N₂ 5.0) : 1 Yes

Water Vapour: (Water Vapour in Zero gas)
Dewpoint: 18.0 °C

Signature: HHZ Date: 160204

Figure H.1: Calibration certificate of the N₂O filter of the Brüel & Kjær Multi-gas monitor Type1302

Table H.1: Error from zero point (0 °C)

Thermocouple	Mean (°C)	Standard deviation (°C)
T2	0,326	0,016
T3	0,462	0,022
T4	0,591	0,018
T5	0,411	0,024
T6	0,450	0,025
T7	0,579	0,026
T8	0,539	0,025
T9	0,142	0,024
T10	0,212	0,033
T11	0,274	0,022
T12	0,206	0,017
T13	0,713	0,021
T14	0,922	0,056
T15	0,974	0,267
T16	0,900	0,044

Appendix I

Data Sheet for Damper and Channel fan

The following data sheets are used for calculation of airflow rates in the model. The CK100C channel fan comes paired with a dimmer that allow for speed control. The DIRU Iris-damper has pressure measurement tubes that allow for flow rate calculations. The position of the damper gives a certain k-factor. The k-factor, together with the pressure drop allow for the flow rate to be calculated by the formula found on the side of the damper:

$$q = k * \sqrt{p_i}$$

where:

q = air flow rate

p_i = pressure drop

Flödesmätspjäll

DIRU

- 1
- 2
- 3
- 4
- 5
- 6
- 7
- 8
- 9
- 10
- 11
- 12
- 13
- 14
- 15
- 16
- 17
- 18



Beskrivning

DIRU är ett irisspjäll för mätning och injustering av luftflöden. DIRU har följande egenskaper: låg ljudnivå, centriskt flöde, fasta mätuttag som ger noggrann flödesmätning samt är utrustad med regleringsfunktion som kan öppnas helt, vilket betyder att det inte krävs någon renslucka. Klarar täthetsklass C.

Dimensioneringsdiagrammen ska användas för att bestämma tryckfallet över flödesmätspjället samt ge information om ljudeffektnivå vid olika inställningar.

Vid injustering av spjället ska injusteringsdiagrammen användas. För flödesmätspjäll finns en monterings-, mättings-, injusterings- och skötselansvisningen (MMIS).

Reglerskivorna bildar en mätläns som möjliggör flödesmätning. Avläst tryckfall över donets mätnipplar ger luftflödet efter uträkning med k-faktor. K-faktor och spjällinställning är sammat tal, vilket innebär att man slipper avläsa diagram för att få fram k-faktorn utifrån en viss spjällinställning. Luftflödet regleras med spjällets handtag.

Utförande

Spjället är tillverkat i galvaniserad stålplåt

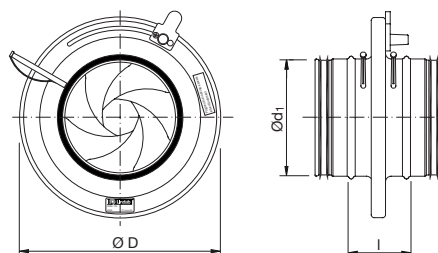
Montering

DIRU injusteringsspjäll monteras så att störningsavståndet beaktas.

Rensning

Genom att ställa spjället i öppet läge kommer man åt att rensa kanalen. Kom ihåg att återställa spjället efter rensning.

Dimensioner



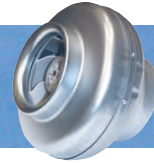
Ød ₁ nom	ØD mm	l mm	m kg
80	135	52	0,60
100	163	54	0,80
125	210	63	1,20
160	230	60	1,40
200	285	62	2,00
250	333	62	2,60
315	406	63	3,40
400	560	70	6,90
500	644	60	7,90
630	811	60	11,9

Beställningsexempel

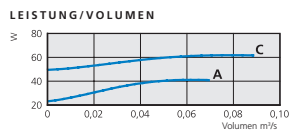
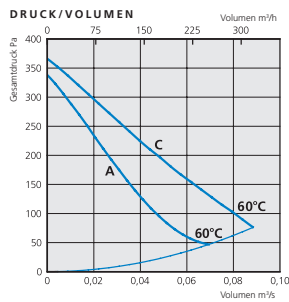
Produkt **DIRU** 160
Dimension Ød₁

CK 100 A/C CK 125 A/C

Rohrventilator mit rückwärts gekrümmtem Laufrad



CK 100 A/C



TECHNISCHE ANGABEN

CK	100 A	100 C
Spannung, V/Hz	230/50	230/50
Strom, A	0,18	0,27
Leistung, W	41	62
Drehzahl, rpm	1730	2530
Gewicht, kg	2,4	2,4
Schaltplan	4040002	4040001
Kondensator, µF	3	2
Isolationsklasse, Motor	F	F
Motorschutz, Motor	IP 44	IP 44

ZUBEHÖR

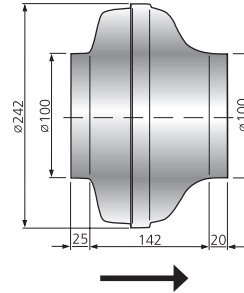
Befestigungsmanschette, Halterung, Schutzgitter, Thermostat, Lüftungsgitter & Rohrverschlussklappe, Drehzahlsteller

SCHALLDATEN

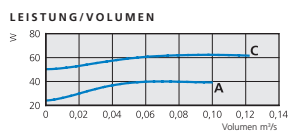
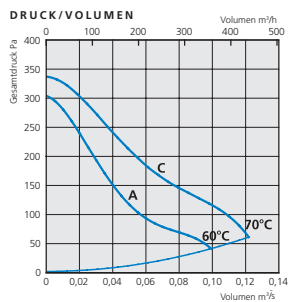
CK 100 A, 144 m ³ /h 125 Pa	LpA	LwA tot dB (A)	63	125	250	500	1K	2K	4K	8K
Umgebung	36	43	35	21	33	35	39	37	37	31
Ansaugstutzen		66	45	56	64	60	58	52	45	38

CK 100 C, 216 m ³ /h 170 Pa	LpA	LwA tot dB (A)	63	125	250	500	1K	2K	4K	8K
Umgebung	42	49	34	23	40	40	44	42	44	38
Ansaugstutzen		70	50	61	66	65	65	59	52	46

ABMESSUNGEN (mm)



CK 125 A/C



TECHNISCHE ANGABEN

CK	125 A	125 C
Spannung, V/Hz	230/50	230/50
Strom, A	0,18	0,27
Leistung, W	40	62
Drehzahl, rpm	1640	2480
Gewicht, kg	2,4	2,5
Schaltplan	4040002	4040001
Kondensator, µF	3	2
Isolationsklasse, Motor	F	F
Motorschutz, Motor	IP 44	IP 44

ZUBEHÖR

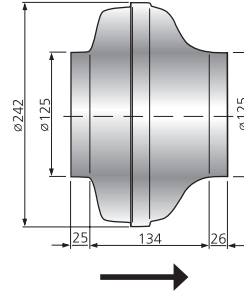
Befestigungsmanschette, Halterung, Schutzgitter, Thermostat, Lüftungsgitter & Rohrverschlussklappe, Drehzahlsteller

SCHALLDATEN

CK 125 A, 144 m ³ /h 130 Pa	LpA	LwA tot dB (A)	63	125	250	500	1K	2K	4K	8K
Umgebung	36	43	35	20	35	34	38	38	36	30
Ansaugstutzen		67	44	51	66	60	56	52	47	39

CK 125 C, 288 m ³ /h 145 Pa	LpA	LwA tot dB (A)	63	125	250	500	1K	2K	4K	8K
Umgebung	42	49	36	25	39	39	44	43	45	36
Ansaugstutzen		70	49	55	64	67	64	60	55	48

ABMESSUNGEN (mm)



Appendix J

Risk Assessment Report

The following risk assessment report was performed prior to the experiments in the reduced-scale model.

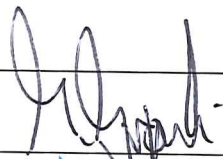
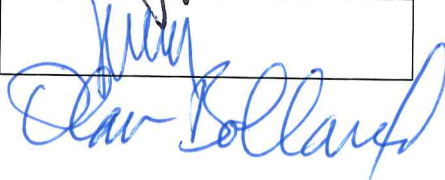
Risk Assessment Report

Klimarom: Reduced scale model

Prosjektnavn	Analysis of ventilation strategies for ZEB
Apparatur	Klimarom: Reduced scale model
Enhet	NTNU
Apparaturansvarlig	Hans Martin Mathisen
Prosjektleder	Hans Martin Mathisen
HMS-koordinator	Morten Grønli
HMS-ansvarlig (linjeleder)	Olav Bolland
Plassering	NTNU-E 302
Romnummer	C247C
Risikovurdering utført av	Magnus Owren Sangnes

Approval:

Apparatur kort (UNIT CARD) valid for:	12 months
Forsøk pågår kort (EXPERIMENT IN PROGRESS) valid for:	12 months

Rolle	Navn	Dato	Signatur
Prosjektleder	Hans Martin Mathisen		
HMS koordinator	Morten Grønli	26/5-2016	
HMS ansvarlig (linjeleder)	Olav Bolland	30/5-2016	

31/5-2016

TABLE OF CONTENTS

1	INTRODUCTION	1
2	ORGANISATION	1
3	RISK MANAGEMENT IN THE PROJECT	1
4	DESCRIPTIONS OF EXPERIMENTAL SETUP.....	1
5	EVACUATION FROM THE EXPERIMENTAL AREA	3
6	WARNING	3
6.1	Before experiments.....	3
6.2	Abnormal situation.....	4
7	ASSESSMENT OF TECHNICAL SAFETY	4
7.1	HAZOP.....	4
7.2	Flammable, reactive and pressurized substances and gas	5
7.3	Pressurized equipment.....	5
7.4	Effects on the environment (emissions, noise, temperature, vibration, smell)	5
7.5	Radiation	5
7.6	Chemicals.....	5
7.7	Electricity safety (deviations from the norms/standards)	6
8	ASSESSMENT OF OPERATIONAL SAFETY	6
8.1	Procedure HAZOP	6
8.2	Operation procedure and emergency shutdown procedure.....	6
8.3	Training of operators.....	6
8.4	Technical modifications.....	6
8.5	Personal protective equipment.....	6
8.6	General Safety	6
8.7	Safety equipment	6
8.8	Special predations	7
9	QUANTIFYING OF RISK - RISK MATRIX.....	7
10	REGULATIONS AND GUIDELINES.....	8
11	DOCUMENTATION.....	8

1 INTRODUCTION

A reduced-scale model of a ventilated office building has been built. The ventilation efficiency of the model will be evaluated by performing tracer gas experiments. Temperature and air velocities in the model will be measured. The working conditions of the test is listed in the table below:

Parameters	Conditions
Working media	Air with atmospheric pressure
Air temperature	15°C – 30°C
Air relative humidity	20 % - 60 %
Air-flow rate	40-80 m ³ /h
Pressure	± 100 Pa

2 ORGANISATION

Rolle	
Prosjektleder	Hans Martin Mathisen
Apparaturansvarlig	Hans Martin Mathisen
Romansvarlig	(Lars Konrad Sørensen)
HMS koordinator	Morten Grønli
HMS ansvarlig (linjeleder):	Olav Bolland

3 RISK MANAGEMENT IN THE PROJECT

Hovedaktiviteter risikostyring	Nødvendige tiltak, dokumentasjon	DATE
Prosjekt initiering	Prosjekt initiering mal	
Veiledningsmøte Guidance Meeting	Skjema for Veiledningsmøte med pre-risikovurdering	
Innledende risikovurdering Initial Assessment	Fareidentifikasjon – HAZID Skjema grovanalyse	
Vurdering av teknisk sikkerhet Evaluation of technical security	Prosess-HAZOP Tekniske dokumentasjoner	
Vurdering av operasjonell sikkerhet Evaluation of operational safety	Prosedyre-HAZOP Opplæringsplan for operatører	
Sluttvurdering, kvalitetssikring Final assessment, quality assurance	Uavhengig kontroll Utstedelse av apparaturkort Utstedelse av forsøk pågår kort	

4 DESCRIPTIONS OF EXPERIMENTAL SETUP

The test rig consists of a physical model. The model is connected to the ventilation system in the laboratory and a separate fan, which provide the air needed for experiments.

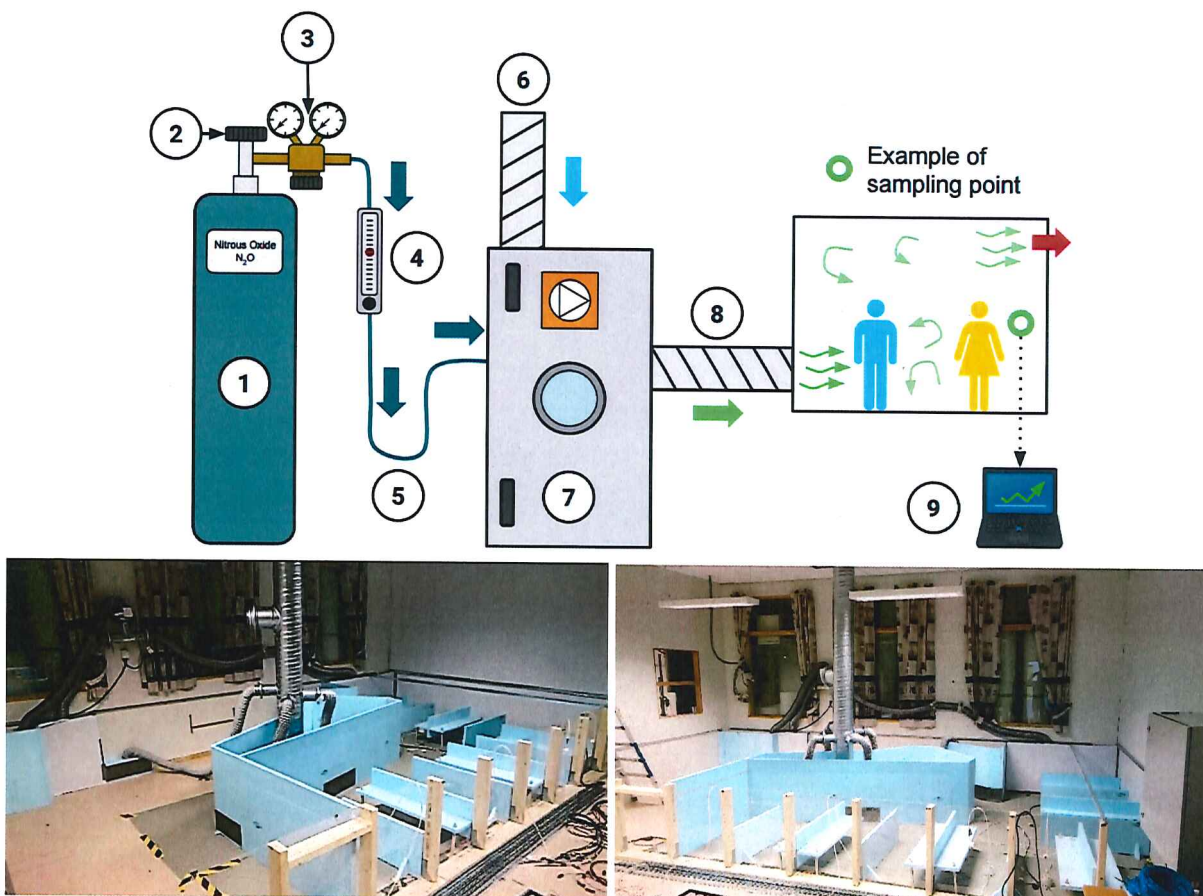


Figure 1.1: Description of the tracer gas setup and pictures of the test rig. The gas will be injected straight into the vertical duct seen on the pictures, not into the air-handling unit.

The air states will be monitored by thermocouples and anemometers. The tracer gas concentrations are monitored by a gas sampler and analyser. The tracer gas used for experiments are nitrous oxide (N_2O). The equipment and instruments are described in the tables below.

Instrument list		
Description	Manufacture	Model
Anemometer	TSI	
Anemometer	TSI	VelociCalc 8388
Tracer gas sampler	Brüel & Kjær	Type 1303
Tracer gas monitor	Brüel & Kjær	Type 1302
Thermocouple T1-T16	Lab	T type
Data logger	National Instruments	NI cDAQ-9172
Air handling unit	Systemair	Gold-08 RX
Fan	Lindab	CK 100C

Equipment list			
Description	Manufacture	Material	Model
Reduced-scale model	Lab	extruded polystyrene foam (Styrofoam), wood, Poly-methyl methacrylate (Plexiglas)	Custom made
Ducts, dampers, diffusers	Lindab	Steel, plastic	PSU, CK, DIRU, FHDD

Shutdown procedure consist by switching off the channel fan in the test room and the air handling system placed on the floor directly below the test room. Delivered air is stopped by switching off the fans. The tracer gas supply is stopped by turning the valve on top of the tank clockwise until it is shut. The heat sources are disconnected by unplugging them.

5 EVACUATION FROM THE EXPERIMENTAL AREA

Evacuate at signal from the alarm system or local gas alarms with its own local alert with sound and light outside the room in question, see 6.2

Evacuation from the rigging area takes place through the marked emergency exits to the assembly point, (corner of Old Chemistry Kjelhuset or parking 1a-b.)

Action on rig before evacuation:

- Shut off the N₂O gas supply by closing valve on the tank
- Switch off the fan connected to the model
- Unplug the heat sources

6 WARNING

6.1 Before experiments

Send an e-mail with information about the planned experiment to:

iept-experiments@ivt.ntnu.no

The e-mail must include the following information:

- Name of responsible person:
- Experimental setup/rig:
- Start Experiments: (date and time)
- Stop Experiments: (date and time)

You must get the approval back from the laboratory management before start up. All running experiments are notified in the activity calendar for the lab to be sure they are coordinated with other activity.

6.2 Abnormal situation

FIRE

If you are NOT able to extinguish the fire, activate the nearest fire alarm and evacuate area. Be then available for fire brigade and building caretaker to detect fire place. If possible, notify:

NTNU	SINTEF
Morten Grønli, Mob: 918 97 515	Harald Mæhlum, Mob: 930 14 986
Olav Bolland: Mob: 918 97 209	Petter Røkke, Mob: 901 20 221
NTNU – SINTEF Beredskapstelefon	800 80 388

GAS ALARM

If a gas alarm occurs, close gas bottles immediately and ventilate the area. If the level of the gas concentration does not decrease within a reasonable time, activate the fire alarm and evacuate the lab. Designated personnel or fire department checks the leak to determine whether it is possible to seal the leak and ventilate the area in a responsible manner.

Alert Order is in the above paragraph.

PERSONAL INJURY

- First aid kit in the fire / first aid stations
- Shout for help
- Start life-saving first aid
- **CALL 113** if there is any doubt whether there is a serious injury

OTHER ABNORMAL SITUATIONS

NTNU:

You will find the reporting form for non-conformance on:
<https://innsida.ntnu.no/wiki/-/wiki/Norsk/Melde+avvik>

SINTEF:

Synergi

7 ASSESSMENT OF TECHNICAL SAFETY

7.1 HAZOP

The experiment set up is divided into the following nodes:

Node 1	Tracer gas dosage unit
Node 2	Air handling unit
Node 3	Model environment

Attachments, Form: Attachment B: HAZOP REPORT

Conclusion: Treat the tracer gas unit according to guidelines for safe handling of gas

7.2 Flammable, reactive and pressurized substances and gas

Are any flammable, reactive and pressurized substances and gases in use?

YES	Explosion document has to be made and/or documented pressure test, (See 8.3)
-----	--

Attachments:

Conclusion: Tracer gas (N₂O) is an oxidizing gas and must be treated according to the data sheet and the guidelines for safe handling of gas. Unit Responsible has certificate for safe handling of gas.

7.3 Pressurized equipment

Is any pressurized equipment in use?

NO	
----	--

Attachments:

Conclusion: T

7.4 Effects on the environment (emissions, noise, temperature, vibration, smell)

Will the experiments generate emission of smoke, gas, odour or unusual waste?

Is there a need for a discharge permit, extraordinary measures?

YES	
-----	--

Attachments:

Conclusion: Tracer gas (N₂O) is considered a greenhouse gas, but the amount released is so small that discharge permits or extraordinary measures are unnecessary.

7.5 Radiation

NO	
----	--

Attachments:

Conclusion: No radiation

7.6 Chemicals

Will any chemicals or other harmful substances be used in the experiments? Describe how the chemicals should be handled (stored, disposed, etc.) Evaluate the risk according to safety datasheets, MSDS. Is there a need for protective actions given in the operational procedure?

NO	
----	--

Attachments: MSDS

Conclusion: No harmful substances will be used in the experiments.

7.7 Electricity safety (deviations from the norms/standards)

NO	
----	--

8 ASSESSMENT OF OPERATIONAL SAFETY

Ensure that the procedures cover all identified risk factors that must be taken care of. Ensure that the operators and technical performance have sufficient expertise.

8.1 Procedure HAZOP

The method is a procedure to identify causes and sources of danger to operational problems.

Attachments: Attachment D: HAZOP Procedure

8.2 Operation procedure and emergency shutdown procedure

The operating procedure is a checklist that must be filled out for each experiment. Emergency procedure should attempt to set the experiment set up in a harmless state by unforeseen events.

Attachments: Attachment E: Procedure for running experiments

Emergency shutdown procedure: Shut of the supply of tracer gas by closing valve on tank, unplug heat sources and channel fan.

8.3 Training of operators

A Document showing training plan for operators

- *What are the requirements for the training of operators?*
- *What it takes to be an independent operator*
- *Job Description for operators*

Attachments: Training program for operators

8.4 Technical modifications

- *Technical modifications made by the operator (e.g.Replacement of components, equal to equal)*

8.5 Personal protective equipment

Conclusion: No personal protective equipment are required during operation of the rig.

8.6 General Safety

- *Gantry crane and truck driving should not take place close to the experiment.*
- *Gas cylinders shall be placed in an approved carrier with shut-off valve within easy reach.*

8.7 Safety equipment

- *The rig equipment itself is a gas detector, though not outfitted with alarms.*
- *Warning signs, see the Regulations on Safety signs and signalling in the workplace*

8.8 Special predations

- *Flammable / toxic gases or chemicals*

9 QUANTIFYING OF RISK - RISK MATRIX

The risk matrix will provide visualization and an overview of activity risks so that management and users get the most complete picture of risk factors.

IDnr	Aktivitet-hendelse	Frekv-Sans	Kons	RV
1	<i>Excessive gas leakage</i>	1	D	D1
2	<i>Overheating of heat sources</i>	2	C	C2

Conclusion: The risks of the activity are acceptable.

CONSEQUENCES	Catastrophic	E1	E2	E3	E4	E5
	Major	D1	D2	D3	D4	D5
	Moderate	C1	C2	C3	C4	C5
	Minor	B1	B2	B3	B4	B5
	Insignificant	A1	A2	A3	A4	A5
		Rare	Unlikely	Possible	Likely	Almost
PROBABILITY						

Table 8. Risk Matrix

Table 9. The principle of the acceptance criterion. Explanation of the colors used in the matrix

COLOUR	DESCRIPTION
Red	Unacceptable risk Action has to be taken to reduce risk
Yellow	Assessment area. Actions has to be considered
Green	Acceptable risk. Action can be taken based on other criteria

10 REGULATIONS AND GUIDELINES

Se <http://www.arbeidstilsynet.no/regelverk/index.html>

- Lov om tilsyn med elektriske anlegg og elektrisk utstyr (1929)
- Arbeidsmiljøloven
- Forskrift om systematisk helse-, miljø- og sikkerhetsarbeid (HMS Internkontrollforskrift)
- Forskrift om sikkerhet ved arbeid og drift av elektriske anlegg (FSE 2006)
- Forskrift om elektriske forsyningsanlegg (FEF 2006)
- Forskrift om utstyr og sikkerhetssystem til bruk i eksplosjonsfarlig område NEK 420
- Forskrift om håndtering av brannfarlig, reaksjonsfarlig og trykksatt stoff samt utstyr og anlegg som benyttes ved håndteringen
- Forskrift om Håndtering av eksplosjonsfarlig stoff
- Forskrift om bruk av arbeidsutstyr.
- Forskrift om Arbeidsplasser og arbeidslokaler
- Forskrift om Bruk av personlig verneutstyr på arbeidsplassen
- Forskrift om Helse og sikkerhet i eksplosjonsfarlige atmosfærer
- Forskrift om Høytrykksspyling
- Forskrift om Maskiner
- Forskrift om Sikkerhetsskiltning og signalgivning på arbeidsplassen
- Forskrift om Stillaser, stiger og arbeid på tak m.m.
- Forskrift om Sveising, termisk skjæring, termisk sprøyting, kullbuemeisling, lodding og sliping (varmt arbeid)
- Forskrift om Tekniske innretninger
- Forskrift om Tungt og ensformig arbeid
- Forskrift om Vern mot eksponering for kjemikalier på arbeidsplassen (Kjemikalieforskriften)
- Forskrift om Vern mot kunstig optisk stråling på arbeidsplassen
- Forskrift om Vern mot mekaniske vibrasjoner
- Forskrift om Vern mot støy på arbeidsplassen

Veiledninger fra arbeidstilsynet

se: <http://www.arbeidstilsynet.no/regelverk/veiledninger.html>

11 DOCUMENTATION

- Tegninger, foto, beskrivelser av forsøksoppsetningen
- Hazop_mal
- Sertifikat for trykkpåkjent utstyr
- Håndtering avfall i NTNU
- Sikker bruk av LASERE, retningslinje
- HAZOP_MAL_Prosegyre
- Forsøksprosedyre
- Opplæringsplan for operatører
- Skjema for sikker jobb analyse, (SJA)
- Apparatorkortet
- Forsøk pågår kort

Attachment to Risk Assessment report

Klimarom: Reduced scale model

Prosjektnavn	Analysis of ventilation strategies for ZEB
Apparatur	Klimarom: Reduced scale model
Enhet	NTNU
Apparaturansvarlig	Hans Martin Mathisen
Prosjektleder	Hans Martin Mathisen
HMS-koordinator	Morten Grønli
HMS-ansvarlig (linjeleder)	Olav Bolland
Plassering	NTNU-E 302
Romnummer	C247C
Risikovurdering utført av	Magnus Owren Sangnes

TABLE OF CONTENTS

ATTACHMENT A: PROCESS AND INSTRUMENTATION DIAGRAM	1
ATTACHMENT B: HAZOP REPORT.....	2
ATTACHMENT C: TEST CERTIFICATE FOR LOCAL PRESSURE TESTING.....	3
ATTACHMENT D: HAZOP PROCEDURE (TEMPLATE).....	4
ATTACHMENT E: PROCEDURE FOR RUNNING EXPERIMENTS.....	5
ATTACHMENT F: TRAINING OF OPERATORS.....	7
APPARATURKORT / UNITCARD.....	8
FORSØK PÅGÅR /EXPERIMENT IN PROGRESS	9

ATTACHMENT A: PROCESS AND INSTRUMENTATION DIAGRAM

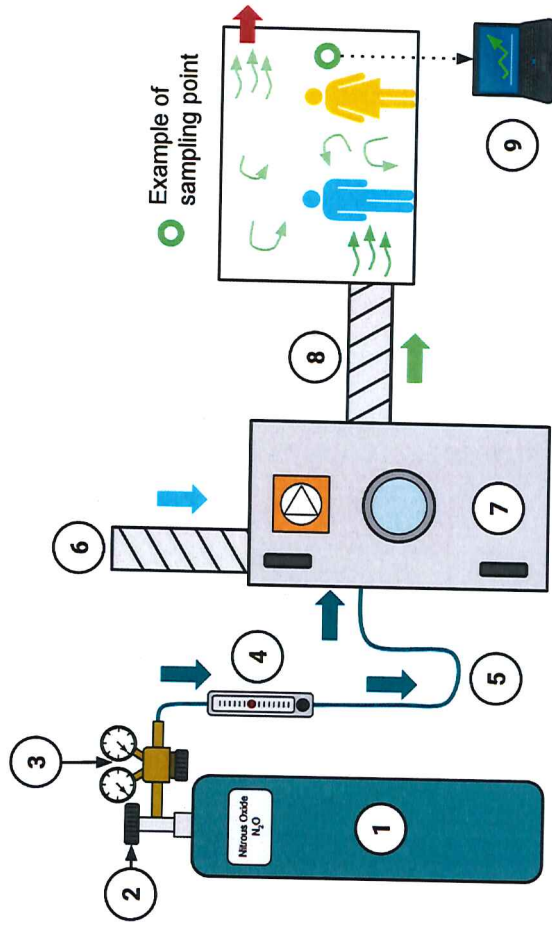


Figure A.1: Description of the tracer gas setup and pictures of the test rig. The gas will be injected straight into the vertical duct (red arrow) seen on the pictures, not into the air-handling unit.

ATTACHMENT B: HAZOP REPORT

Project: Analysis of ventilation strategies for ZEB Node: 1. Tracer gas dosage unit						Page	
Ref	Guideword	Causes	Consequences	Safeguards	Recommendations	Action	Date/Sign
1	More flow	Leakage	Danger of suffocation	Correct operation			
Project: Analysis of ventilation strategies for ZEB Node: 3. Model environment						Page	
Ref	Guideword	Causes	Consequences	Safeguards	Recommendations	Action	Date/Sign
2	More temperature	Overheating of heat sources	Fire hazard	Correct placement, restrict excessive use			

ATTACHMENT C: TEST CERTIFICATE FOR LOCAL PRESSURE TESTING

Trykkpåkjent utstyr:	
Benyttes i rigg:	
Design trykk for utstyr (bara):	
Maksimum tillatt trykk (bara): (i.e. burst pressure om kjent)	
Maksimum driftstrykk i denne rigg:	

Prøvetrykket skal fastlegges i følge standarden og med hensyn til maksimum tillatt trykk.

Prøvetrykk (bara):	
X maksimum driftstrykk: I følge standard	
Test medium:	
Temperatur (°C)	
Start tid:	Trykk (bara):
Slutt tid:	Trykk (bara):
Maksimum driftstrykk i denne rigg:	

Eventuelle repetisjoner fra atm. trykk til maksimum prøvetrykk:.....

Test trykket, dato for testing og maksimum tillatt driftstrykk skal markers på (skilt eller innslått)

Sted og dato

Signatur

ATTACHMENT D: HAZOP PROCEDURE (TEMPLATE)

Project: Node: 1		Page					
Ref#	Guideword	Causes	Consequences	Safeguards	Recommendations	Action	Date/Sign
	Not clear procedure	Procedure is too ambitious, or confusingly					
	Step in the wrong place	The procedure can lead to actions done in the wrong pattern or sequence					
	Wrong actions	Procedure improperly specified					
	Incorrect information	Information provided in advance of the specified action is wrong					
	Step missing	Missing step, or step requires too much of operator					
	Step unsuccessful	Step has a high probability of failure					
	Influence and effects from other	Procedure's performance can be affected by other sources					

ATTACHMENT E: PROCEDURE FOR RUNNING EXPERIMENTS

Prosjekt Analysis of ventilation strategies for ZEB	Dato	Signatur
Apparatur Klimarom: Reduced scale model	30/5-16	Morten G. Sævi
Prosjektleder Hans Martin Mathisen	30/5-2016	[Signature]

	Completed
Conditions for the experiment:	
Experiments should be run in normal working hours, 08:00-16:00 during winter time and 08.00-15.00 during summer time. Experiments outside normal working hours shall be approved.	✓
One person must always be present while running experiments, and should be approved as an experimental leader.	✓
An early warning is given according to the lab rules, and accepted by authorized personnel.	✓
Be sure that everyone taking part of the experiment is wearing the necessary protecting equipment and is aware of the shut down procedure and escape routes.	✓
Preparations	
Post the "Experiment in progress" sign.	✓
<i>Start up procedure</i> <i>The start-up sequence consist of turning Air handling unit and fans on, turning the heat sources on, initializing measurement equipment and start the supply of tracer gas.</i>	✓
During the experiment	
<i>Control of tracer gas dosage, temperature, and air flow</i>	✓
End of experiment	
Shut down procedure: <i>The shut-up sequence consist of shutting the supply of tracer gas, turning the air handling unit and fans off, unplugging the heat sources and shutting down the measurement equipment.</i>	✓
Emergency shut down procedure: <i>Shut of the supply of tracer gas by closing valve on tank, unplug heat sources and channel fan.</i>	
Remove all obstructions/barriers/signs around the experiment.	✓
Tidy up and return all tools and equipment.	✓
Tidy and cleanup work areas.	✓
Return equipment and systems back to their normal operation settings (fire alarm)	✓
To reflect on before the next experiment and experience useful for others	
Was the experiment completed as planned and on scheduled in professional terms?	✓
Was the competence which was needed for security and completion of the	✓

	experiment available to you?	
	Do you have any information/ knowledge from the experiment that you should document and share with fellow colleagues?	✓

Operator(s):

Navn	Dato	Signatur
Magnus Owren Sangnes	28/5 - 16	<i>Magnus Owren Sangnes</i>

ATTACHMENT F: TRAINING OF OPERATORS

Prosjekt	Dato	Signatur
Analysis of ventilation strategies for ZEB		
Apparatur Klimarom: Reduced scale model	30/6	Magnus B. Sangnes
Prosjektleder Hans Martin Mathisen	30/5-2016	<i>[Signature]</i>

Knowledge about EPT LAB in general	
Lab	
<ul style="list-style-type: none"> • Access • routines and rules • working hour 	
Knowledge about the evacuation procedures.	
Activity calendar for the Lab	
Early warning, iept-experiments@ivt.ntnu.no	
Knowledge about the experiments	
Procedures for the experiments	
Emergency shutdown.	
Nearest fire and first aid station.	

I hereby declare that I have read and understood the regulatory requirements has received appropriate training to run this experiment and are aware of my personal responsibility by working in EPT laboratories.

Operator(s):

Navn	Dato	Signatur
Magnus Owren Sangnes	30/5-16	Magnus B. Sangnes

APPARATURKORT

Enhet (unit) og bygg/romnr. (building/room no.):

NTNU-E 302

C247C

2. etg

Laboratorium

Klimarom VVSLab

Dette kortet SKAL henges godt synlig ved maskinen!
This card MUST be posted on a visible place on the unit!

Apparatur (Unit) Klimarom: Reduced scale model	Dato Godkjent (Date Approved) 23. mai 2016
Prosjektleder (Project Leader) Hans Martin Mathisen	Telefon mobil/privat (Phone no. mobile/private) 930 59 175
Apparaturansvarlig (Unit Responsible) Hans Martin Mathisen	Telefon mobil/privat (Phone no. mobile/private) 930 59 175
Sikkerhetsrisikoer (Safety hazards) Nitrous oxide (N ₂ O) gas leakage, hot surface on light bulbs.	
Sikkerhetsregler (Safety rules) Do not interfere with the gas equipment without the consent of Unit Responsible. Be careful of hot surfaces.	
Nødstopprosedyrer (Emergency shutdown) Shut the gas supply by closing vavle on top of tank. Unplug the heat sources and channel fan.	
Her finner du (Here you will find):	
Prosedyrer (Procedures)	In the room
Bruksanvisning (User manual)	In the room
Brannslukningsapparat (Fire extinguisher)	1. etasje VVSLab (syd)
Førsthjelpsskap (First aid cabinet)	1. etasje VVSLab (syd)

NTNU

Institutt for energi og prosessteknikk

Dato 31/5 - 2016

Signert *Olav Bell*

FORSØK PÅGÅR

Enhet (unit) og bygg/romnr. (building/room no.):

NTNU-E 302

C247C

2. etg

Laboratorium

Klimarom VVSLab

Dette kortet SKAL henges opp før forsøk kan starte!
This card MUST be posted on the unit before the experiment startup!

Apparatur (Unit)

Klimarom: Reduced scale model

Dato godkjent (Date Approved)

23. mai 2016

Prosjektleder (Project Leader)

Hans Martin Mathisen

Telefon mobil/privat (Phone no. mobile/private)

930 59 175

Apparaturansvarlig (Unit Responsible)

Hans Martin Mathisen

Telefon mobil/privat (Phone no. mobile/private)

930 59 175

Godkjente operatører (Approved Operators)

Navn/Name

Telefon/Phone Mobil

Sanges, Magnus Owren

90657630

Prosjekt (Project)

Analysis of ventilation strategies for ZEB

Forsøksstid / Experimental time (start - stop)

23.05.2016 - 23.05.2017

Kort beskrivelse av forsøket og relaterte farer (Short description of the experiment and related hazards)

A reduced-scale model of a ventilated office building has been built. The ventilation efficiency of the model will be evaluated by performing tracer gas experiments. Temperature and air velocities in the model will be measured.

NTNU

Institutt for energi og prosessteknikk

Dato

31/5 - 2016

Signert

NTNU

SINTEF